AN AUTOMATIC FACILITY

FOR

NEUTRON ACTIVATION ANALYSIS

AN AUTOMATIC FACILITY FOR NEUTRON ACTIVATION ANALYSIS

by

RANDY N. MACDONALD, B.Sc.

A Thesis

Submitted to the Faculty of Graduate Studies

in Partial Fulfillment of the Requirements

for the Degree

Master of Science

McMaster University

June 1973

MASTER OF SCIENCE (1973) McMaster University
Hamilton, Ontario

TITLE: An Automatic Facility for Neutron Activation Analysis

AUTHOR: Randy N. MacDonald, B.Sc. (University of Alberta)

SUPERVISOR: Dr. T. J. Kennett

NUMBER OF PAGES: vii, 155

SCOPE AND CONTENTS:

The development of a unified system for the automatic neutron activation analysis of large numbers of samples is described. The realization of the system entailed the automation of a gamma ray spectrometer system by means of a data and control link to a small computer (PDP-15) and the development of a reliable and fast data reduction algorithm suited to the small computer system. A detailed study of the algorithm and the errors associated with it has been included.

ACKNOWLEDGEMENTS

Thanks are extended to all of may associates for their assistance in the completion of this work. In particular I would like to thank my supervisor, Dr. T.J. Kennett, for his insight and advice on the more difficult aspects of the work. Discussions with Mr. A. Robertson and Dr. W.V. Prestwich have been of great value and are highly appreciated. I am grateful to Mr. J. Skene and Dr. F. Vajda for their assistance with the electronics, and to my wife, Hilary, for the typing of the manuscript.

TABLE OF CONTENTS

TABLE OF CONTENTS (cont.)

LIST OF ILLUSTRATIONS

LIST OF ILLUSTRATIONS (cont)

CHAPTER I

INTRODUCTION

In recent years the growing concern over pollution and environmental protection has precipitated a need for an economical and convenient method of performing elemental analysis on large numbers of samples. It is believed that in many cases neutron activation analysis will provide a viable answer to this need.

The neutron activation process involves irradiating the sample to be analysed in a thermal neutron flux. The stable nuclei of the sample are removed from the line of stability (Fig. 1a) by absorbing thermal neutrons. The resulting nuclei are liable to be β^- unstable and return to the line of stability via the reaction.

$$n \longrightarrow p + e^- + \bar{\upsilon}_e$$

Typical lifetimes for β decay are 1.0 to 10^9 seconds. The resultant nucleus (which has atomic number one greater than the original) is often left in an excited state. The quantum nature of the atomic nucleus results in the establishment of discrete energy levels within the nuclear structure and a

Fig. 1a

Line of Stability

The stable nuclei tend to cluster around the line indicated on the graph. The inset shows the process of neutron capture and subsequent β decay.

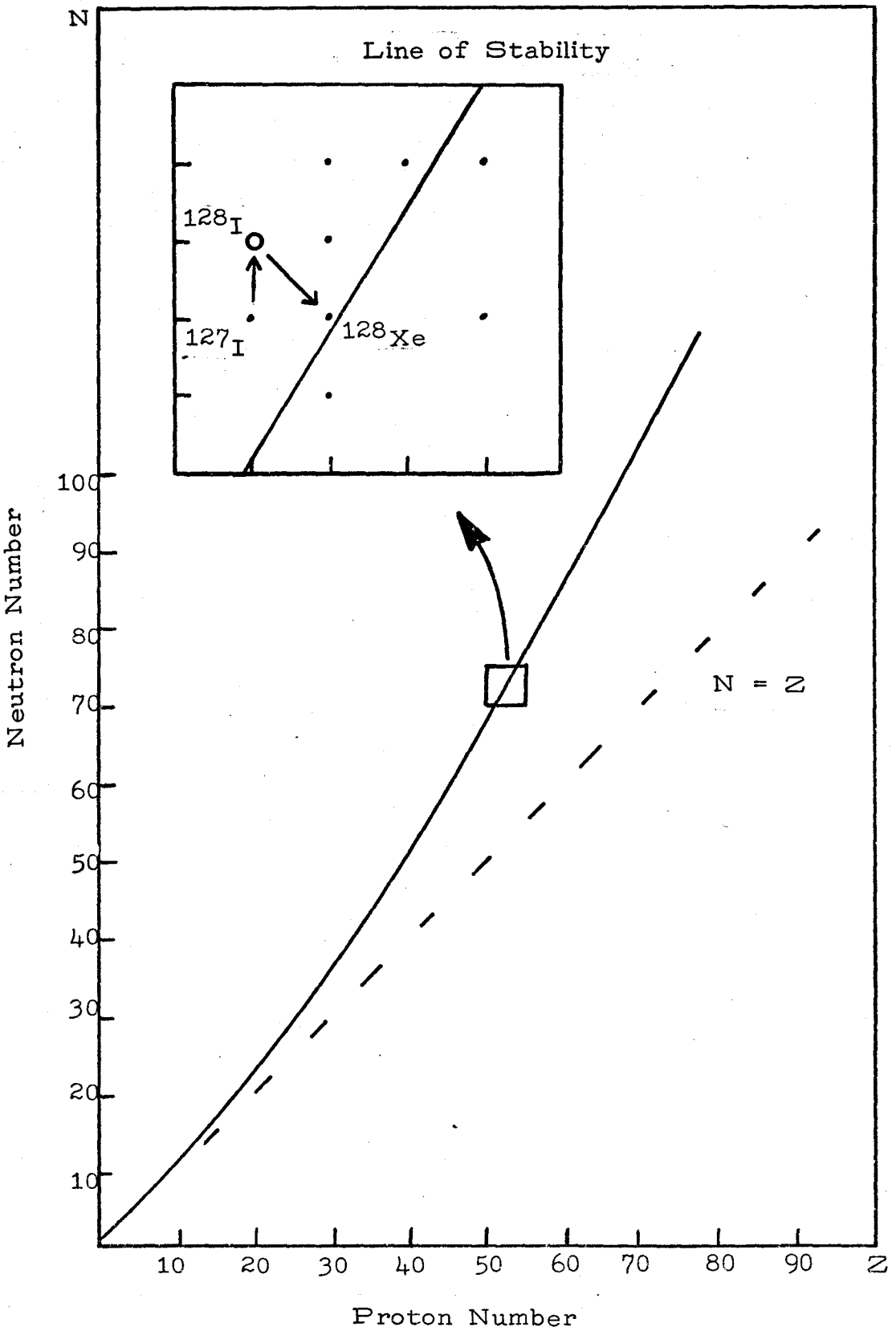
N
Line of Stability
^{128}I
^{127}I
^{128}Xe
100
90
80
70
60
50
40
30
20
10
Neutron Number
N = Z
10
20
30
40
50
60
70
80
90
Z
Proton Number

nucleus in an excited state will usually decay to its ground state by emitting its energy in the form of one or more gamma rays, also of discrete energies. Although long lived states do occur the half life for this process is much shorter than for the β decay process. The typical range is from several pico-seconds to several microseconds. The gamma ray energies are determined by the difference between energy levels of the decaying nucleus and the intensities by the probability that the transition will occur. As each isotope has a distinct and unique structure the de-excitation spectrum of each isotope will likewise be unique. Hence neutron activation provides a source of excited nuclei which may be identified from their decay spectrum. If, after irradiation, the sample under analysis contains more than one radioactive isotope the decay spectrum of each of these constituents will be superimposed and may be identified from the observed spectrum. Further, it is possible to relate the intensity of each component of the spectrum to the actual amount of source material present.

The typical neutron activation analysis procedure is depicted in Fig. 1b. The procedure is shown as being broken into the two major blocks: "Data Acquisition" and "Data Reduction". The topic of the present work is the automation of these two stages in order to provide a unified

Fig. 1b

The Activation Analysis Procedure

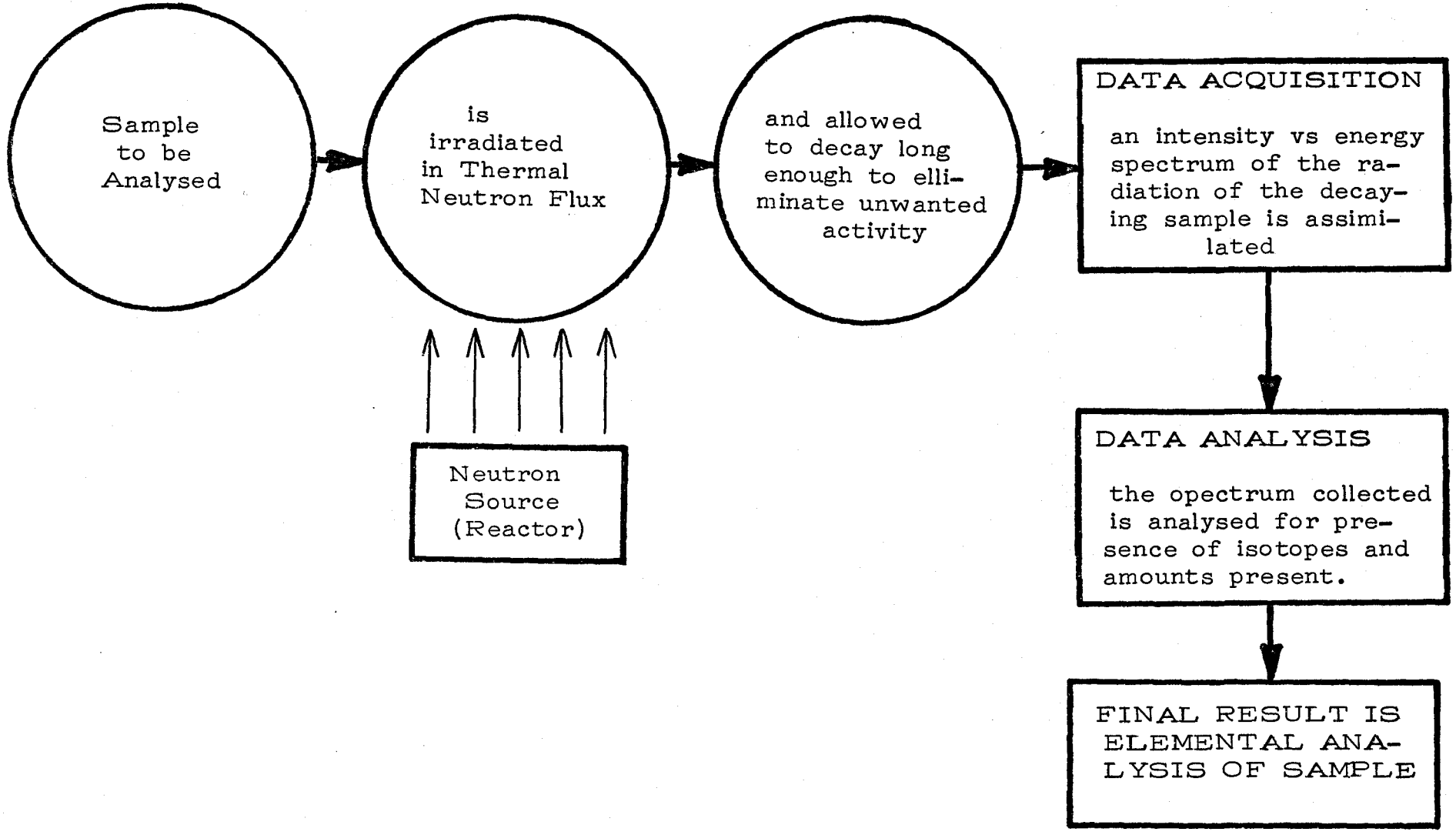
Sample to be Analysed
is irradiated in Thermal Neutron Flux
and allowed to decay long enough to eliminate unwanted activity
DATA ACQUISITION
an intensity vs energy spectrum of the radiation of the decaying sample is assimilated
Neutron Source (Reactor)
DATA ANALYSIS
the opectrum collected is analysed for presence of isotopes and amounts present.
FINAL RESULT IS ELEMENTAL ANALYSIS OF SAMPLE

facility for neutron activation analysis. The data acquisition stage and its automation are discussed in Chapter II and Appendix A. The implementation of the data reduction stage required the development of a new algorithim. The presentation and a discussion of the testing of this algorithim is included in Chapters III and IV.

CHAPTER II

THE DATA ACQUISITION SYSTEM

The data acquisition system includes the radiation detector, the pulse height analyser, the data storage system and the data output device. In order to resolve the gamma ray energies of multi-constituent samples the resolution capabilities of either of two lithium drifted germanium (Ge(Li)) detectors may be used. One of these offers 3 keV resolution at 1.17 MeV and is in demand for several other applications as well. The other is more available, however is capable of only 5 keV resolution. A brief description of the operation of these detectors is included in Section 2.1. The pulse height analysis system consists of a FET preamplifier (CI-1408) a double delay line (DDL) spectroscopy amplifier (CI-1417) and a Nuclear Data analog to digital converter (ND-161 F) which feed a Nuclear Data 4-K memory unit (ND-160 M). The operation of these components is described in Section 2.2. Data is output directly to a PDP-15 computer via a data and control interface described in Section 2.3 and Appendix A. The present PDP-15 facilities include 8-K of core storage, 256-K drum storage, a 7-track magnetic tape drive, fast and slow paper tape readers and punches, a teletype, a graphic display ter-

minal, a CRT display and numerous peripheral devices including the data acquisition system described above. The computer facilities are being expanded.

2.1 The Germanium Detector.

The introduction of the lithium drifted germanium detector in 1963 by Tavendale and Ewan (Tav-20) was a large step forward in nuclear spectroscopy. The device in prior use was the NaI(Tl) scintillation detector whose resolving capabilities are of the order of 100 keV (FWHM) at 1 MeV. Typical Ge(Li) detectors have resolution capabilities between 2 keV and 8 keV (FWHM) at 1 MeV. The increase in resolution is greater than an order of magnitude. As will be seen in Chapter III a high degree of resolution is required for accurate quantitative neutron activation analysis.

The detector consists of a reverse biased gallium doped P-I-N junction with a large intrinsic region provided by the lithium drifting technique (Wal-21). Since about 3eV is required to form an ion pair in the intrinsic region approximately 3.4×10^5 ion pairs will be formed with the capture of a 1 MeV gamma ray. These ion pairs are swept quickly out of the intrinsic region by the high reverse bias ($\sim$1000 Volts) and the resulting current pulse is integrated and amplified by a FET preamplifier. Fig. 2.1a shows an idealized detector.

Fig. 2.1a

An Ideal Ge(Li) Detector

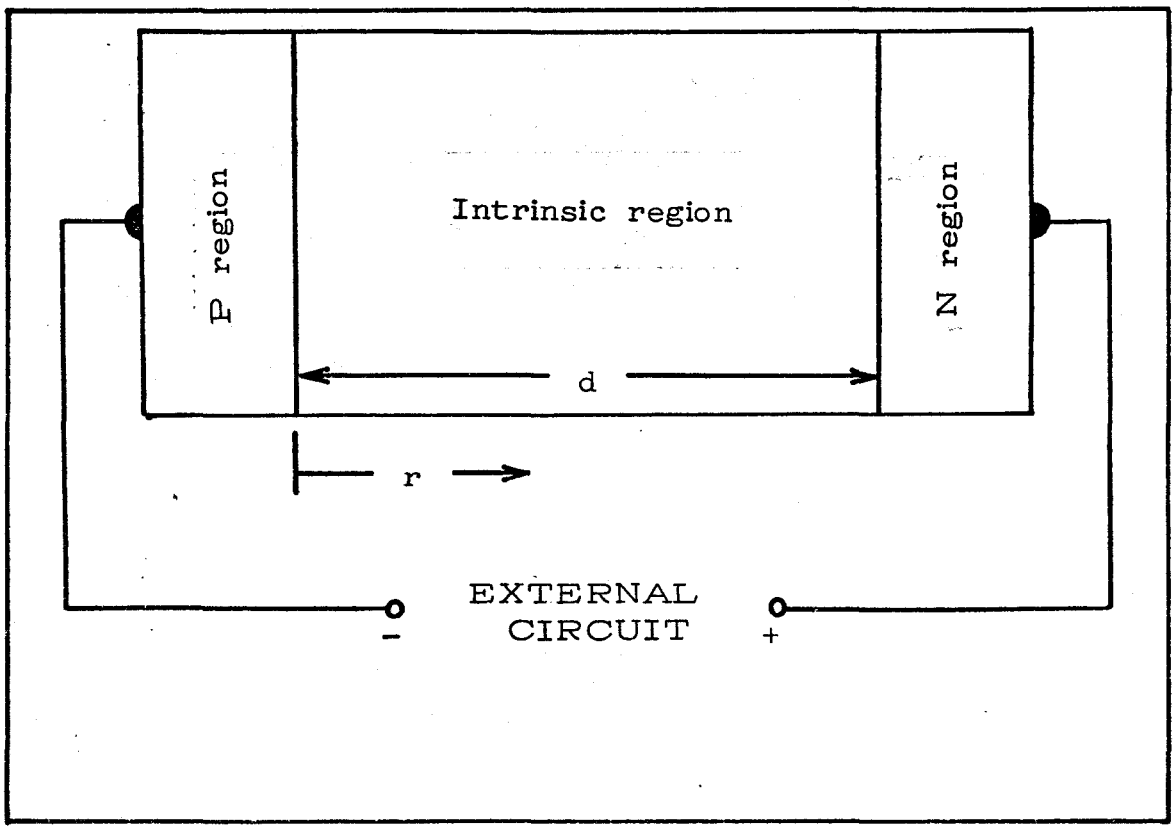

Fig. 2.1b

Charge Collection for Ideal Detector

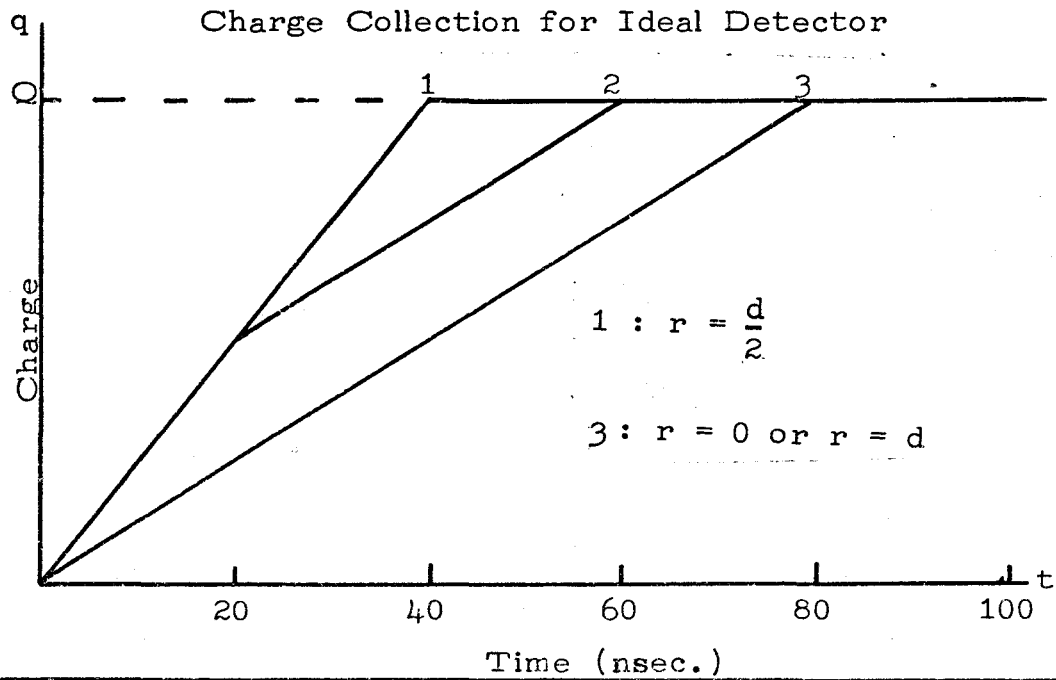

The form of the charge collection pulse will depend upon where in the intrinsic region the ion pairs are formed. Fig. 2.1b shows typical charge collection functions for the ideal detector. Fig. 2.1c shows the output of the preamplifier. This signal, whose height is proportional to the energy deposited in the counter by the gamma ray, is fed into a double delay line spectroscopy amplifier resulting in an output signal as shown in Fig. 2.1d. This signal also will have a height proportional to the energy deposited in the detector by the incident gamma ray.

2.2 The Pulse Height Analyser.

The pulse shape from the DDL amplifier (Fig. 2.1d) is an appropriate form for input to the Nuclear Data (ND-161 F) analog to digital converter (ADC). The ADC is a 12-bit Wikinson type converter. The input pulse is converted into a time duration proportional to its height and a 16 MHz clock feeds a 12-bit address scaler for this time duration. Thus the number in this scaler will be proportional to the energy which was originally deposited in the Ge(Li) detector. The digital output of the ADC is used to select a specific memory location or "channel" in the associated ND-161 M memory-arithmetic unit. The number in this channel is then increased (or decreased) by one count to tally the event of a deposition of

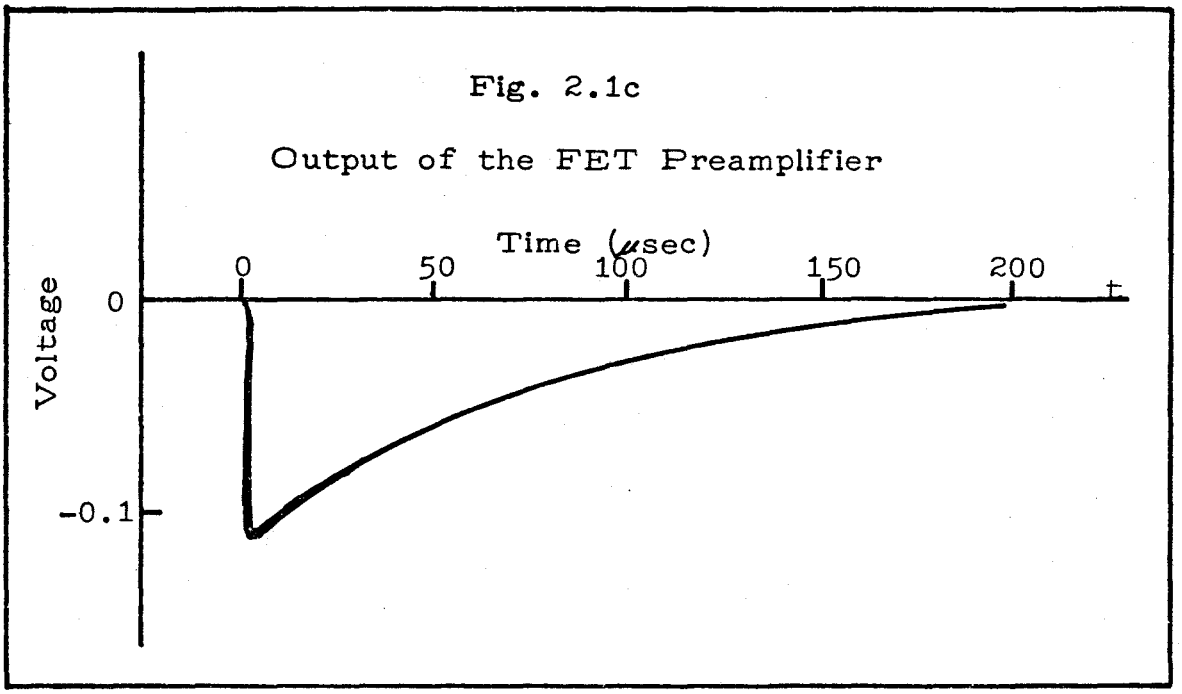

Fig. 2.1c

Output of the FET Preamplifier

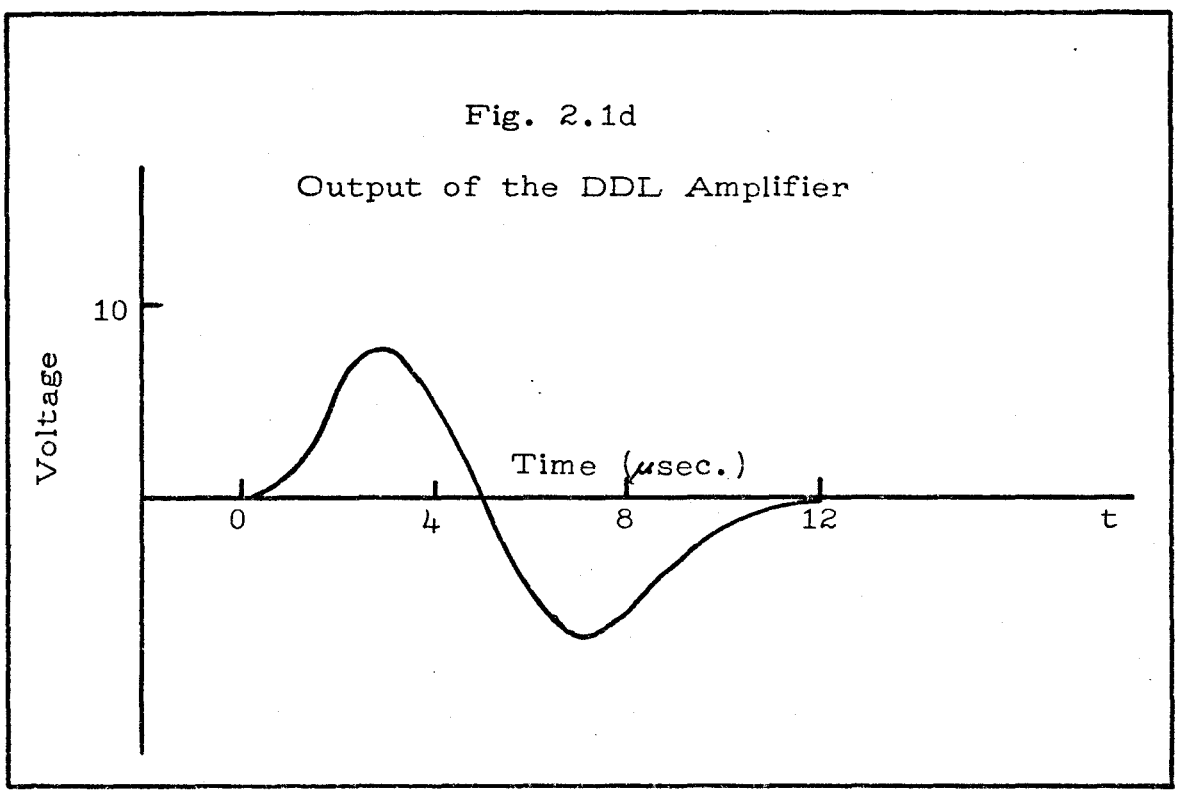

Fig. 2.1d

Output of the DDL Amplifier

a corresponding energy in the Ge(Li) detector. Thus the gamma ray spectrum is accumulated in the memory unit, the channel number being proportional to energy and the contents proportional to the intensity of the corresponding energy. Spectrum stabilization may be included if desired by using two spectral peaks as stabilizer references or by feeding a dual reference pulser into the "test" input provided on the pre-amplifier. The stabilizers automatically adjust the zero and gain of the ADC in order to maintain a constant centroid position for the reference peaks. Generally reference peaks which bracket the region of interest are selected. Fig. 2.2a is a block diagram of the analyser system.

2.3 The Interface.

To facilitate the practicality of the analysis method and minimize analyst interaction a direct data and control link to a PDP-15 computer was designed and built. A detailed description of the interface including operating instructions, software description and schematics is included in Appendix A. The data link was designed to facilitate bi-directional block data transfers between the ND-160 M unit and the PDP-15 computer. This makes it possible to process the data immediately or to output the data on any of the peripherals associated with the PDP-15. The bi-directional nature of the

Fig. 2.2a

An Analyser System

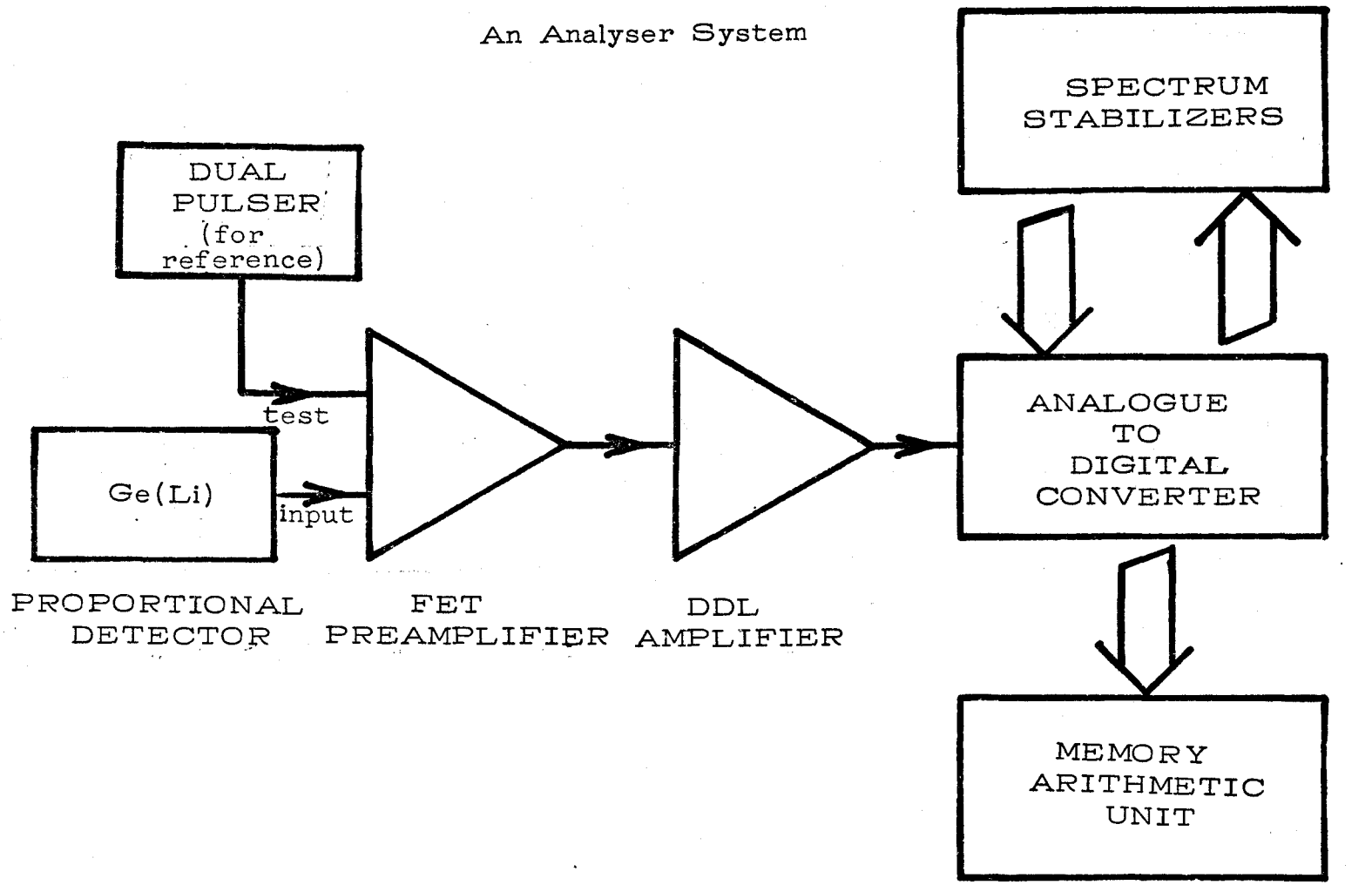

data link effectively provides the computer with an additional 4-K of memory which is sequentially accessible via its accumulator. This proves to be exceptionally practical for the method of data analysis described in Section 3.2. The more important analyser control functions (ANALYSE, STOP, READOUT, etc.) we re also interfaced to the computer to allow completely automatic analysis.

CHAPTER III

DATA ANALYSIS TECHNIQUE

3.1 Automatic Activation Analysis.

3.1.1 Quantitative Spectral Analysis.

In general the neutron activation Ge(Li) spectrum consists of a number of more or less Guassian peaks ("lines") on a roughly exponential background (Fig. 3.1.1a). The manual method of analysis involves establishing the source of each line and its intensity. Usually there are several possible sources which could fit each line; however each of these sources will likely be associated with several other lines and a cross referencing technique will establish the actual source. In the case the line is due to more than a single source the cross reference will determine the extent of the interference. The actual amount of the constituent isotopes may then be found either by comparison of the intensities (peak areas) with the intensities derived from analysis of a known quantity of that isotope or by knowing the cross section, neutron flux and efficiency of the detection system. Usually, for ease of calculation, peaks in which interferences between isotopes occur are omitted from the analysis. It will be seen quite

Fig. 3.1.1a

A Typical Neutron Activation Analysis Spectrum

Observed With A Ge(Li) Detector

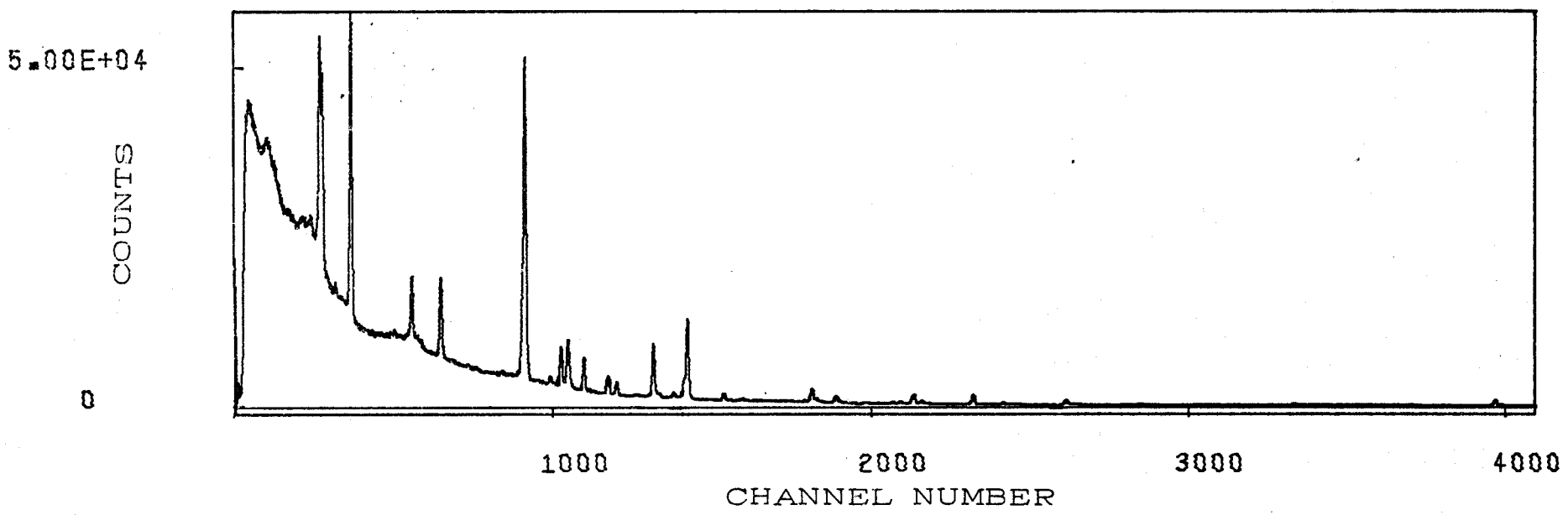

clearly how the manual method of peak identification, cross reference and peak area determination has had a strong influence on the automatic and computer assisted methods of activation analysis available.

3.1.2 Methods Involving Peak Extraction.

Computerized methods of activation analysis relying on peak extraction procedures have developed from two directions. Since the manual method relies on individual peak identification it is natural that computer aided and totally automated schemes would develop in the same way. Other schemes have been adapted from peak finding programmes in use for other purposes. However developed, automatic peak search and fitting programmes and analysis methods which apply them are abundant in the literature (Mar-1, Bow-2, Rob-3, Rou-4, Var-5, Kos-6, Gos-7, Sla-8, Con-9, Ino-10) as are discussions of relevant aspects of peak fitting procedures (Tom-11, Hea-12, Qui-13, Cas-14). Analysis methods involving peak extraction have some advantage in the versatility they allow by giving centroids, areas and widths of peaks. Such quantities as these are of interest to physicists and others for a variety of reasons. Unfortunately there is a price to pay for this wider range of applicability.

Although there is at least one notable exception (Rob-3), most peak extraction methods involve a least squares fit of some chosen line shape to each peak and surrounding background. These often require a large amount of work on the part of the analyst in setting up first guesses of peak positions, heights, and widths. Further, the choice of a suitable line shape is not a trivial problem as evidenced by the variety of functions used in the literature (Mar-1, Bow-2, Rou-4, Var-5, Kos-6, Gos-7, Sla-8, Con-9). The line shape problem is complicated by the fact that the actual peak shape is a function of several parameters including the counter being used, the energy scale, the count rate, and the detector voltage. Another serious difficulty is that the fitting procedure is a lengthy process in terms of computer central processor (CPU) time. Those routines which economize on CPU time also tend to sacrifice accuracy or reality in the line shape fitted to the peak (Bow-2). One of the most complete peak extraction routines is described by Routti and Prussian (Rou-4). They list eight points which a "good" analysis programme must achieve.

1: The method must be programmed to perform an automatic data analysis (i.e. a minimum requirement of analyst interaction).

2: The method should be capable of handling data measured under a wide variety of experimental conditions, including variable statistics, variable systems gains and detectors of different sizes and quality.

3: The method should be capable of analysis of spectra of high complexity, and no prior knowledge of spectral components should be required. Provisions should be included for recognition and analysis of closely spaced spectral lines (multiplets).

4: The calibration data, if required, should be readily available.

5: The results of the analysis should include gamma ray energies and intensities and the lifetimes of measured lines.

6: The analysis should include calibration procedures for determining energy and efficiency.

7: The accuracy of the results should be as good as the statistics of the data and the calibration information permit.

8: The computation procedures should be efficient enough to make the method feasible for routine analysis using available computer capacities.

If all of these conditions could be met the procedure would be hard to improve upon. Unfortunately condition 8 tends to conflict with most of the other conditions set. The

line shape which the authors chose in this case was a Gaussian with exponential tails matched so that the function and its first derivative are continuous. A straight line approximation is applied to the background continuum. The analyst must choose a number of peaks for energy and line shape calibration data for each different experimental set up, and check the resulting fit for accuracy and omissions by examining a residual spectrum.

The fully automated peak extraction programme must include a peak search routine which will identify those data patterns which represent peaks with a great deal of reliability. The best of these routines are described by Inouye (Ino-10), Mariscotti (Mar-1), and Robertson (Rob-3). Inouye's method involves deleting components in Fourier space in order to achieve smoothing. Mariscotti's method (which is the one used by Routti) is a "smoothed second difference" method and Robertson applies a zero area filter to the spectrum in square root space. The last two methods are attractive because they require relatively little CPU time and elliminate constant and linear background components. The last is extremely attractive because the use of the square root results in a constant noise band and allows discrimination levels to be set very easily.

Having achieved a complete spectral analysis by the method of Routti, or a similar code, it is then necessary to refer to a look-up table and match each line with its proper source. Cross referencing is required to ensure all peaks are present for a given element and that the peaks are of the appropriate heights. This ensures that no unresolved doublets are present. In the case that a quantitative analysis is required the activities of each of the source elements are determined by means of an efficiency calibration of the detector. Then, with a good knowledge of the thermal neutron cross section of the element and the half life of the product, the flux of irradiation and the detector efficiency, the elemental abundance may be determined. It is customary to elliminate the need for flux, cross section and efficiency measurements by irradiating and analysing standard amounts of the elements of interest. If this procedure seems long and complicated, it must be remembered that it is identical to the manual method of analysis.

3.1.3 Methods Involving Combinational Techniques

A second class of analysis methods have developed from the premise that any complex spectrum is a linear superposition of several spectra, each due to a single isotope. (Tan-15, Eck-16, Bla-17)

$$s(E) = \sum_{i=1}^{N} k_i b_i(E) \qquad (1)$$

$s(E)$ represents the complex spectrum and the $b_i(E)$ represents the spectra due to a unit of the i-th isotope. The k_i then represents the weight of the i-th isotope present in the sample. The method delineated in Section 3.2. follows these lines. These methods are derived by minimizing the quantity

$$\int_E W^2(E)\left(s(E) - \sum_{i=1}^{N} k_i b_i(E)\right)^2 dE$$

with respect to the parameters k_i. All these methods reduce to the problem of solving a set of simultaneous linear equations. Tanner et al (Tan-15) are at a strong disadvantage here as they must solve a system of K+1 equations where K is the number of channels in the spectrum. Thus they are forced to reduce the analysis to only those channels containing the most important peak of the component for which they are analysing. Statistical errors are thus increased and analysis for more than one component at a time is not practical. Eckhoff (Eck-16) and Blackburn (Bla-17) fare somewhat better as they reduce the problem to N linear equations where N is the number of isotopes in equation (1). The only difference between the two methods is the method each uses to solve the set of equations. Eckhoff preferring the matrix notation from beginning to end uses a matrix inversion formula.

Blackburn, taking the simultaneous equations viewpoint, prefers an equivalent solution in terms of determinants. All three methods involve the use of a non-constant "weighting" function W(E), and all suffer from the problem of non-orthoganality of unknown components discussed in Section 3.2.1. These methods, while saving greatly on CPU time also lose the versatility mentioned in conjunction with peak extraction processes. This is not liable to be a detriment however if the system is to be dedicated to elemental analysis. Further, for such a dedicated system the analyst is interested only in the amount of the constituents in his sample and has no interest in the energies and intensities of particular lines or efficiencies of detection. In fact the analyst has no interest in even the mechanism of analysis other than as it may be used as a tool and the less he is required to know to operate the tool, the better the tool is. Clearly Routti's rules 5 and 6 (Rou-4) are not applicable to such a "black box" system of analysis.

3.2 The Present Method.

3.2.1 The Cross Correlation Technique

Any spectra to be analysed in terms of its constituents will hopefully obey a linear superposition principle. This is the case for gamma-ray spectra arising from radio-isotopes

as well as most other spectral types. Certain non-linear effects do occur in the detection procedure and these are discussed in Section 3.3.4. The primary assumption is:

$$s(E) = \sum_{i=1}^{N} k_i b_i(E) \qquad (1)$$

where the function $s(E)$, the sample spectrum, is taken as being the superposition of the functions $b_i(E)$, the spectra of one unit of each of the sample's constituents taken alone. The weighting factors k_i then are the amounts of the constituents in the sample.

In the case where all "N" of the $b_i(E)$ are known it is possible to resolve $s(E)$ in terms of the $b_i(E)$ as follows.

Consider the N-vector $\{v_i\}_N$ defined by:

$$v_i \equiv s(E) \circ b_i(E)$$

where the inner product is defined in the usual way:

$$s(E) \circ b_i(E) = \int_E s(E) b_i(E) \, dE$$

in the continuous case, or:

$$s(E) \circ b_i(E) = \sum_{\varepsilon} s(E) b_i(E)$$

for the discrete case. Applying equation (1) we find

$$v_i = \left(\sum_{j=1}^{N} k_j b_j(E) \right) \circ b_i(E)$$

$$= \sum_{j=1}^{N} k_j b_j(E) \circ b_i(E)$$

$$= \sum_{j=1}^{N} k_j C_{ji}$$

where C_{ji} is defined by

$$C_{ji} = b_j(E) \circ b_i(E) = C_{ij}$$

In matrix notation

$$\vec{v} = \vec{k} \circ \underline{C}$$

or

$$\vec{k} = \vec{v} \circ \underline{C}^{-1}$$

Finding the amount of each constituent then becomes simply a matter of inverting the matrix $\underline{C}$. The method can be shown to be identical to an unweighted least squares fit

Section (3.2.3). It is noted that the inner product between two spectra is identical to their cross correlation at zero lag. The cross correlation is

$$d(r) = \int_E s(E+r)b_i(E)\,dE$$

where "r" specifies the lag.

The greatest difficulty with this method of analysis is the rigid requirement that all of the constituent spectra be known and included in the calculation. Most real sample groups will consist of a number of constituents common to the group and large number of possible "unexpected" constituents. The vectorial viewpoint is adequate to examine the effect of omitting these unexpected spectral contributants from the analysis. The degree of orthogonality of two vectors $\vec{A}$ and $\vec{B}$ is defined as

$$d_o \equiv \frac{(\vec{A}\circ\vec{B})(\vec{B}\circ\vec{A})}{(\vec{A}\circ\vec{A})(\vec{B}\circ\vec{B})} \qquad (2)$$

and may be identified with $\cos^2\theta$ in the geometrical case. We may rewrite equation (1) as

$$\vec{s} = \sum_{i=1}^{N} k_i\vec{b}_i + \sum_{i=N+1}^{M'} k_i\vec{b}_i \qquad (3)$$

$\vec{s}$ is a linear combination of the M' basis vectors, $\vec{b}_i$, and we are trying to resolve the components k_i $(1 \leq i \leq N)$ without any knowledge of the vectors $\vec{b}_i$ $(N < i \leq M')$ (the unexpected constituents). In the usual geometrical case we deal with an ortho-normal set of basis vectors and any component of a general vector is simply the projection of that vector along the corresponding basis vector (Fig. $3.2.1a_i$). It is clear that in such a case no knowledge of the unexpected constituents is required in order to determine the desired components. In the present case however the basis set is not orthogonal and hence interference between the basis vectors are liable to occur (Fig. $3.2.1a_{ii}$). If we let the unknown components in equation (3) $\vec{b}_i$ $(N < i \leq M')$ be represented by $\vec{d}_i$ $(1 \leq i \leq M)$ we may rewrite (3) as

$$\vec{s} = \sum_{i=1}^{N} k_i \vec{b}_i + \sum_{i=1}^{M} l_i \vec{d}_i$$

where $l_i = k_{i+N}$.

Following through with the analysis in the same way as before we arrive at the matrix equation

$$\begin{pmatrix} \vec{v} \\ \vec{w} \end{pmatrix} = \begin{pmatrix} \vec{k} \\ \vec{l} \end{pmatrix} \left(\begin{array}{c|c} \vec{b}\cdot\vec{b} & \vec{b}\cdot\vec{d} \\ \vec{d}\cdot\vec{b} & \vec{d}\cdot\vec{d} \end{array} \right) \qquad (4)$$

Fig. 3.2.1a

A simple example: Resolution of a two dimensional vector in terms of only one basis vector.

a_i - When the basis vectors are orthogonal

a_{ii} - When the basis vectors are non-orthogonal

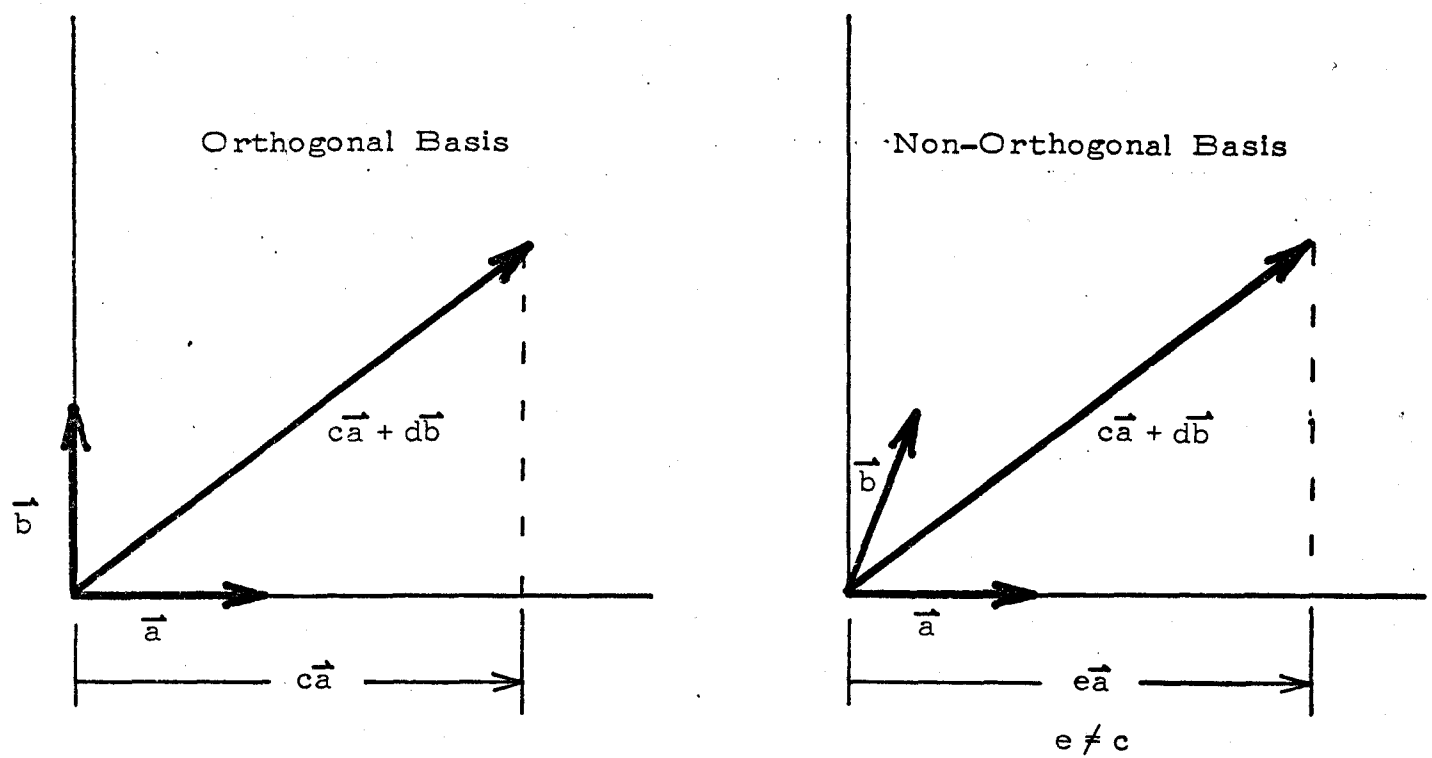
Orthogonal Basis
$c\vec{a} + d\vec{b}$
$\vec{b}$
$\vec{a}$
$c\vec{a}$
Non-Orthogonal Basis
$c\vec{a} + d\vec{b}$
$\vec{b}$
$\vec{a}$
$e\vec{a}$
$e \neq c$

where $\vec{w} = \{w_i\} = \{\vec{s} \circ \vec{d}_i\}$ $(1 \leq i \leq M)$ and $\vec{b} \circ \vec{b}$ represents all the cross correlation terms between the known vectors, $\vec{d} \circ \vec{d}$ represents all the cross correlation terms between the unknown vectors and $\vec{d} \circ \vec{b}$ and $\vec{b} \circ \vec{d}$ represent all the cross correlation terms between the known and unknown vectors. It is clear that it is not possible to invert the matrix without a precise knowledge of the vectors $\vec{d}_i$. The orthogonality of a pair of vectors is represented by a zero entry in the corresponding locations of the cross correlation matrix. In the case that each vector, $\vec{d}_i$, is orthogonal to every vector, $\vec{b}_i$, the off diagonal matrices of equation (4) are zero and the equation becomes

$$\begin{pmatrix} \vec{v} \\ \vec{w} \end{pmatrix} = \begin{pmatrix} \vec{k} \\ \vec{l} \end{pmatrix} \left(\begin{array}{c|c} \underline{C} & 0 \\ \hline 0 & \underline{D} \end{array} \right)$$

where $\underline{C} = \vec{b} \circ \vec{b}$ and $\underline{D} = \vec{d} \circ \vec{d}$. This breaks into the two independent matrix equations

$$\vec{v} = \vec{k} \circ \underline{C} \tag{5}$$

and

$$\vec{w} = \vec{l} \circ \underline{D} \tag{6}$$

Naturally equation (6) can not be solved as neither $\vec{w}$ nor $\underline{D}$ are known, however equation (5) may be solved in the usual

manner.

Thus, ignoring the spectra of the unexpected constituents is equivalent to assuming that they are orthogonal to all the spectra of the desired components. The errors introduced by the lack of validity of this assumption have been analysed in Section 3.3.3 and are shown in Fig. $3.3.3_a$. Table $3.2.2f_i$ shows typical orthogonality data for Ge(Li) spectra. Together these illustrate the undesirability of neglecting any possible constituent in the sample. On the other hand, if all possible constituents are considered "N" will be rather large and the inversion of the matrix $\underline{C}$ will be a lengthy and inaccurate task for even a large computer. Thus the major problem of the cross correlation technique is seen to be the non-orthogonality of the basis vectors. For maximum orthogonality then we require the inner product of the normalized spectra to be close to zero. Recall that this is

$$A \circ B = \int_E \hat{A}(E)\hat{B}(E)\,dE$$

Both $\hat{A}$ and $\hat{B}$ in the present case are positive definite and consist of peaks riding on a relatively large smooth background. For spectral analysis most of the relevant information is contained in the peaks and relatively little in the background. Since the background is the major non-orthogonality contributant to $\hat{A} \circ \hat{B}$ it is desirable to elliminate it.

This could be achieved by the subtraction of a fit to the background although this method has some disadvantages. First, the background fit is liable to require a large amount of computing time, depending upon the order and extent of the fit. Further, there could be difficulty insuring that the fitting technique adopted represents a linear operator. Secondly, the resultant spectra still have a net positive area and therefore it is not likely that a high degree of orthogonality will be achieved.

The method of background ellimination selected here involves the use of the zero-area filter described by Robertson et al (Rob-3). The spectra resulting from use of this method have a net area of zero and thus will achieve the state of maximum possible orthogonality. Other advantages of the method such as noise band reduction and maintainence of non-photo peak features of the spectra (Compton edges,

back scatter peaks etc.) make the method most attractive.

3.2.2 The Zero Area Filter

In order to elliminate "background" or low frequency components from the spectrum, a convolution of the data with a symmetric "filter" function is conducted. The filter function has a net area of zero and is intended to closely resemble the spectral line shape involved. It can be shown that the signal to noise ratio of the spectrum is optimized if the filter is identical to the shape of the signal (optimum filter, Appendix B.1). Since the line shape is approximately Gaussian this would seem the ideal filter to use, the width being determined by the peak width of the corresponding spectrum. However it is found in practice that the calculation of the exponential requires relatively large amounts of central processor time and floating point arithmetic. As a result the selected filter is the rectangular function depicted in Fig. 3.2.2a_i which may be achieved simply by addition and subtraction of points. The two following diagrams (3.2.2a_{ii} and a_{iii}) show two possible forms of Gaussian filters.

The convolution of the spectrum $s(x)$ with the filter $F(x)$ results in the convolute spectrum $S(y)$ as

Fig. 3.2.2a

The three graphs on the following page depict three possible filter functions.

a_i - The chosen filter, the difference of two rectangular filters.

a_{ii} - A limited range Gaussian minus a rectangular function.

a_{iii} - The difference between two Gaussian functions

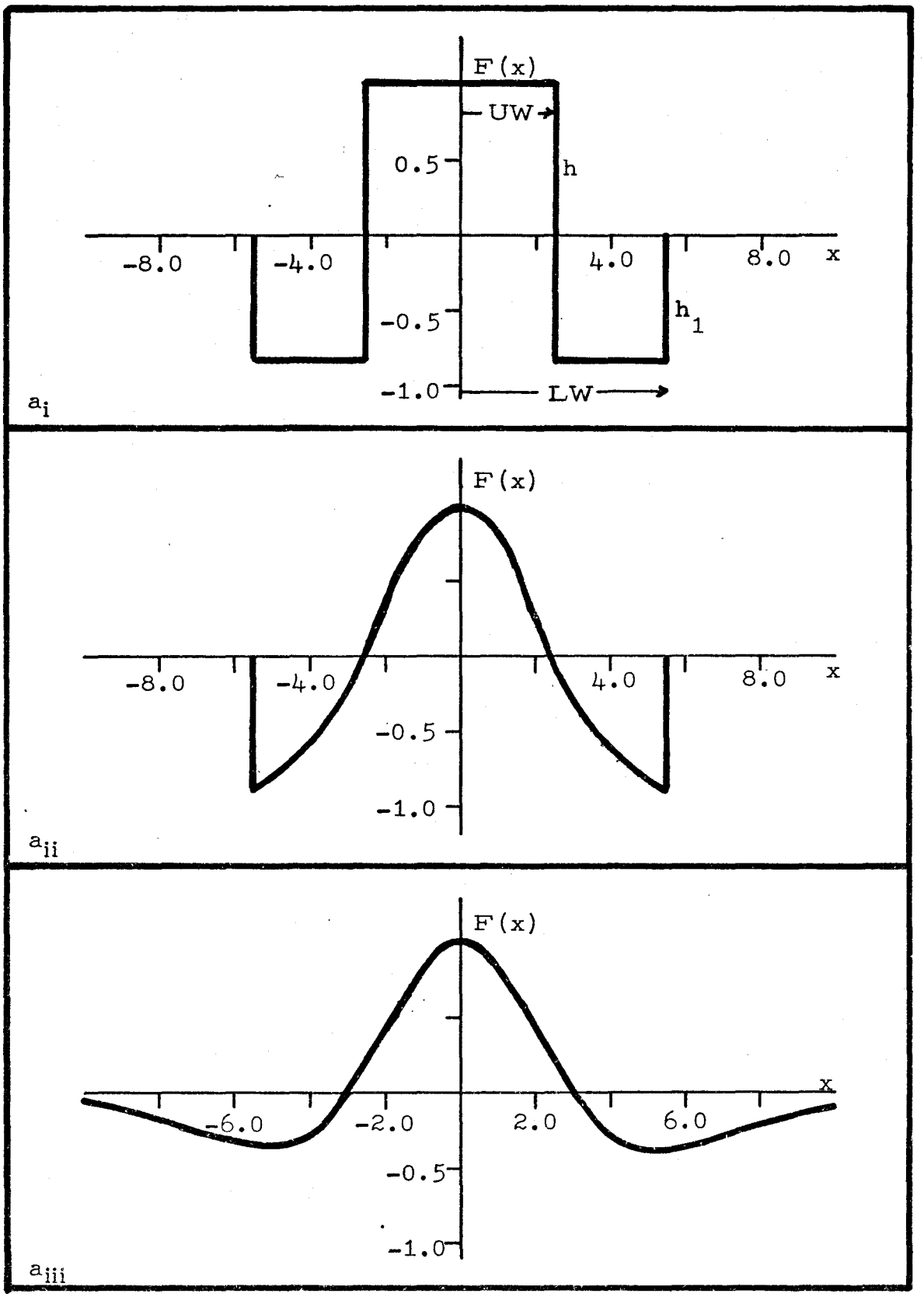
F(x)
UW
0.5
h
-8.0
-4.0
4.0
8.0
x
-0.5
h_1
-1.0
LW
a_i
F(x)
-8.0
-4.0
4.0
8.0
x
-0.5
-1.0
a_{ii}
F(x)
x
-6.0
-2.0
2.0
6.0
-0.5
-1.0
a_{iii}

$$S(y) = \int_{x=-\infty}^{\infty} F(y-x)\,s(x)\,dx$$

or

$$S(y) = \sum_{x=y-p}^{y+p} F(y-x)\,s(x)$$

in the discrete case. The summation need only extend over the non-zero portion of F(x) as indicated by the term "p". Note, as shown below, that the convolute spectrum is independent of constant and first order terms in the original data.

We write the spectrum in terms of its Taylor series

$$s(x) = \sum_{n=0}^{\infty} a_n x^n$$

Then the convolute spectrum becomes

$$S(y) = \int_{x=y-p}^{y+p} F(y-x) \sum_{n=0}^{\infty} a_n x^n dx$$

$$= \int_{x=-p}^{p} F(x') \sum_{n=0}^{\infty} a_n (y+x')^n \, dx$$

$$= \int_{x=-p}^{p} F(x') \sum_{n=0}^{\infty} a_n \sum_{m=0}^{n} \binom{m}{n} x'^m y^{n-m} dx'$$

$$S(y) = \sum_{n=0}^{\infty}\sum_{m=0}^{n} a_n \binom{m}{n} y^{n-m} * \int_{x=-p}^{p} F(x') x'^{m} dx'$$

Since F(x) is an even function the parity of the integrand is determined by the parity of m. As the range of integration is symmetric about zero no odd parity terms will contribute to the summation. Further, for m=0 the integral is simply the area of the filter, in this case zero. Then the summation terms n=0 and n=1 will both be zero since the only contributants to these terms are m=0 and m=0, m=1 respectively. Thus only the terms of second order and higher in n contribute. Since the peak width is narrow ($\sigma \ll E$) for Ge(Li) spectra the background across the corresponding filter width may be considered to be approximately linear and therefore will be elliminated by the convolution. Attention is directed to Fig. 3.2.2b which clearly demonstrates the removal of the background components from the spectrum.

Observation of the filters (Fig. 3.2.2a) in frequency space (Fig.3.2.2c) shows the ellimination of low frequency and high frequency effects. In Fourier space the convolution is

$$S_F(w) = F_F(w) s_F(w)$$

Fig. 3.2.2b

The effect of the zero area rectangular filter on a Ge(Li) spectrum.

b_i - The original spectrum

b_{ii} - The convolute spectrum

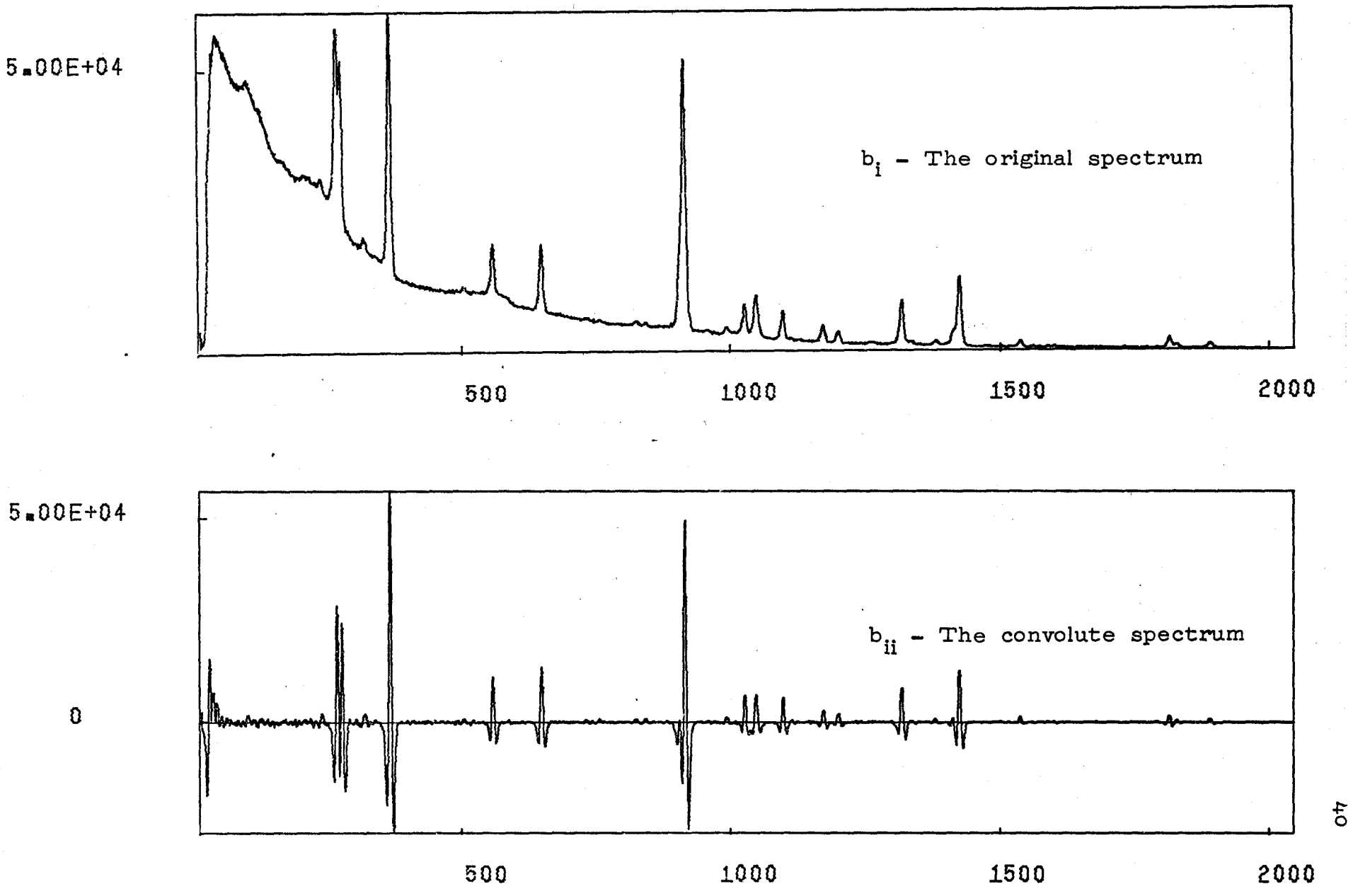
5.00E+04
b_i - The original spectrum
500
1000
1500
2000
5.00E+04
0
b_{ii} - The convolute spectrum
500
1000
1500
2000

Fig. 3.2.2c

Fourier Transforms of Zero Area Filters

c_i - Transform of the rectangular-rectangular filter (Fig. $3.2.2b_i$)

c_{ii} - Transform of the Gaussian-rectangular filter (Fig. $3.2.2b_{ii}$)

c_{iii} - Transform of the Gaussian-Gaussian filter (Fig. $3.2.2b_{iii}$)

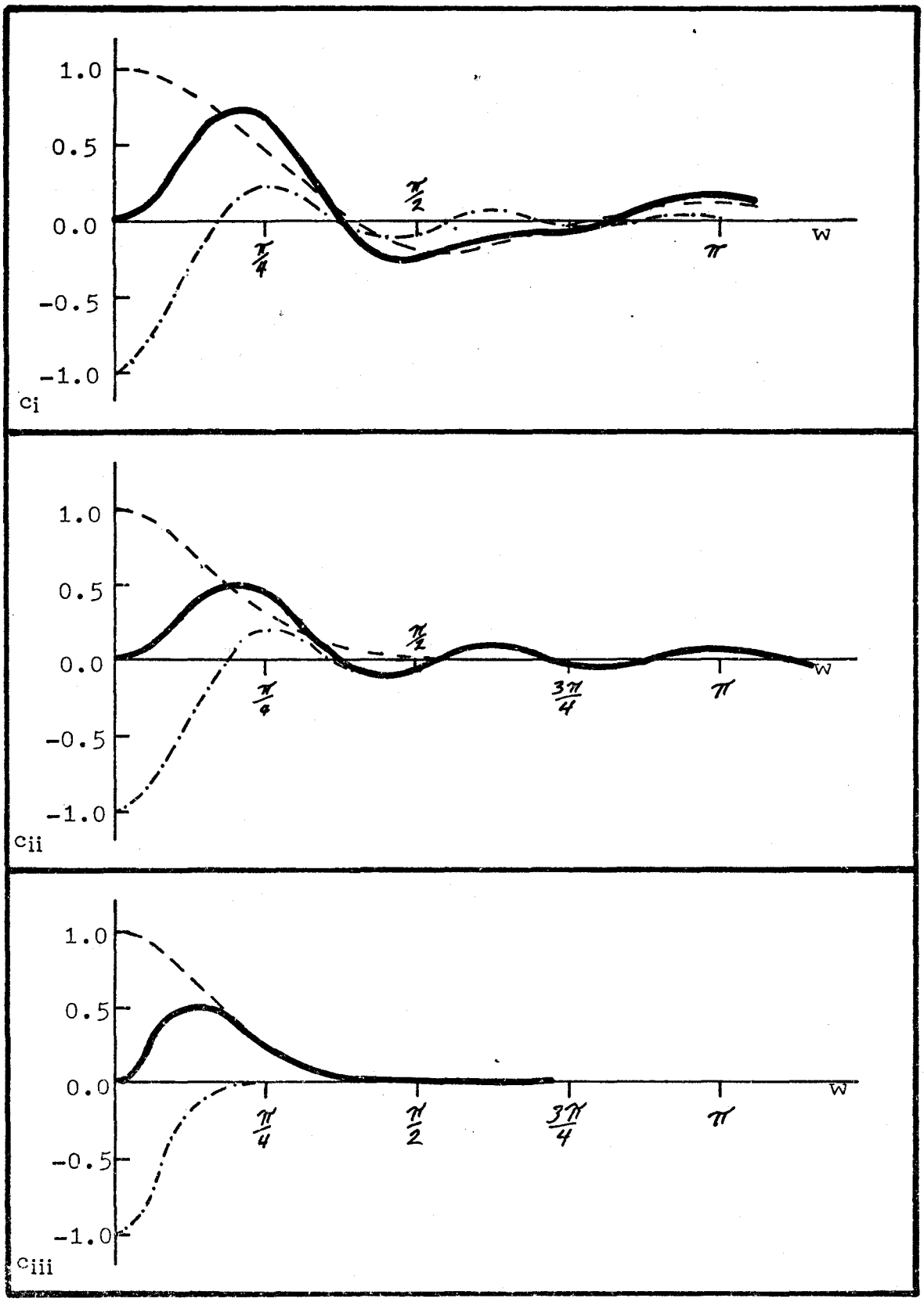
1.0
0.5
0.0
-0.5
-1.0
π/2
π/4
π
w
ci
1.0
0.5
0.0
-0.5
-1.0
π/2
π/4
3π/4
π
w
cii
1.0
0.5
0.0
-0.5
-1.0
π/4
π/2
3π/4
π
w
ciii

where -

$$S_F(w) = \mathcal{F}\, S(y)$$

$$F_F(w) = \mathcal{F}\, F(x)$$

$$s_F(w) = \mathcal{F}\, s(x)$$

The calculation of the Fourier transforms of the filters is performed in Appendix B.2. Work by Robertson (Rob-3) shows the effect of a zero area filter on a simulated peak and Compton edge as well as trends in signal to noise ratio and width of the convolute peak for the rectangular filter. The results of this work are shown in Fig. 3.2.2d and 3.2.2e. As can be seen from these plots the signal to noise ratio is optimized for a filter having an upper width approximately equal to the HWHM of the peak. It is seen also that the greater the lower width the greater the signal to noise ratio. An important consideration here however is the decrease in resolution (increase in ΔW) with increasing lower width. This decrease in resolution implies a decrease in the orthogonality of the spectra. The optimum lower width then will depend upon the quality of the statistics and the degree of orthogonality of the spectral components.

Fig. 3.2.2d

d_i - Simulated peak and its filtered equivalent.

d_{ii} - Simulated Compton edge and its filtered equivalent.

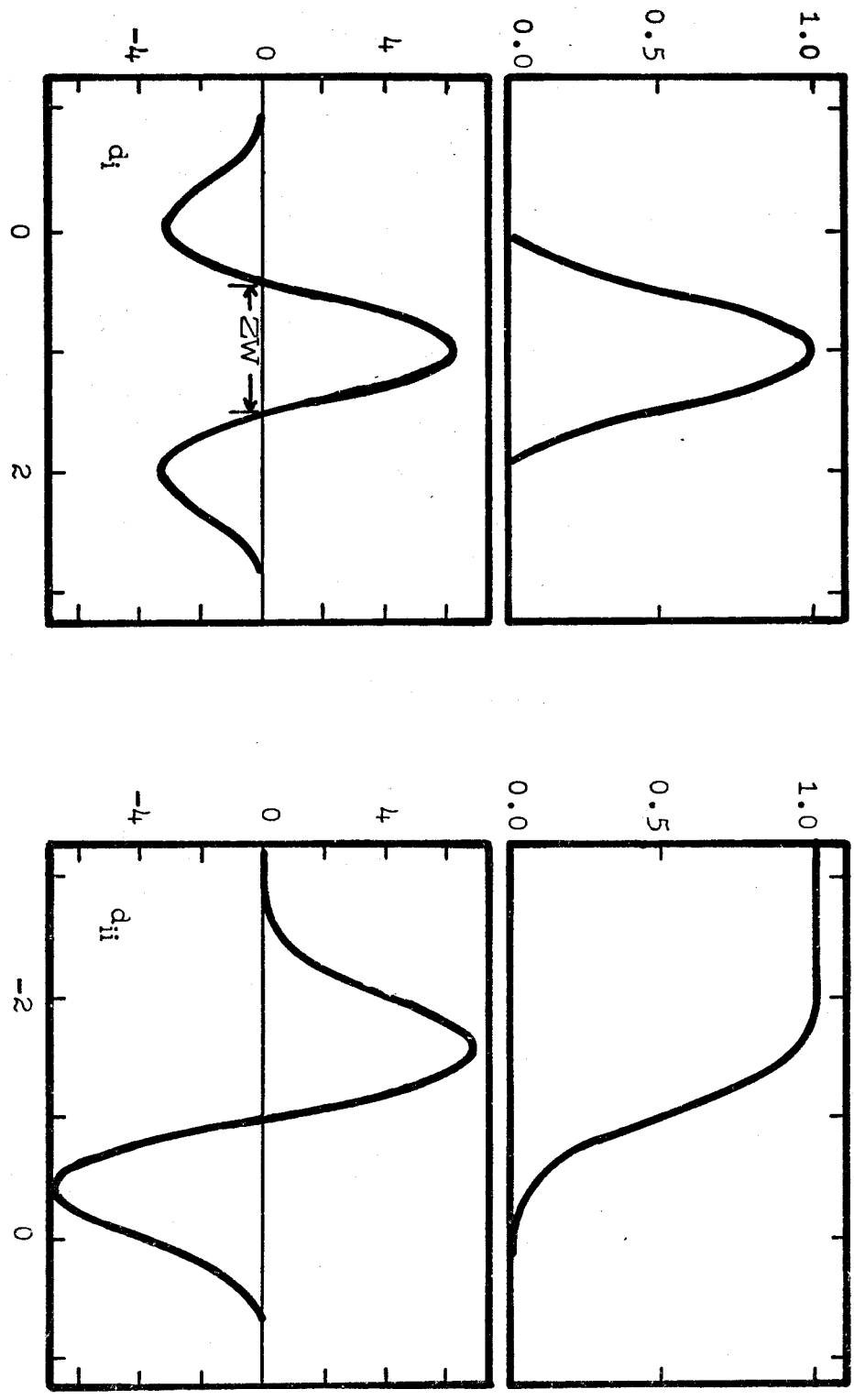
1.0
0.5
0.0
4
0
-4
d_i
2W
0
2
d_{ii}
-2

Fig. 3.2.2e

e_i - Convolute Signal to Noise Ratio

e_{ii} - Convolute Peak Width

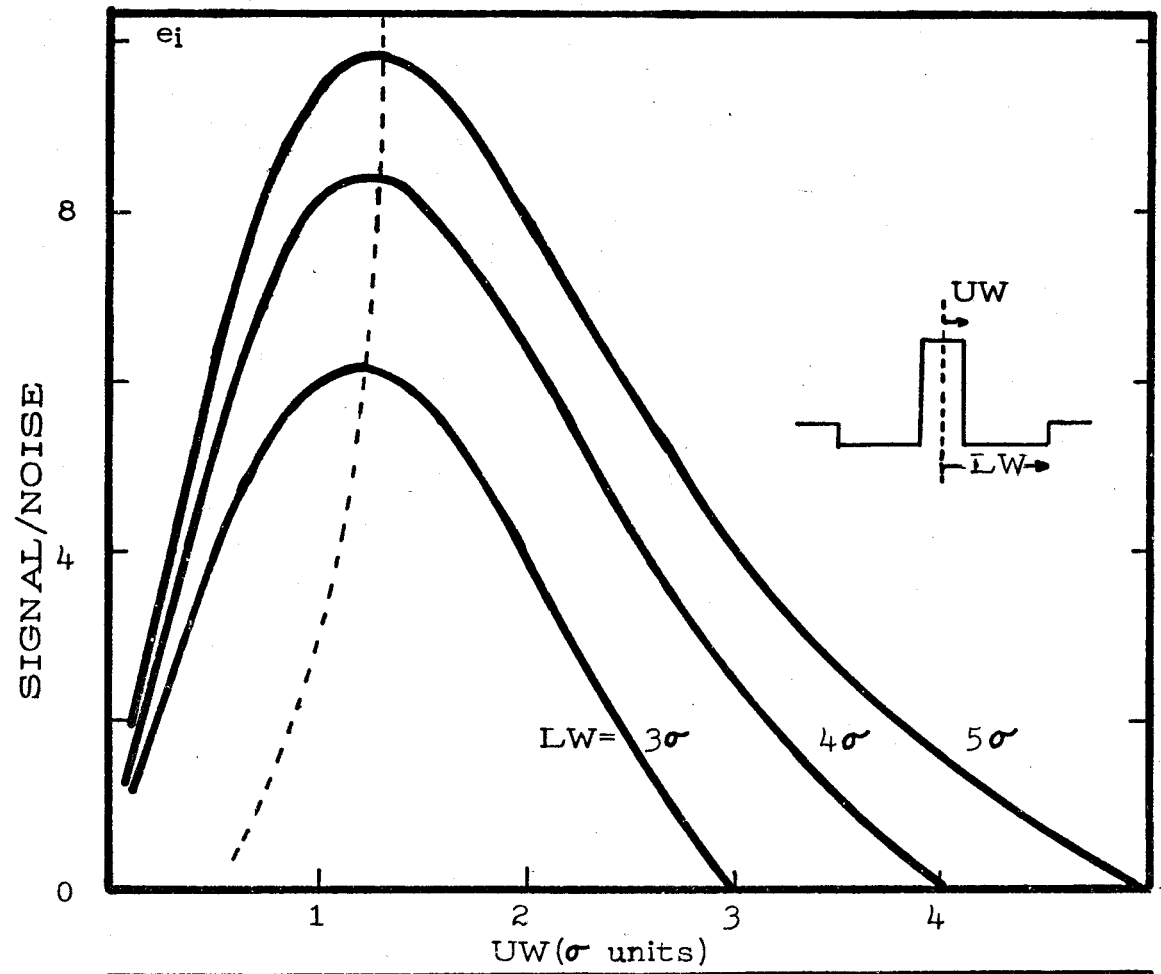
eᵢ
SIGNAL/NOISE
8
4
0
UW
LW
LW= 3σ
4σ
5σ
1
2
3
4
UW(σ units)

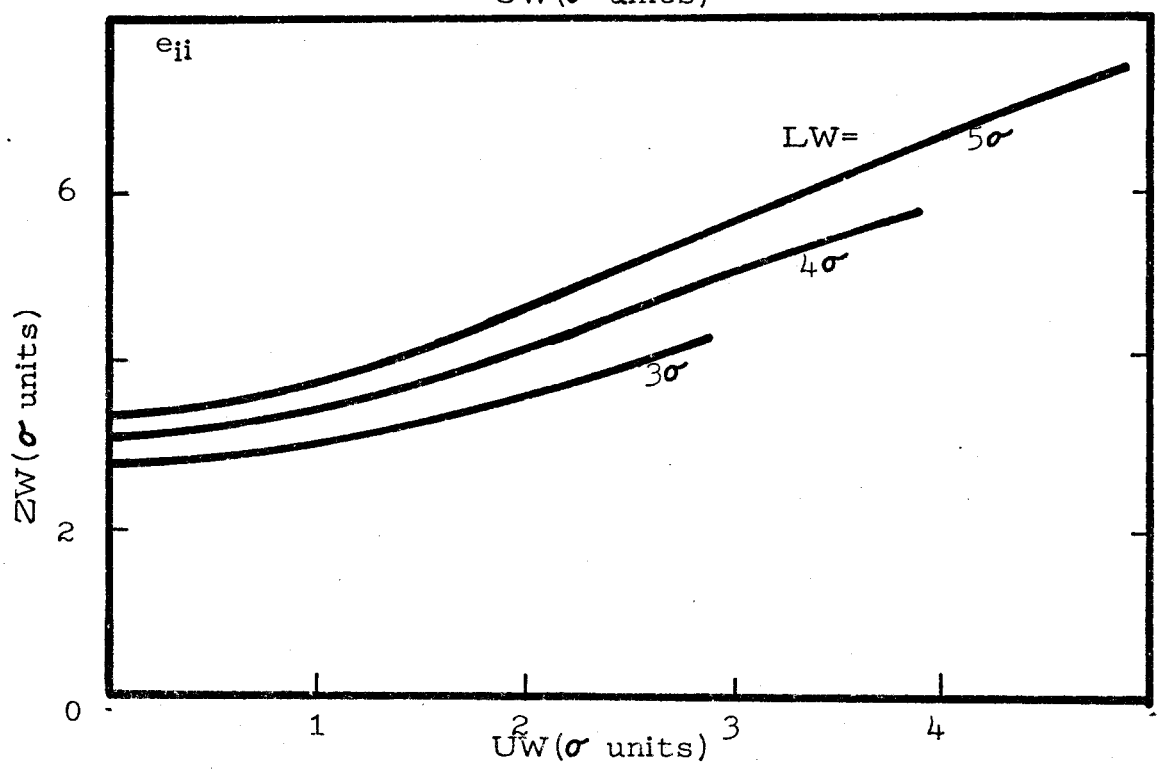
eᵢᵢ
ZW(σ units)
6
2
0
LW=
5σ
4σ
3σ
1
2
3
4
UW(σ units)

The only requirement necessary to allow the use of the filtered spectra in place of the original is that the application of the filter be a linear operation. An operator "H" is defined to be linear if

$$H\left(\sum_i k_i b_i(E)\right) = \sum_i k_i H b_i(E)$$

For the filter

$$H(y) = \int dx F(y-x)$$

it is trivial to show

$$\int dx\, F(y-x)\left(\sum_{i=1}^{N} k_i b_i(x)\right) = \sum_{i=1}^{N} k_i \int dx\, F(y-x)\, b_i(x)$$

or

$$S(y) = \sum_{i=1}^{N} k_i B_i(y)$$

where $S(y)$ is the convolute of $s(x)$

$$S(y) = \int F(y-x)\, s(x)\, dx$$

and $B_i(y)$ is the convolute of the $b_i(x)$ in equation (1)

$$B_i(y) = \int F(y-x)b_i(x)\,dx$$

The advantageous increase in orthogonality of the zero-area filtered spectra over their unfiltered counterparts is clearly demonstrated by the data in Table 3.2.2f.

3.2.3 Equivalence to Least Squares Fit and Weighting

In this section it will be demonstrated that the cross correlation method delineated in Section 3.2.1 is equivalent to a least squares fit of the basis spectra to the sample spectra.

The least squares approach stipulates maximizing the likelihood function

$$L(s,k_i) = \prod_{E} P_{k_i}(s(E))$$

by variation of the parameters k_i. Here $P_{k_i}(s(E))$ refers to the probability of a measurement of 's' at energy E given the correct distribution is specified by the k_i. If there are enough counts in each channel "E" we may assume a Gaussian distribution about the expected value, i.e.

Table 3.2.2f

The data presented here represents the orthogonality matrices for 5 typical spectra obtained with a Ge(Li) detector. The first matrix refers to the original data and the second to the filtered data. The spectra and their filtered counterparts are shown in the diagrams on the following pages.

The five spectra are:

i room background

ii As - neutron activation

iii Br - neutron activation

iv Ga - neutron activation

v Ge - neutron activation

Orthogonality

i) Before filtering

	i	ii	iii	iv	v
i	1.000	0.485	0.893	0.745	0.633
ii	0.485	1.000	0.581	0.575	0.389
iii	0.893	0.581	1.000	0.802	0.627
iv	0.745	0.515	0.802	1.000	0.549
v	0.633	0.389	0.627	0.549	1.000

ii) After filtering

	i	ii	iii	iv	v
i	1.00	1.75×10^{-3}	2.65×10^{-3}	6.20×10^{-4}	2.45×10^{-3}
ii	1.75×10^{-3}	1.00	7.15×10^{-2}	2.46×10^{-5}	9.81×10^{-5}
iii	2.65×10^{-3}	7.15×10^{-2}	1.00	1.15×10^{-4}	1.06×10^{-3}
iv	6.02×10^{-4}	2.46×10^{-5}	1.15×10^{-4}	1.00	3.32×10^{-5}
v	2.45×10^{-3}	9.81×10^{-5}	1.06×10^{-3}	3.32×10^{-5}	1.00

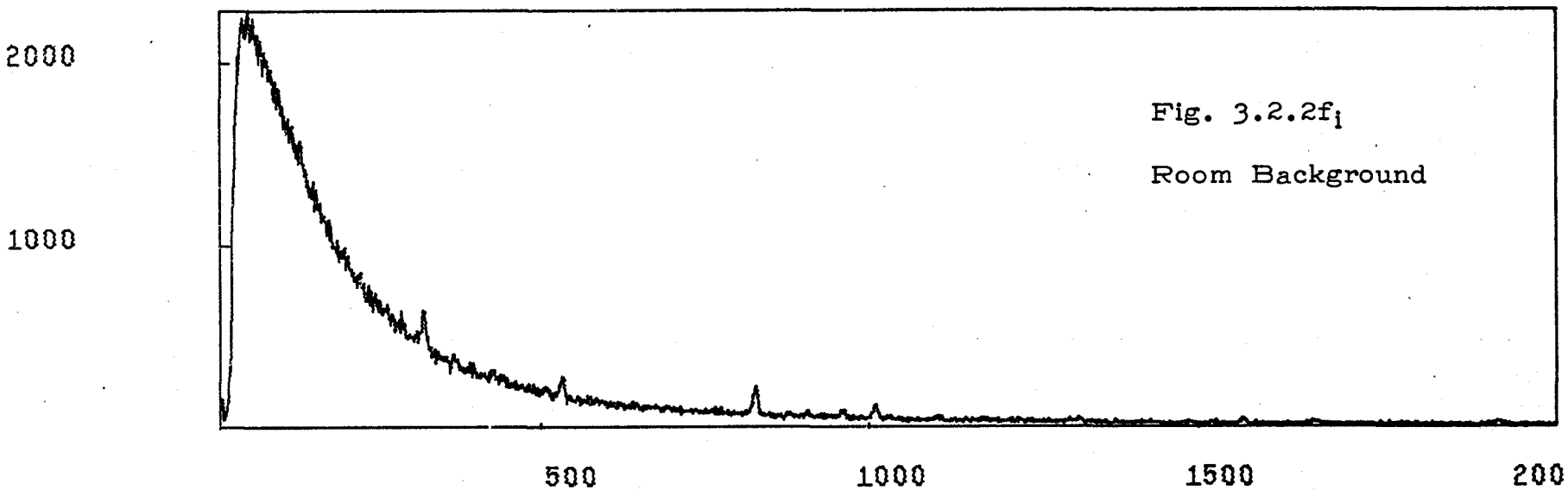

Fig. 3.2.2f$_i$

Room Background

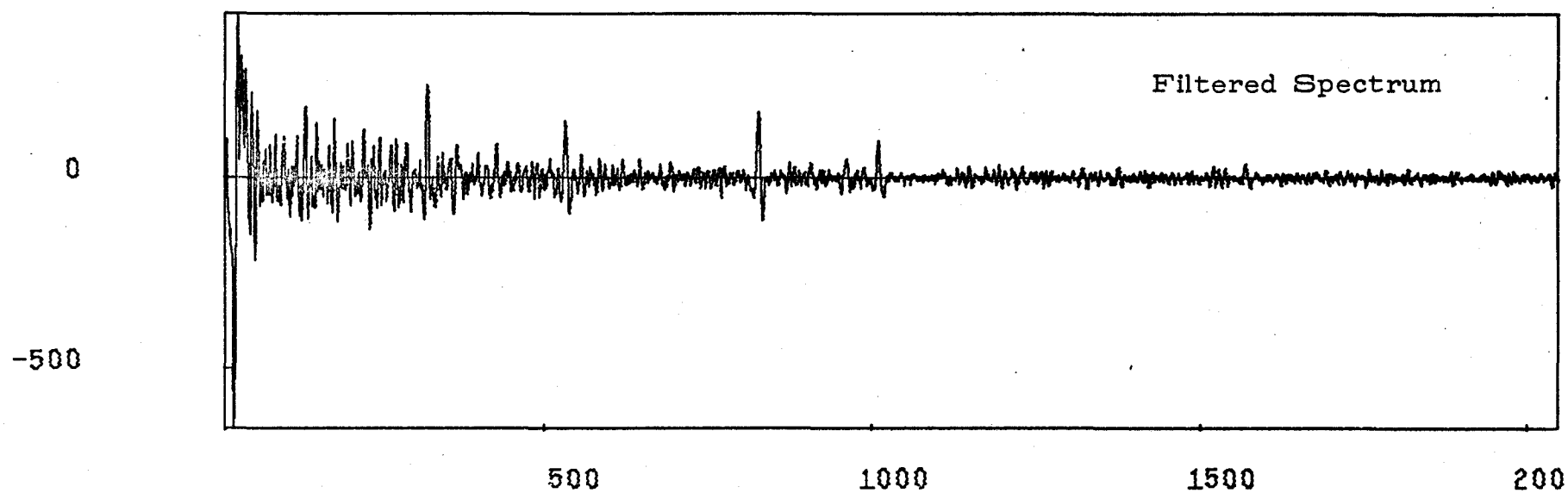

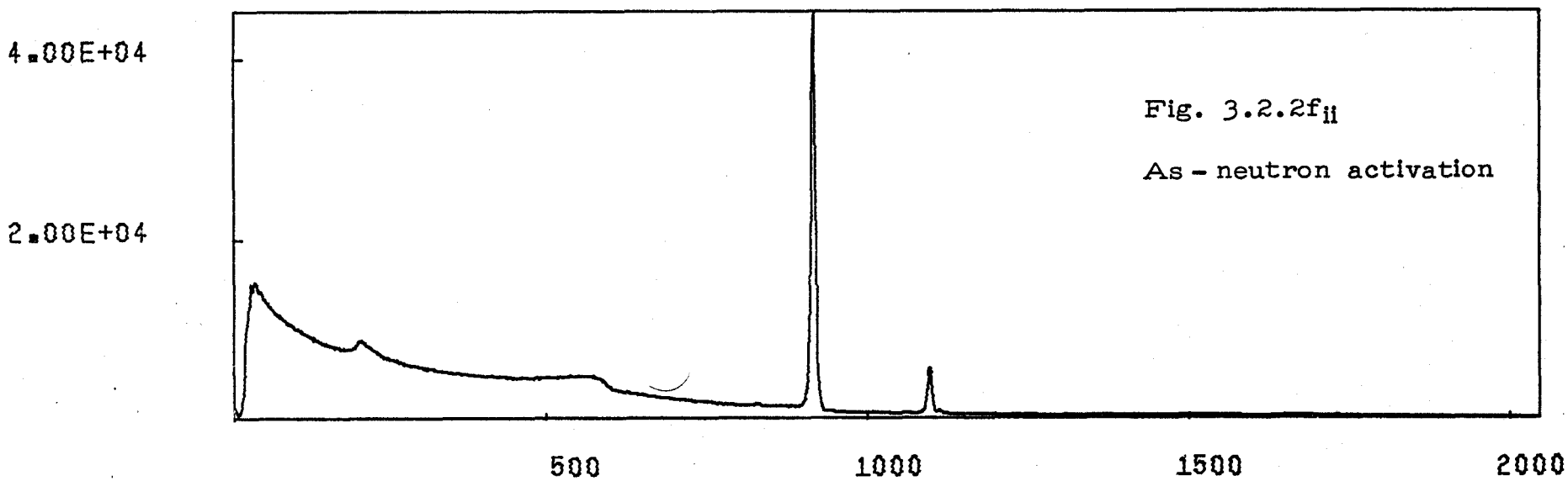

Fig. 3.2.2f$_{ii}$

As - neutron activation

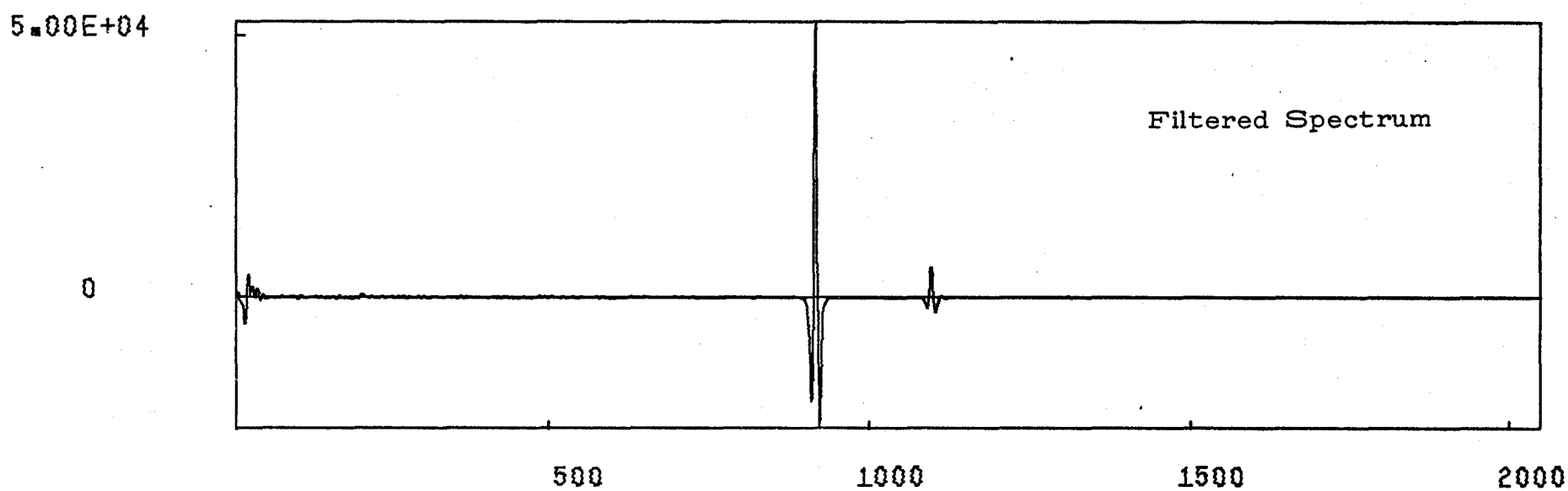

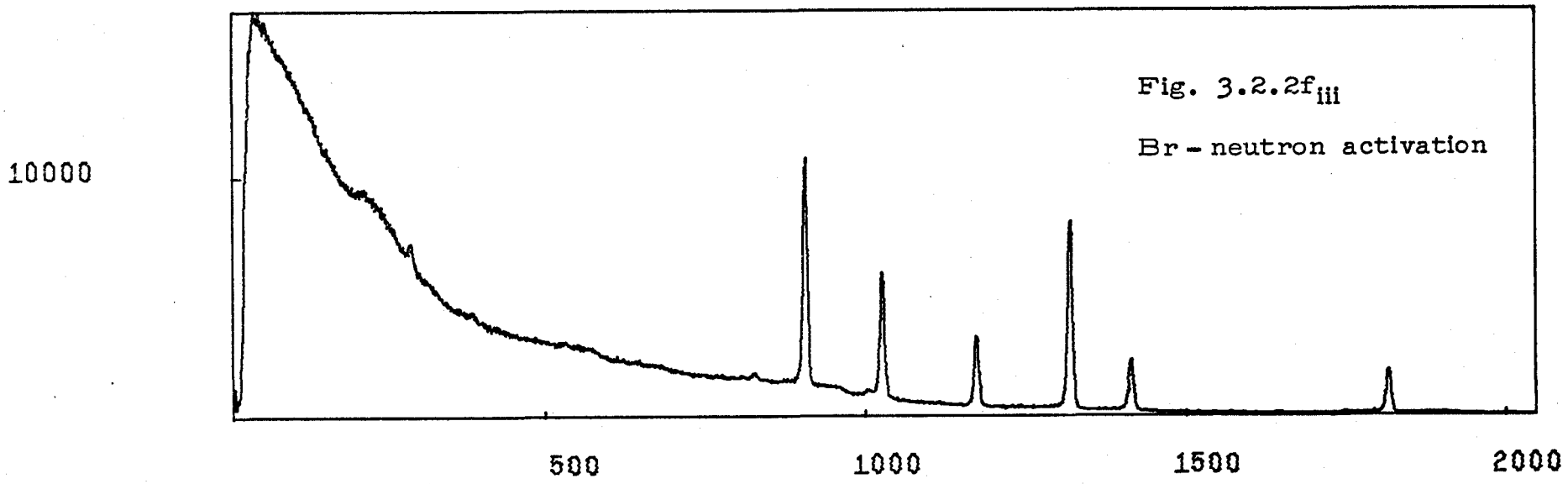

Fig. 3.2.2f$_{iii}$

Br - neutron activation

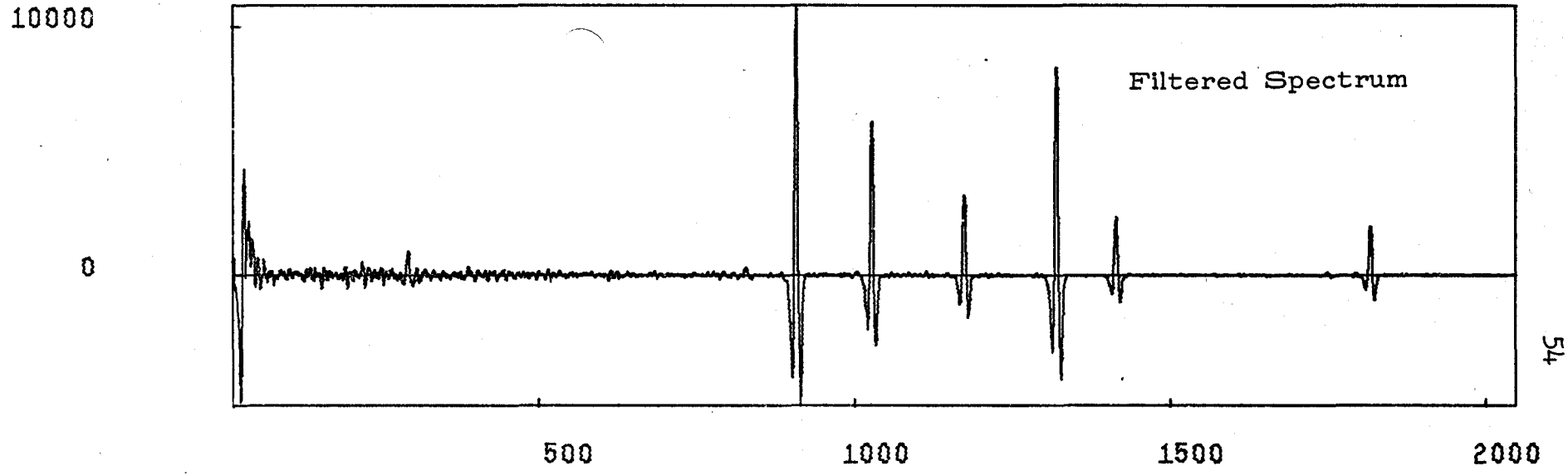

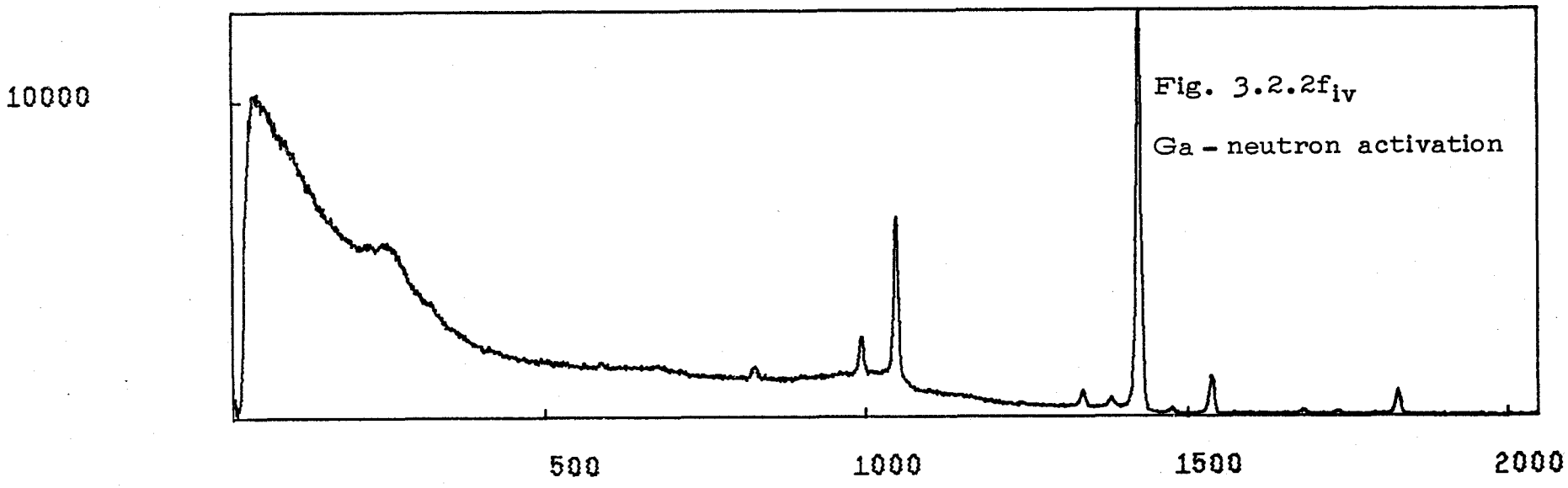
10000
Fig. 3.2.2f$_{iv}$
Ga - neutron activation
500
1000
1500
2000

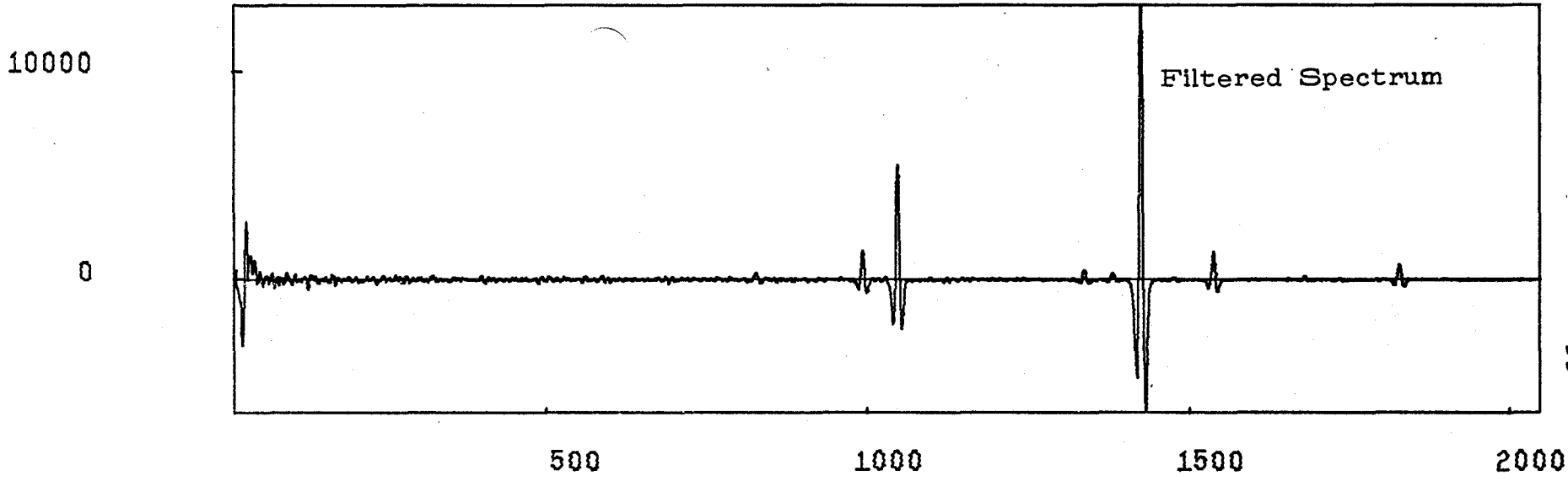
10000
0
Filtered Spectrum
500
1000
1500
2000

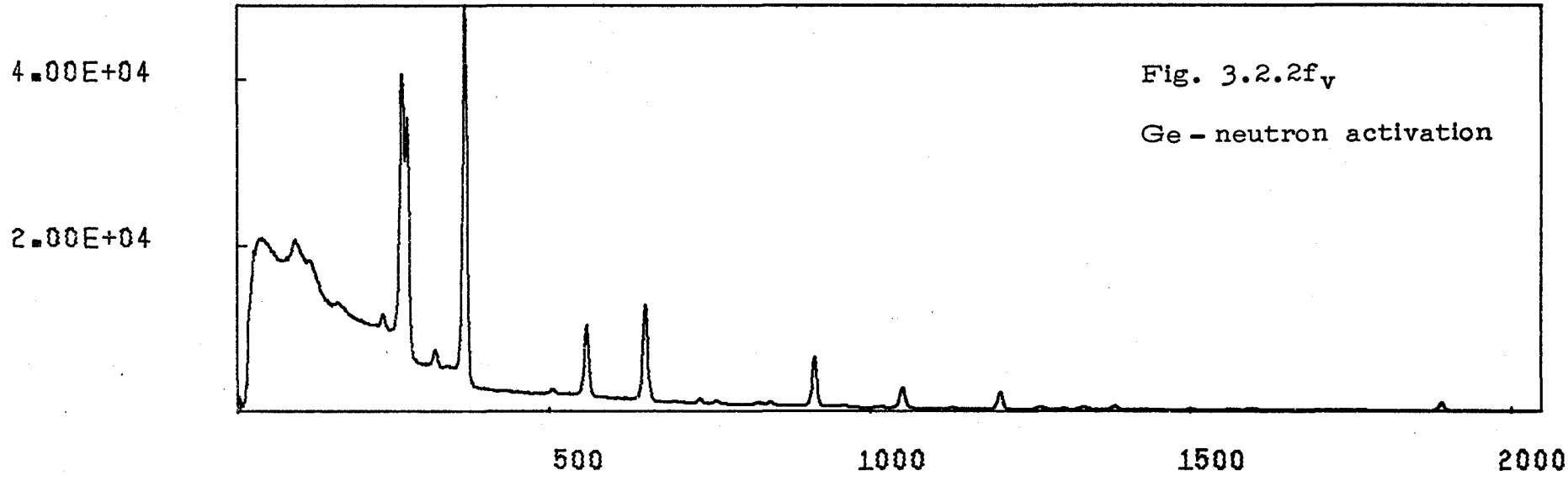

Fig. 3.2.2f$_v$

Ge - neutron activation

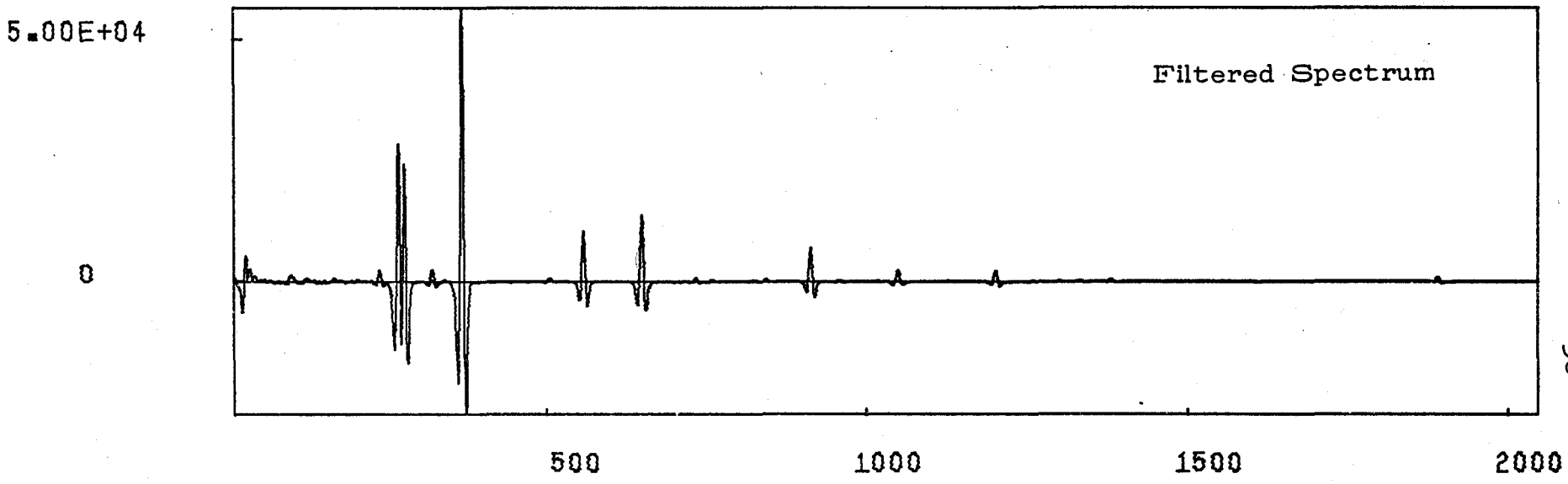

$$L(s,k_i) = \prod_E EXP \frac{(s(E) - \sum_{i=1}^{N} k_i b_i(E))^2}{2\sigma_E^2}$$

Maximizing the log of the likelihood function will correspondingly maximize the likelihood function. Define Q by

$$\frac{Q}{2} = \ln L(s,k_i) = \sum_E \frac{(s(E) - \sum_{i=1}^{N} k_i b_i(E))^2}{2\sigma_E^2}$$

Then Q is recognized as being the usual least squares sum with weighting factor $1/\sigma_E^2$. We require

$$\frac{dQ}{dk_j} = 0$$

for all j.

$$\frac{dQ}{dk_j} = \frac{d}{dk_j} \sum_E \frac{1}{\sigma_E^2} \left\{ s^2(E) - 2s(E) \sum_i k_i b_i(E) + \right.$$

$$\left. + \sum_{i,k} k_i k_k b_i(E) b_k(E) \right\}$$

$$\frac{dQ}{dk_j} = -2 \sum \frac{s(E)}{\sigma_\varepsilon^2} \frac{d}{dk_j} \sum k_i b_i(E) + 2 \sum k_i \sum \frac{b_i(E) b_j(E)}{\sigma_\varepsilon^2} = 0$$

Then

$$\sum_E \frac{s(E)}{\sigma_\varepsilon^2} b_j(E) = \sum_I k_i \sum_E \frac{b_i(E) b_j(E)}{\sigma_\varepsilon^2}$$

In the case σ^2 is constant this is

$$\sum_E s(E) b_j(E) = \sum_I k_i \sum_E b_i(E) b_j(E)$$

which will be recognized as

$$s(E) \circ b_j(E) = \sum_I k_i b_i(E) \circ b_j(E)$$

or with the notation of Section 3.2.1

$$v_j = \sum_I k_i C_{ij}$$

$$\vec{k} = \vec{v} \underline{C}^{-1}$$

Thus the cross correlation technique is equivalent to an "unweighted" least squares fit. Weighting can be included in the cross correlation technique by redefining the terms v_i and C_{ij} as

$$v_i \equiv \sum_E \frac{s(E)b_i(E)}{\sigma_\epsilon^2}$$

$$C \equiv \sum_E \frac{b_i(E)b_j(E)}{\sigma_\epsilon^2}$$

σ^2 in this more complete analysis is dependent on the sample spectrum s(E). Thus including it means recalculating and re-inverting the matrix $\underline{C}$ for each new sample spectrum. Further, the variance is not usual 1/s(E) but due to the effect of the filter is

$$\sigma_\epsilon^2 = \sum_E F^2(E-E')\, s(E)$$

It is clear that the inclusion of the weighting factor is costly in terms of central processor time. Further, consideration

of the problem in terms of information content leads one to believe that it is better to fit the peaks preferentially to the smooth portions of the spectrum. As peaks tend to contain more counts than background and therefore have a higher variance, the ommission of the weighting may be advantageous. In any case there is no weighting included in the calculations and examples which follow.

3.3 Error Analysis

3.3.1 Statistical Analysis of Results

The evaluation of the variance of the final result is performed under the assumption that there is no significant uncertainty in the set of basis spectra. In fact this assumption is expected to be valid in the usual case because the basis spectra will be standard spectra used to analyse many samples and it will be advantageous to obtain good statistics for these spectra.

It will be necessary to find the variance in the filtered spectrum and it is important to note that covariance exists between neighboring channels due to the effect of the filter. The data of the original spectrum are statistically independent. As a result of the convolution of the original data (x_i) by the filter ($F_{ij} = F(i-j)$) we have the resultant spectrum (y_j).

$$y_j = \sum_i F_{ij} x_i \qquad (7)$$

The covariance matrix in y is defined by

$$\sigma_{y_j, y_k} \equiv \langle y_j - y_j \rangle \langle y_k - y_k \rangle$$

Substitution of equation (7) gives

$$\sigma_{y_j, y_k} = \langle \sum_i F_{ij} x_i - \sum_i F_{ij} \bar{x}_i \rangle \langle \sum_l F_{lk} x_l - \sum_l F_{lk} \bar{x}_l \rangle$$

$$= \langle \sum_i F_{ij} (x_i - \bar{x}_i) \rangle \langle \sum_l F_{lk} (x_l - \bar{x}_l) \rangle$$

$$= \sum_i F_{ij} \langle x_i - \bar{x}_i \rangle * \sum_l F_{lk} \langle x_l - \bar{x}_l \rangle$$

$$= \sum_{i,l} F_{ij} F_{lk} \langle x_i - \bar{x}_i \rangle \langle x_l - \bar{x}_l \rangle$$

$$= \sum_{i,l} F_{ij} F_{lk} \sigma_{x_i, x_l}$$

but

$$\sigma_{x_i, x_l} = \sigma^2_{x_i} \delta_{il}$$

by virtue of the statistical independence of the original data x_i.

Hence

$$\sigma_{y_j, y_k} = \sum_{i,l} E_{ij} E_{lk} \sigma^2_{x_i} \times \delta_{il}$$

$$= \sum_{l} E_{ij} E_{lk} \sigma^2_{x_i}$$

$$\sigma_{y_j, y_k} = \sum E_{ij} E_{ik} x_i \qquad (8)$$

since $\sigma^2_{x_i} = x_i$

Next the variance in the correlation of y_j with the basis vectors is determined. Recall we are assuming that the base vector data (b^l_j) are exact. The correlation with the

l-th basis vector

$$v_l = y \circ b^l = \sum_j y_j b^l_j$$

has the variance

$$\sigma^2_{v_l} = \left(\sum_j \sigma_{y_j} b^l_j \right)^2$$

$$= \sum_{j,k} b^l_j b^l_k \sigma_{y_j, y_k}$$

associated with it. Using the previous result (8) for σ_{y_j, y_k} this becomes

$$\sigma^2_{v_l} = \sum_{j,k} b^l_j b^l_k \sum_i F_{ij} F_{ik} x_i$$

$$= \sum_{i,j,k} b^l_j b^l_k F_{ij} F_{ik} x_i \qquad (9)$$

Recalling that the intensity is given by

$$\vec{k} = \vec{v}_l \underline{C}^{-1}$$

and that the basis set have no error, $\underline{C}^{-1}$ can be treated as if error free. To find the variance in the coefficient k_i then we note

$$k_m = \sum_j v_j C^{-1}_{mj}$$

Then

$$\sigma^2_{k_m} = \sum_l \sigma^2_{v_l} \left(C^{-1}_{ml} \right)^2$$

is the variance in the quantity of the m-th basis spectrum in the sample spectrum. Using equation (9) to expand this we obtain the final result

$$\sigma^2_{k_m} = \sum_{i,j,k,l} \left(C^{-1}_{ml} \right)^2 b^l_j b^l_k F_{ij} F_{ik} x_i \qquad (10)$$

It is clear that equation (10) represents a lengthy calculation and yet even with its complexity the expression is not rigourously correct due to the assumption of very good statistics on the basis spectra b^1. To follow the variances in the basis spectra through the matrix inversion alone would be a horrendous task, although some simplification could be achieved by assuming the matrix to be diagonal. In any case it was found more than one minute of computing time was required on a CDC-6400 computer to evaluate the variance of a single component of a 5 component spectra. Since one of the prime objectives of this work was to develop a simple, fast and adequate algorithm, this evaluation clearly violates our aims. Therefore an alternate approach was sought.

The number of terms involved in the summation of equation (10) is seen to be

$$N \times K \times L^2$$

where N is the number of standards included in the analysis, L is the width of the filter and K is the number of channels involved in the cross correlation. Thus for filter widths of 10 to 30 channels computation time is increased by a factor of

100 to 1000 over the computation time required if no filter were applied. It is useful to examine the statistical deviations ("noise") in the spectral data and the effect of the filters on these deviations in more detail. As was demonstrated in Section 3.2.3 the cross correlation technique is equivalent to an "unweighted" least squares fit. Analysing the fitting procedure in terms of maximizing the likelihood function shows that the correct weighting factor is the variance. By using the unweighted technique it is assumed that the variance on all points is a constant. That is, the noise band is represented by white noise. Fig. 3.3.1a shows the power spectral density of the noise band of a spectrum determined by subtracting the unweighted least squares fit. For white noise the power spectral density would be a constant in the limit of an infinite number of trials. The diagram shown (Fig. $3.3.1a_{ii}$) represents only a single trial and thus contains a large amount of randomness. Fig. $3.3.1a_{iii}$ represents a smoothed version of Fig. $3.3.1a_{ii}$. The important thing to note is the lack of any trend in the data. This indicates that the spectral noise will approach white noise for a large number of trials.

Recall that the filtering operation is represented by the convolution

$$y(x) = \int F(x-x')\,Y(x')\,dx'$$

Fig. 3.3.1a

Spectral Noise Characteristics

i - Noise determined by cross correlation technique

ii - Power spectral distribution of noise in i

iii - Smoothed power spectral distribution

iv - Fourier Transform of rectangular filter function

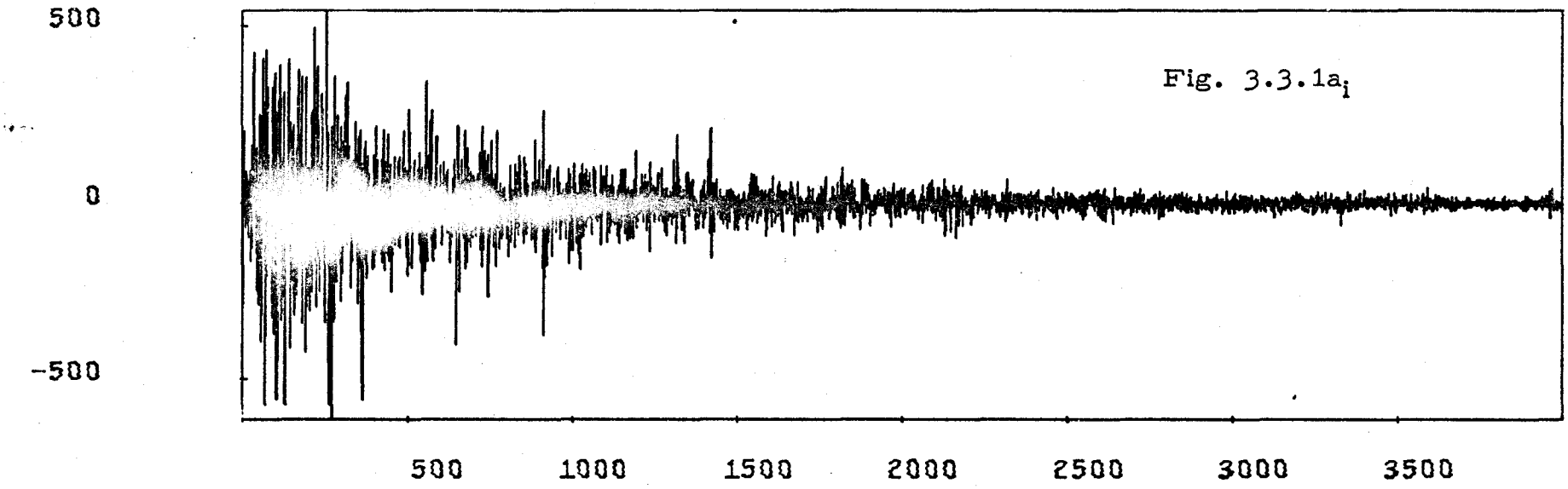

Fig. 3.3.1a$_i$

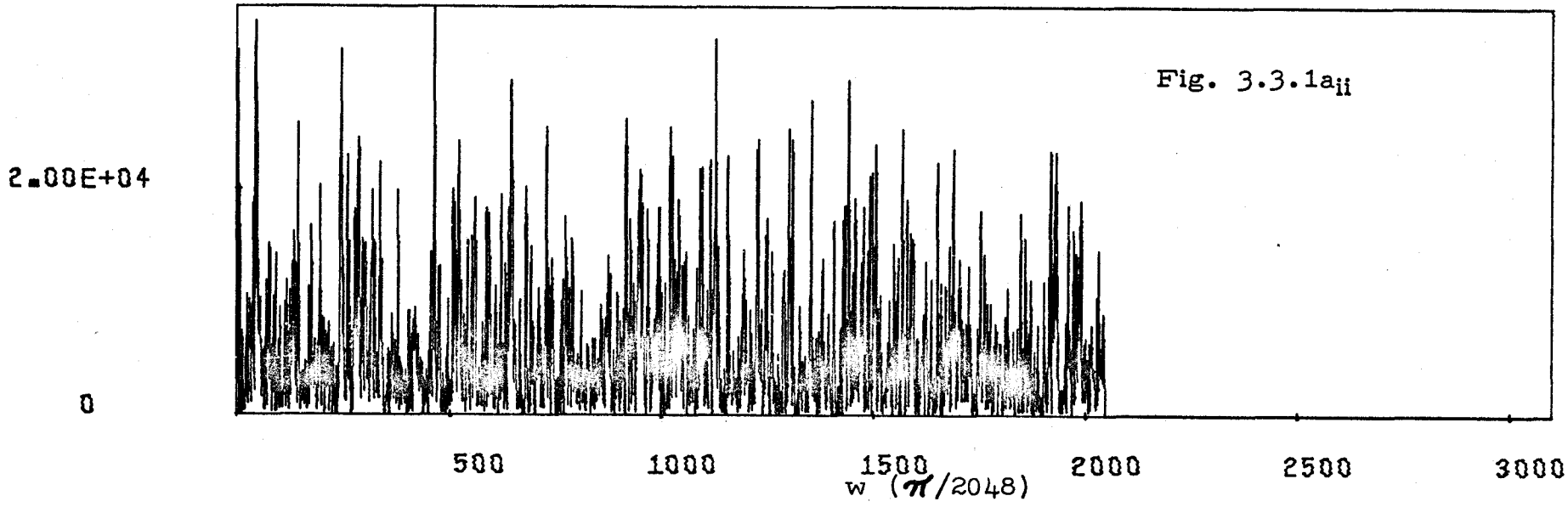

Fig. 3.3.1a$_{ii}$

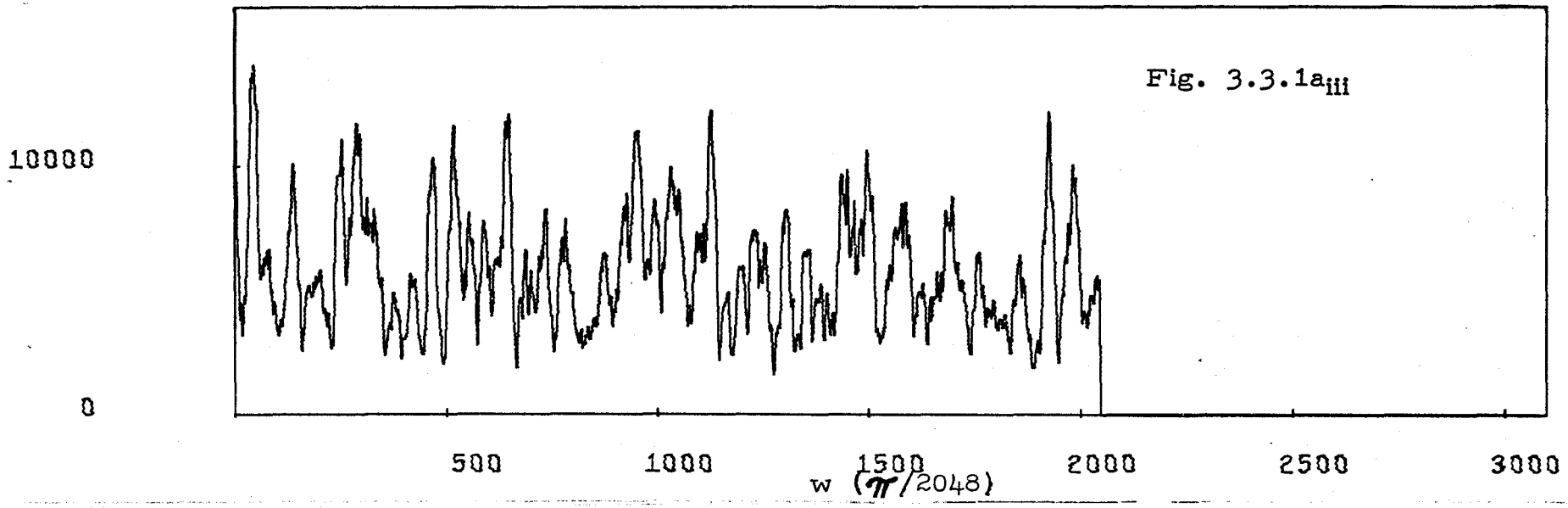

Fig. 3.3.1a$_{iii}$

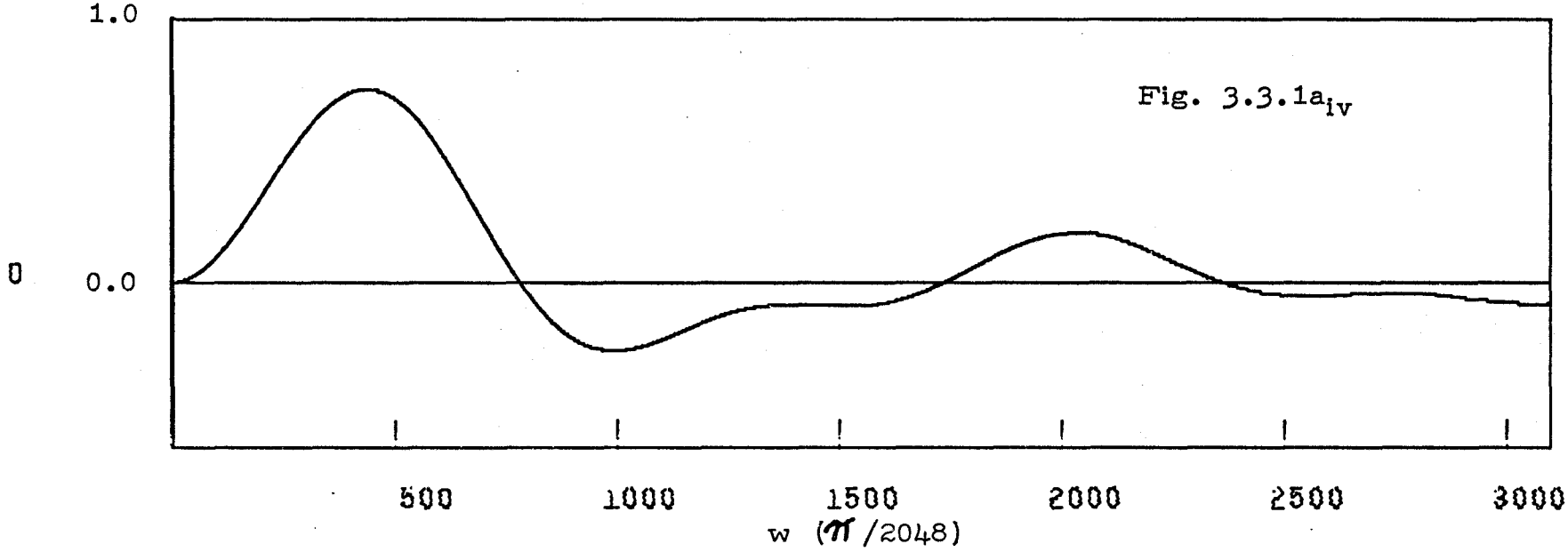

Fig. 3.3.1a$_{iv}$

The original spectrum $Y(x')$ may be considered as consisting of a signal portion $Y_s(x')$ and a noise portion $Y_n(x')$. Then

$$y_s(x) + y_n(x) = \int F(x-x')(Y_s(x') + Y_n(x'))dx'$$

or

$$y_n(x) = \int F(x-x')Y_n(x')dx'$$

If $f(w)$, $X_n(w)$ and $x_n(w)$ represent the Fourier transforms of $F(x)$, $Y_n(x)$ and $y_n(x)$ respectively then the convolution theorem yields

$$x_n(w) = f(w)X_n(w)$$

The Fourier transform of a typical filter is shown in Fig. $3.3.1a_{iv}$. It is clear that the effect of the filter is to reduce

the area of the noise band in frequency space. Further, the amount of reduction depends primarily on the filter used. Hence we can write for equation (9)

$$\sigma^2_{v_l} \doteq R^2(F) \sum_{i,j,k} b^l_j b^l_k \delta_{ij} \delta_{ik} x_i$$

$$= R^2(F) \sum_i b^{l^2}_i x_i \qquad (11)$$

where R(F) is a constant (dependant only on the filter F) which is related to the reduction in area of the noise band. Equation (10) is replaced by the approximate form.

$$\sigma^2_{k_m} = R^2(F) \sum_{i,l} \left(C^{-1}_{ml} \right)^2 b^{l^2}_i x_i \qquad (12)$$

The CPU time saving by using equation (12) in place of equation (10) will be a factor of 100 to 1000 depending upon the filter width L. The constant R(F) may be empirically determined by evaluating both equation (10) and (12) without the factor R. The quantity R^2 is just the ratio of the two quantities evaluated. Table 3.3.1b includes data derived from

Table 3.3.1b

i. The quantity "R" determined by equation (12)

Standard No.	Sample No. 1	2	3	4	5
1	0.21	0.20	0.20	0.20	0.21
2	0.23	0.23	0.23	0.22	0.23
3	0.21	0.22	0.22	0.22	0.22
4	0.22	0.23	0.23	0.23	0.23
5	0.20	0.20	0.21	0.21	0.22

such a calculation. The data included in this table is derived from an analysis of 5 sample spectra in terms of 5 standards. A detailed description of the results is included in Section 4.1.

3.3.2 Noise Auto Correlation in Standard Spectra

A systematic error will ordinarily develop in the calculation of the diagonal terms of the correlation matrix, $\underline{C}$, due to the auto correlation procedure used. The basis spectra may be considered to consist of a statistics or "noise" contribution superimposed upon the pure spectrum (signal). If b^i represents the i-th basis spectrum

$$b^i = b^i_s + b^i_n$$

where b^i_s represents the pure signal and b^i_n represents the noise contribution. The elements of $\underline{C}$ would ideally consist only of the cross correlations of the pure spectra. In fact what we calculate is $\underline{C}'$ where

$$C'_{ij} = b^i \cdot b^j$$

$$C'_{ij} = (b^i_s + b^i_n) \circ (b^j_s + b^j_n)$$

$$= b^i_s \circ b^j_s + b^i_s \circ b^j_n + b^i_n \circ b^j_s + b^i_n \circ b^j_n \qquad (14)$$

Since the elements of b^i_n and b^j_n are normally distributed about zero the second and third terms in equation (14) will have an expectation value of zero. Further, the data of b^i_n and b^j_n are uncorrelated if $i \neq j$ and the expectation value of the fourth term will also be zero. In the case $i = j$ however the fourth term is seen to be positive definite and will clearly have a positive expectation value.

$$\langle C'_{ij} \rangle = b^i_s \cdot b^j_s + \langle b^i_n \cdot b^j_n \rangle$$

$$= C_{ij} + \langle b^{i2}_n \rangle \delta_{ij}$$

$$C_{ij} = \langle C'_{ij} \rangle - \langle b^{i2}_n \rangle \delta_{ij}$$

Thus the calculated diagonal elements will be too large by the amount of the auto correlation of the noise contribution. It would be possible to correct for this effect by estimating the noise auto correlation and subtracting it from the value of C_{ii} determined however this would require a calculation analogous to that defined in equation (9). An alternate procedure which would avoid this problem involves obtaining two statistically independent spectra for each standard basis. If the cross correlation of these pairs of spectra is used to determine the diagonal elements of $\underline{C}$ the noise auto correlation problem will never occur.

3.3.3 Incompleteness and Non-orthogonality

The previous discussion of errors has been primarily directed at the case where all possible components of the sample are known and their spectra included in the set of standard spectra. The problem and solution was formulated in terms of vector algebra as the resolution of an unknown vector in an N-dimensional vector space in terms of N non-orthogonal linearly independent members of the space. (N is the number of standards included in the analysis). As pointed out in Section 3.2.1 however the real samples may contain one or more constituents which are unexpected or uninteresting and inclusion of all possible constituents in the analysis is not ex-

pedient. Ignoring these uninteresting constituents leads to the problem of resolving an N + 1 dimensional vector in terms of N non-orthogonal basis vectors.

Clearly the errors involved are strongly dependent upon the degree of orthogonality of the unknown base spectrum to the standard base spectra. The relationship however is not clear cut due to the non-orthogonalities between the standard spectra. In the simplified case where the vector to be resolved has only two components, the known and the unknown, the error may be easily found. Let

$$\vec{s} = a\vec{x} + b\vec{y}$$

where x will be the known standard and y the unknown component. Then

$$a = \frac{\vec{x} \circ \vec{s}}{\vec{x} \circ \vec{x}} - b\frac{\vec{x} \circ \vec{y}}{\vec{x} \circ \vec{x}}$$

and ignoring the cross term $\vec{x} \circ \vec{y}$ introduces a relative error, Δ_r

$$\Delta_r = \frac{b(\vec{x}\circ\vec{y})}{\vec{x}\circ\vec{s}}$$

Usually the term $b(\vec{x}\circ\vec{y})$ will be small compared to $a(\vec{x}\circ\vec{x})$ and we make the approximation

$$\vec{x}\circ\vec{s} \doteq a(\vec{x}\circ\vec{x})$$

The relative error then becomes

$$\Delta_r = \frac{b(\vec{x}\circ\vec{y})}{a(\vec{x}\circ\vec{x})} \qquad (15)$$

To test this relationship a sample spectrum was artificially created by combining five different spectra taken using a Ge(Li) detector. The resulting spectrum was then analysed using 5 different combinations of 4 of the Ge(Li) spectra. The results plotted in Fig. 3.3.3a show the relationship between the actual relative discrepancy and the quantity Δ_r determined by equation (15). It is clear from equation (15) and Fig. 3.3.3a the important effect which the unknown component

Fig. 3.3.3a

Relative Discrepancy v.s. Δ_r (equation (15)) for a simulated analysis

$$\Delta_r = \frac{b}{a} \frac{\vec{x} \circ \vec{y}}{\vec{x} \circ \vec{x}} \qquad (15)$$

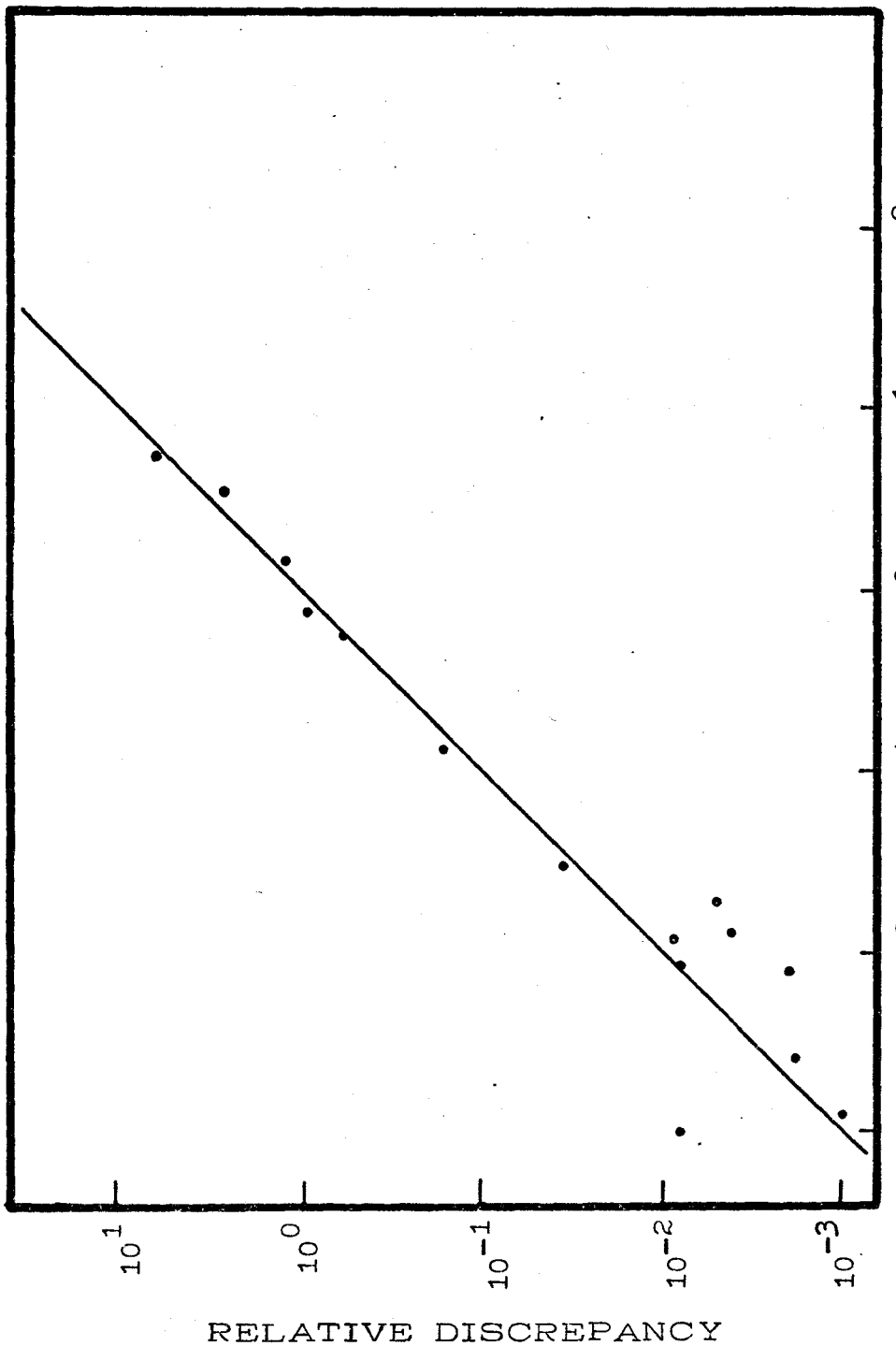
10^{1}
10^{0}
10^{-1}
10^{-2}
10^{-3}
RELATIVE DISCREPANCY
10^{-3}
10^{-2}
10^{-1}
10^{0}
10^{1}
10^{2}
$\Delta_r = \frac{b\,x\,y}{a\,x\,x}$

can have. Fortunately the presence of the unknown component and the extent of its influence may be estimated quite simply by visual examination of a residual or difference spectrum and if the analyst has chosen his set of standard spectra carefully, there will be very few samples requiring re-analysis.

The influence of the unknown is most easily considered in terms of the filtered spectra and their peaks. Non-orthogonality of spectra may be considered to be a measure of degree of overlap of their peaks. Once the analysis has been completed with the assumption that there are no unknown components the "best fit" spectrum is formed and subtracted from the original spectrum. If the spectrum and the unknown component is completely orthogonal to all other spectral components the "difference" spectrum will be identical to the unresolved spectral component. In the case where the spectrum of the unexpected component is not orthogonal to one of the standard spectra, the non-overlapping peaks of the unexpected component will still appear as positive peaks in the difference spectrum. In this case however the amount of the standard spectrum will either be under estimated or over estimated depending on whether the cross correlation of the standard spectrum with the unexpected spectral component is positive or negative. If the standard is under estimated there will be positive peaks

in the difference spectrum corresponding to the standard spectral peaks. If the standard is over estimated there will be inverted peaks in the difference spectrum which match the corresponding standard spectral peaks. These effects are demonstrated in the following difference spectra (Fig. 3.3.3b). By examining the difference spectrum the analyst can tell at a glance if a significant amount of unknown spectrum exists and interferes with the results. Further, equation (15) and the difference spectrum may be used to give a quantitative estimate of Δ_r. As pointed out the difference spectrum is expected to closely resemble the unknown constituent. Then

$$\Delta_r \doteq \frac{b(\vec{x}\circ\vec{y})}{a(\vec{x}\circ\vec{x})} \leq \frac{b|\vec{x}||\vec{y}|}{a|\vec{x}|^2}$$

$$\Delta_r \leq \frac{b|\vec{y}|}{a|\vec{x}|}$$

If $\vec{D}$ is the difference spectrum and $\vec{d}$ its filtered counterpart

Fig. 3.3.3b

Difference spectra compared with Unknown Spectra

i The original spectrum* and difference spectrum in the case there are no unknowns.

ii Unknown spectral component = room background

iii Unknown spectral component = ^{76}As

iv Unknown spectral component = ^{82}Br

v Unknown spectral component = ^{72}Ga

vi Unknown spectral component = ^{77}Ge

* A sample spectrum was artificially created by combining five different spectra taken using a Ge(Li) detector. The resulting spectrum was then analysed using 5 different combinations of 4 of the Ge(Li) spectra.

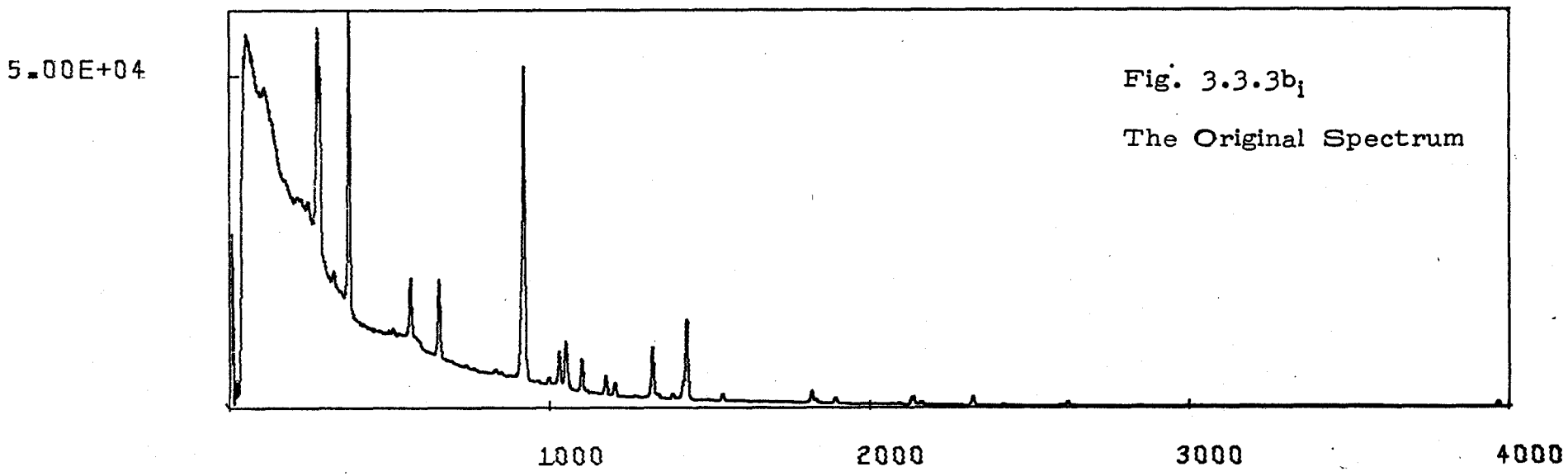

Fig. 3.3.3b$_i$

The Original Spectrum

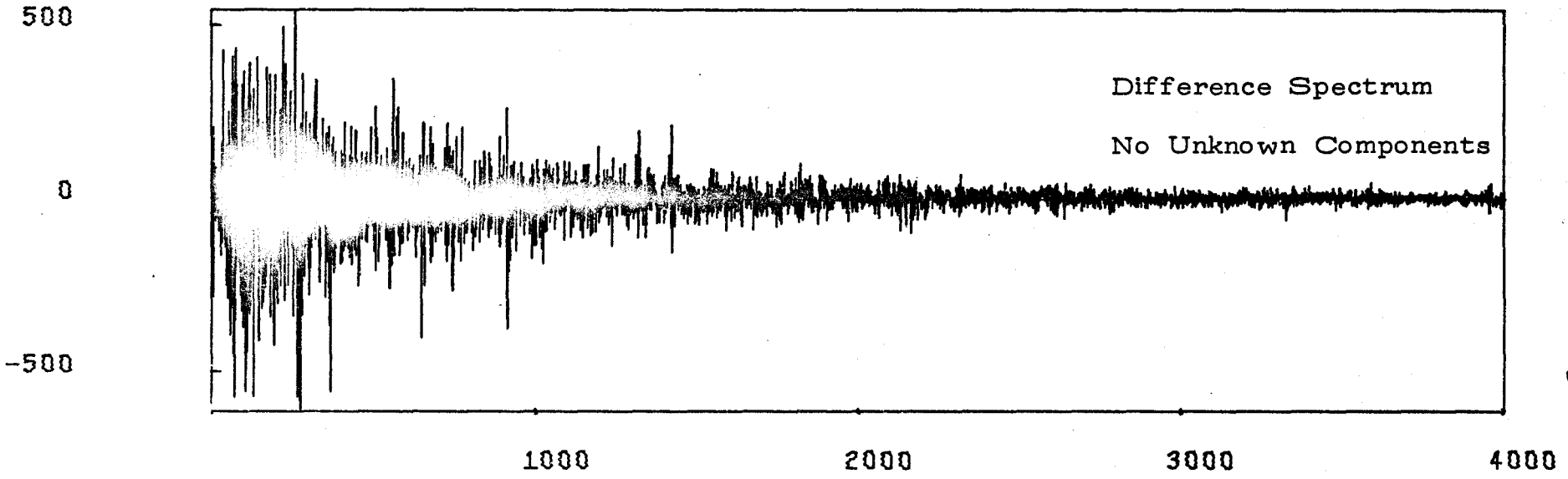

Difference Spectrum

No Unknown Components

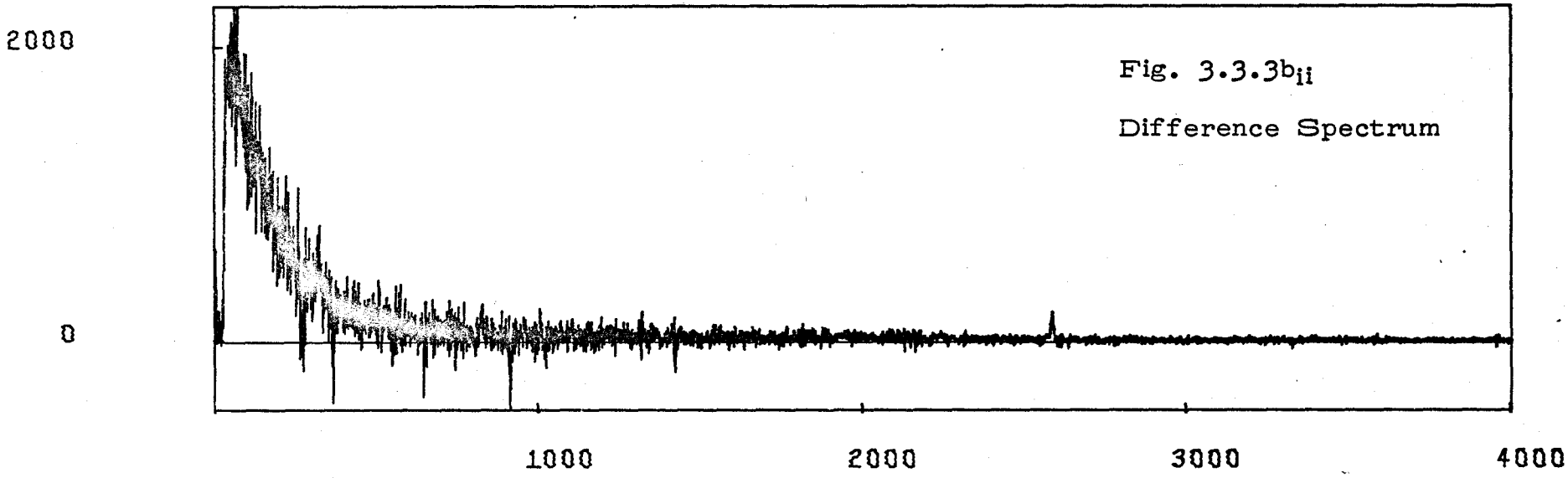

Fig. 3.3.3b$_{ii}$

Difference Spectrum

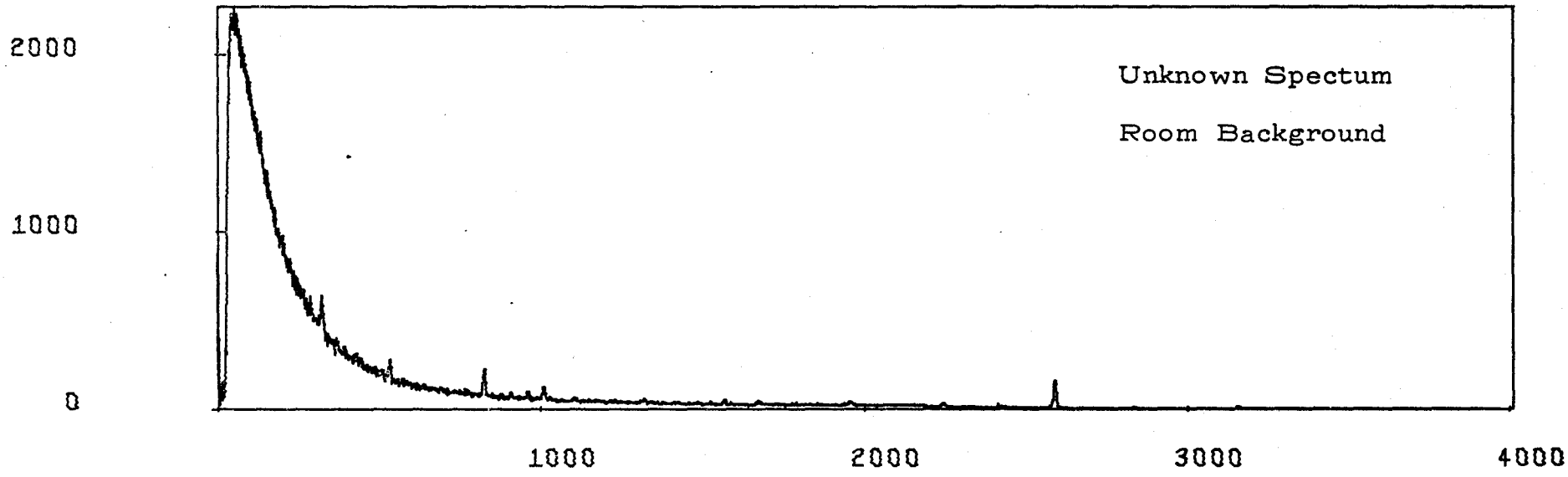

Unknown Spectum

Room Background

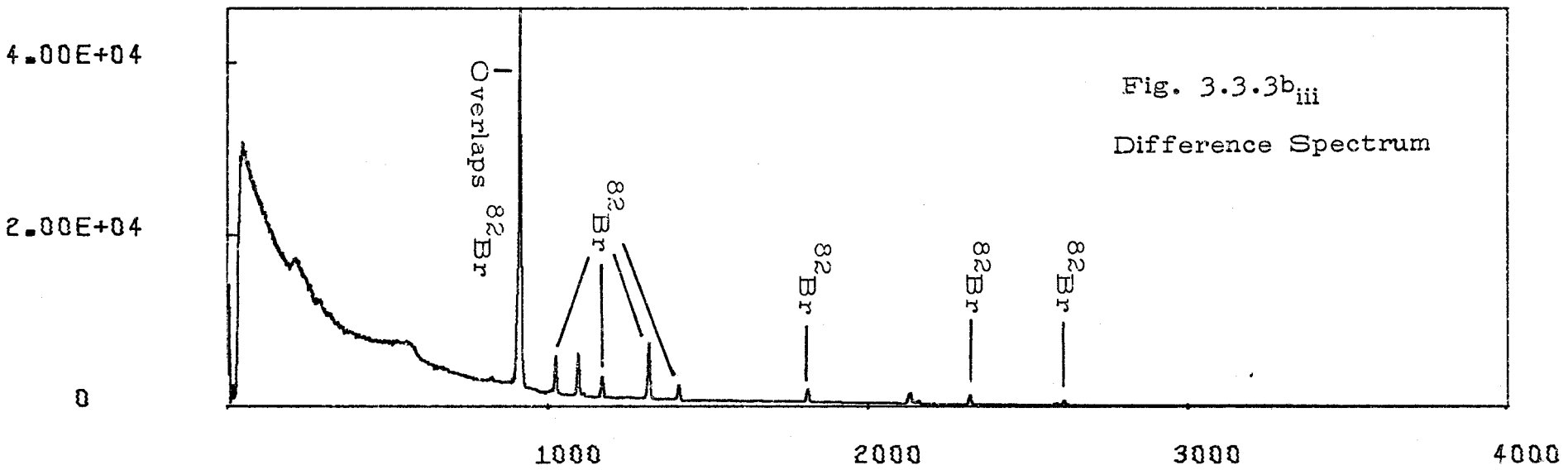

Fig. 3.3.3b$_{iii}$

Difference Spectrum

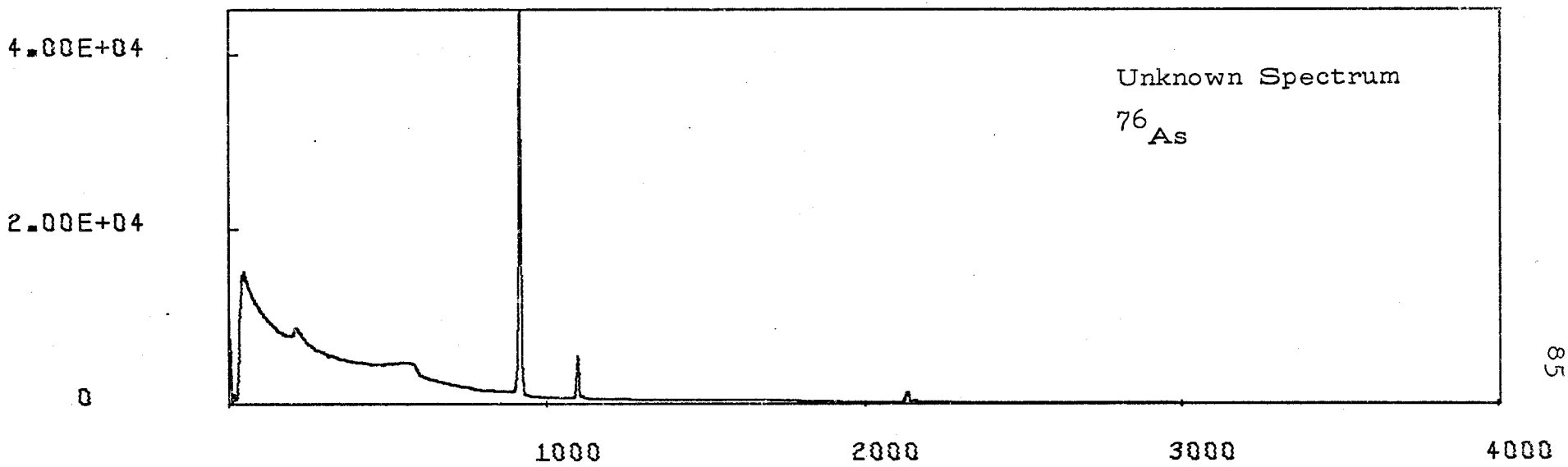

Unknown Spectrum

^{76}As

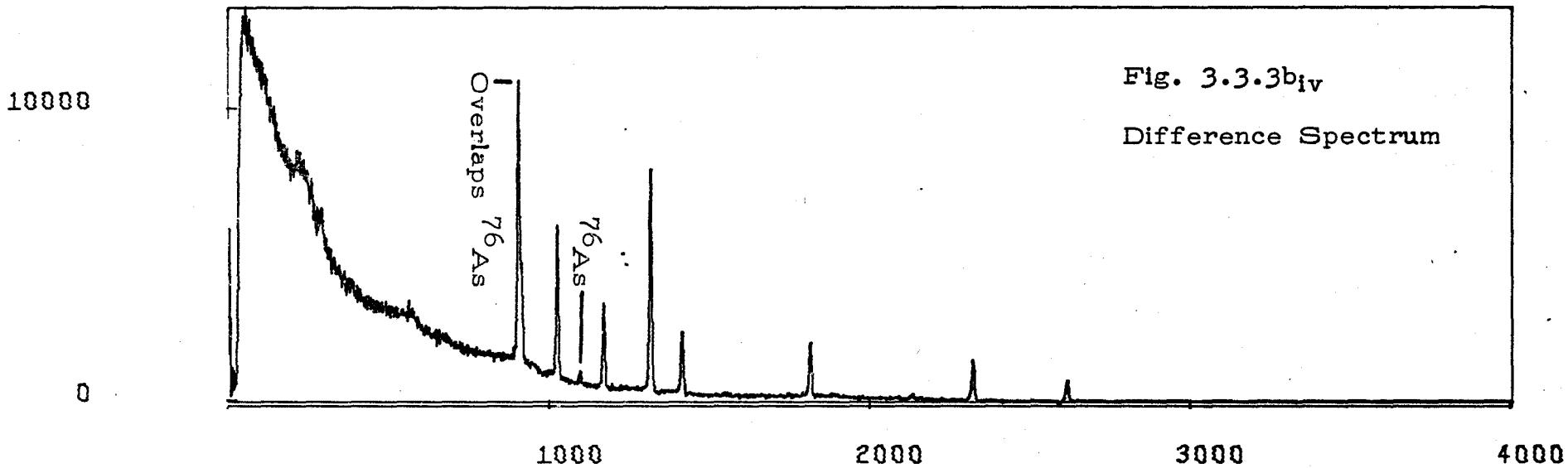

Fig. 3.3.3b$_{iv}$

Difference Spectrum

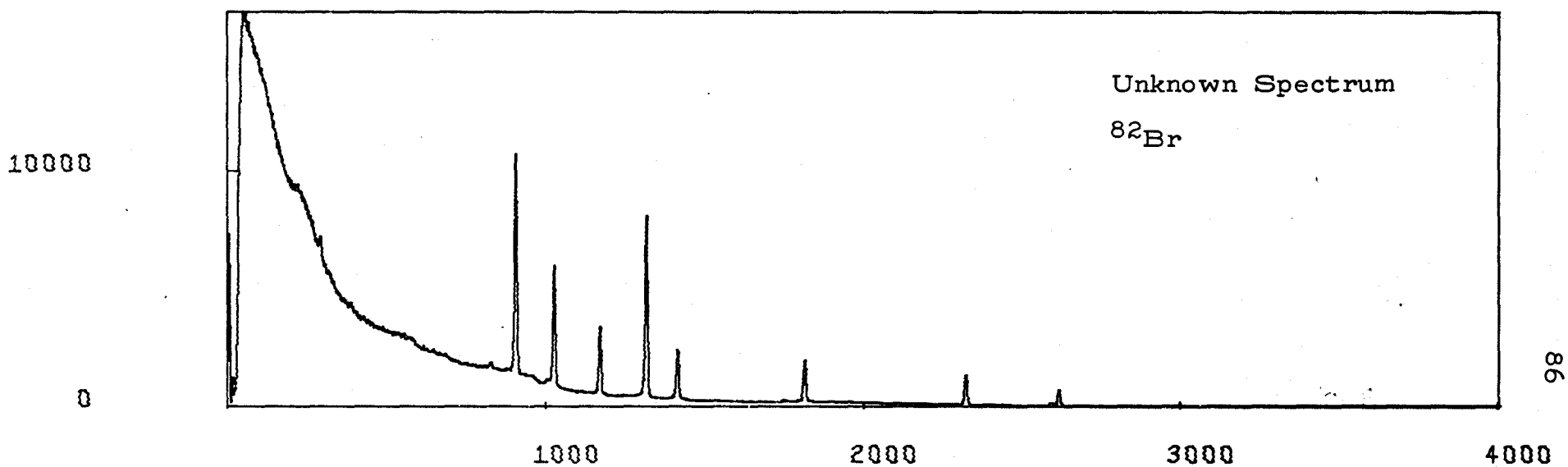

Unknown Spectrum

^{82}Br

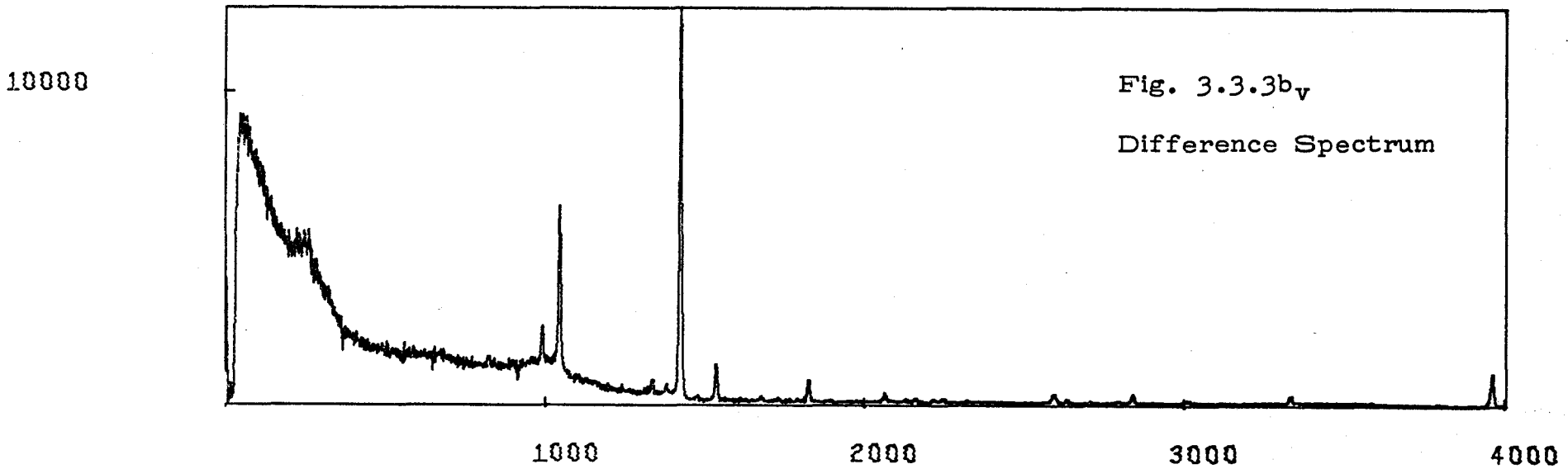

Fig. 3.3.3b$_v$

Difference Spectrum

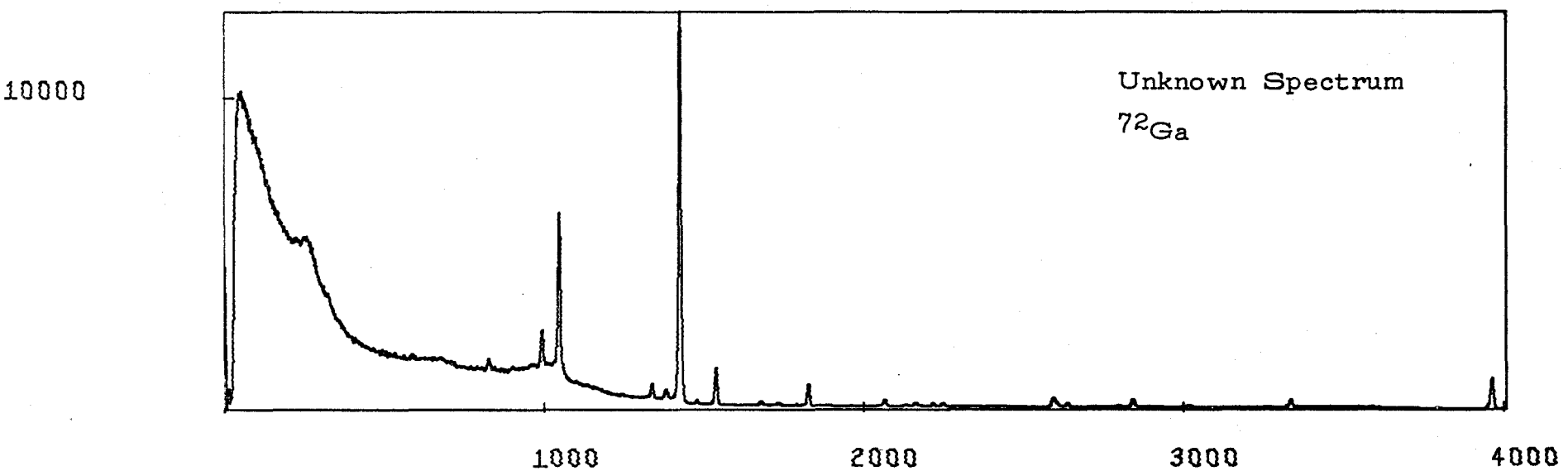

Unknown Spectrum

^{72}Ga

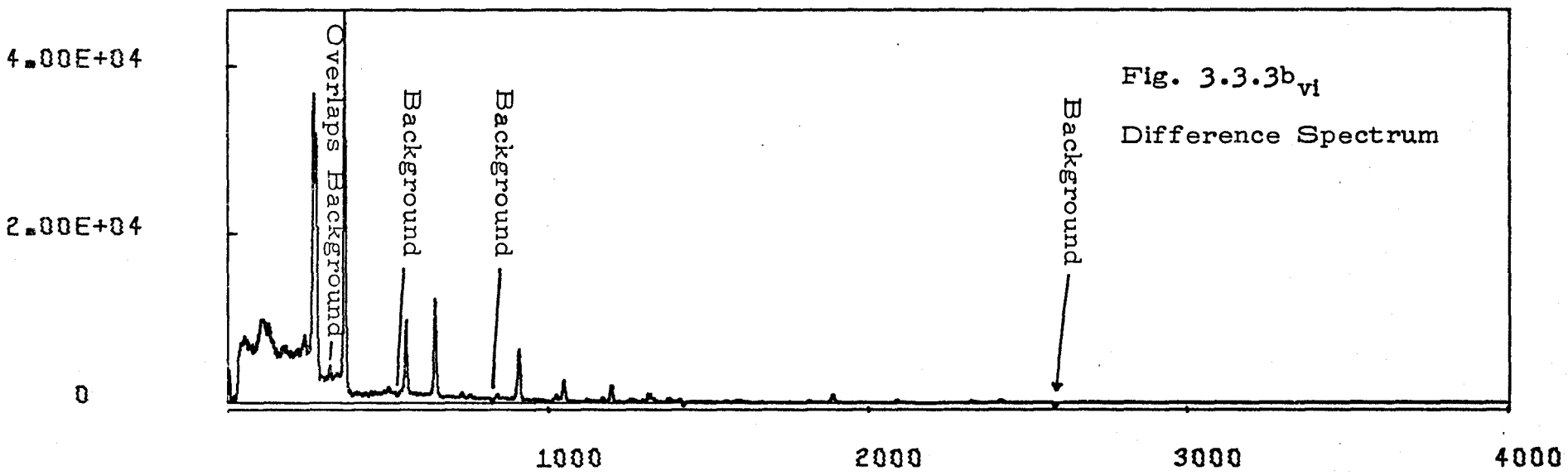

Fig. 3.3.3b$_{vi}$

Difference Spectrum

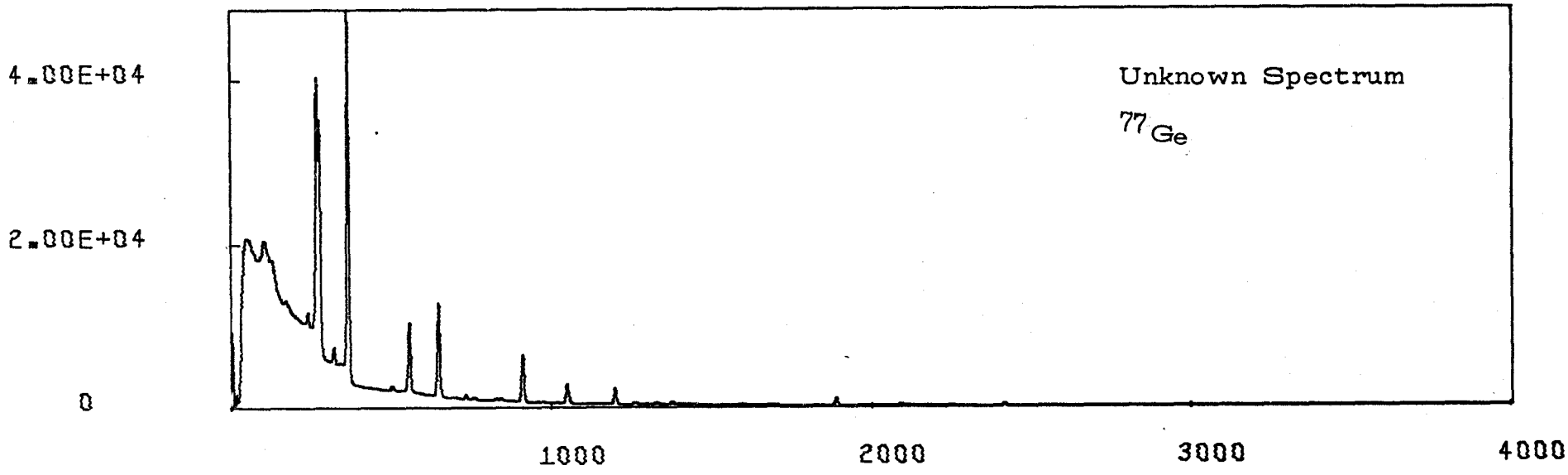

Unknown Spectrum

^{77}Ge

$$|\vec{d}| \doteq b|\vec{y}|$$

and

$$\Delta_r \leq \frac{|\vec{d}|}{a|\vec{x}|}$$

It must be remembered that this quantity is an over estimate of the true error. That is, a large value does not necessarily indicate poor results but a small value does indicate good results. Having decided that a significant interference has occured the analyst may place the spectrum aside for manual analysis or he may estimate the extent of the over or under estimation from the remainder spectrum and make an appropriate correction to the analysed values. Other options include elimination of the interfering regions from the analysis, or identification of the unexpected component and including it in the analysis. The action chosen will depend upon the conditions however if a careful selection of standard spectra has been made very few samples will have to be reconsidered.

3.3.4 Miscellaneous Notes

i) Ellimination of spectral "problem" regions

It was clearly demonstrated that the orthogonality of any possible unknown spectral contributants must be kept at a maximum. In order to aid this end the analyst should elliminate from the analysis certain regions which are liable to provide strong correlations between standard and unknown spectra. Such regions are the low energy cut-off, the region surrounding the 511 keV positron annihilation peak and possibly the backscatter peak area. The last is likely only a minor contributant and since the peak can cover a wide range of energies it may be felt that the loss in information does not justify the gain in orthogonality.

ii) Instrumental Effects

There are several problems related to the collection of the spectral data which will influence the results of the analysis. Most of these problems are due to some non-constancy of the system. One of the most familiar of these difficulties is the problem of analyser gain and zero shift. Because of the high resolution of the Ge(Li) detector the effects of both gain and zero shift on the analysis may be understood as they apply to individual peaks in the filtered spectrum. Ordinary shifts will not alter the peak shape

greatly. The predominant effect is the peak controid shift. This centroid shift corresponds with a non zero lag "r" in the cross correlation of the shifted spectral peaks.

$$d(r) = \int_{\varepsilon} s(E+r)b_i(E)\,dE$$

The effect of the non zero lag will be to reduce the cross correlation term and the error introduced by the shift is expected to be proportional to this reduction.

$$k_{measured} = \frac{d(r)}{d(o)}$$

Fig. 3.3.4a shows the auto correlation as a function of lag for a single Ge(Li) spectrum. Fig. 3.3.4b shows the relationship between analyser zero shift and analysed amount of one unit of a standard. The similarity of these two figures indicates the validity of the above relationship.

A second set of problems fall under the heading "Geometrical effects" and includes such things as position of the sample and standards in the reactor core for irradiation, power level of the reactor, length of irradiation

Fig. 3.3.4a

Auto Correlation of the ^{82}Br Spectrum

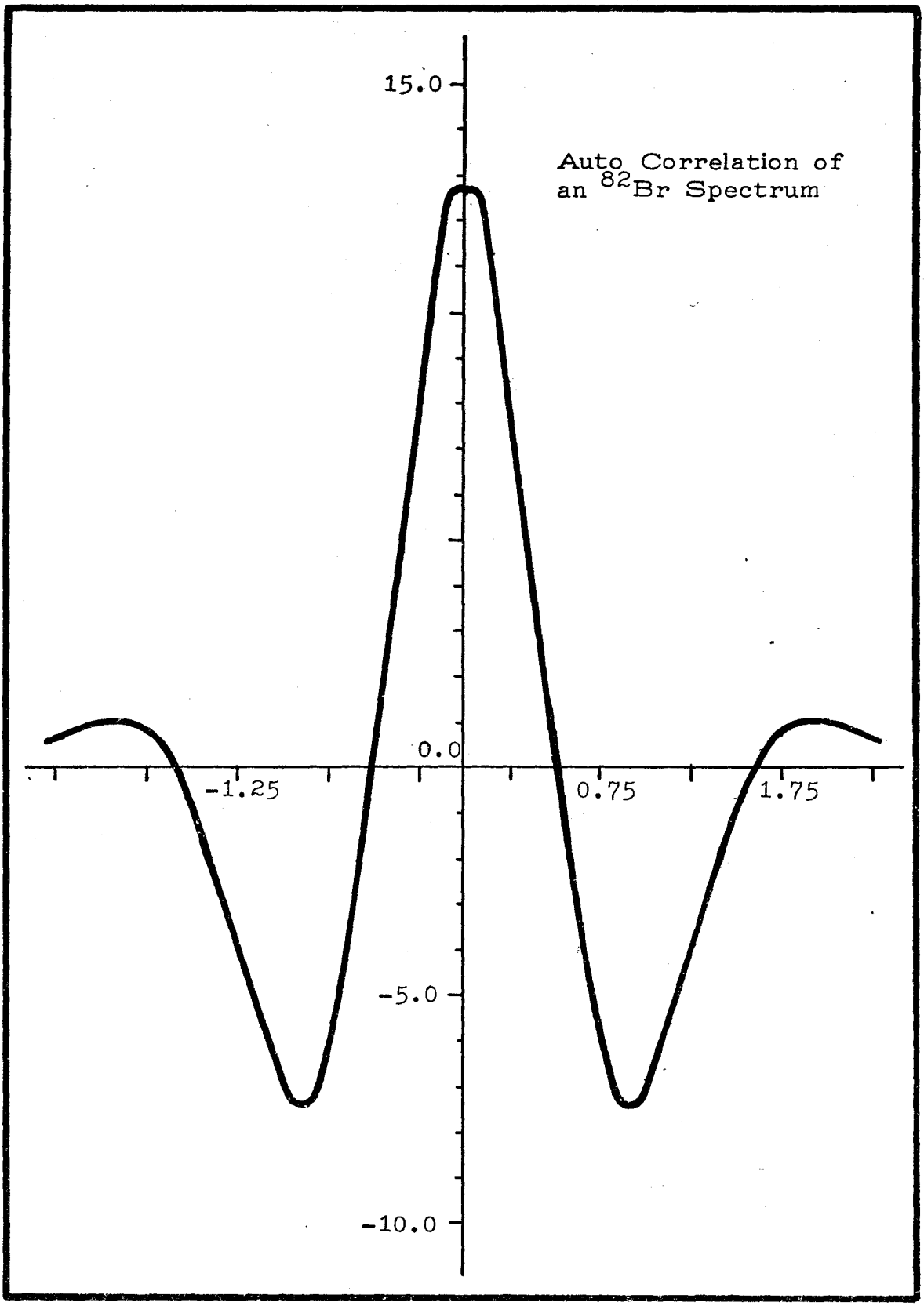
15.0
Auto Correlation of
an ^{82}Br Spectrum
0.0
-1.25
0.75
1.75
-5.0
-10.0

Fig. 3.3.4b

This diagram shows the relative amount of a standard element (^{77}Ge) found by the cross correlation technique as a function of Analyser Zero Position.

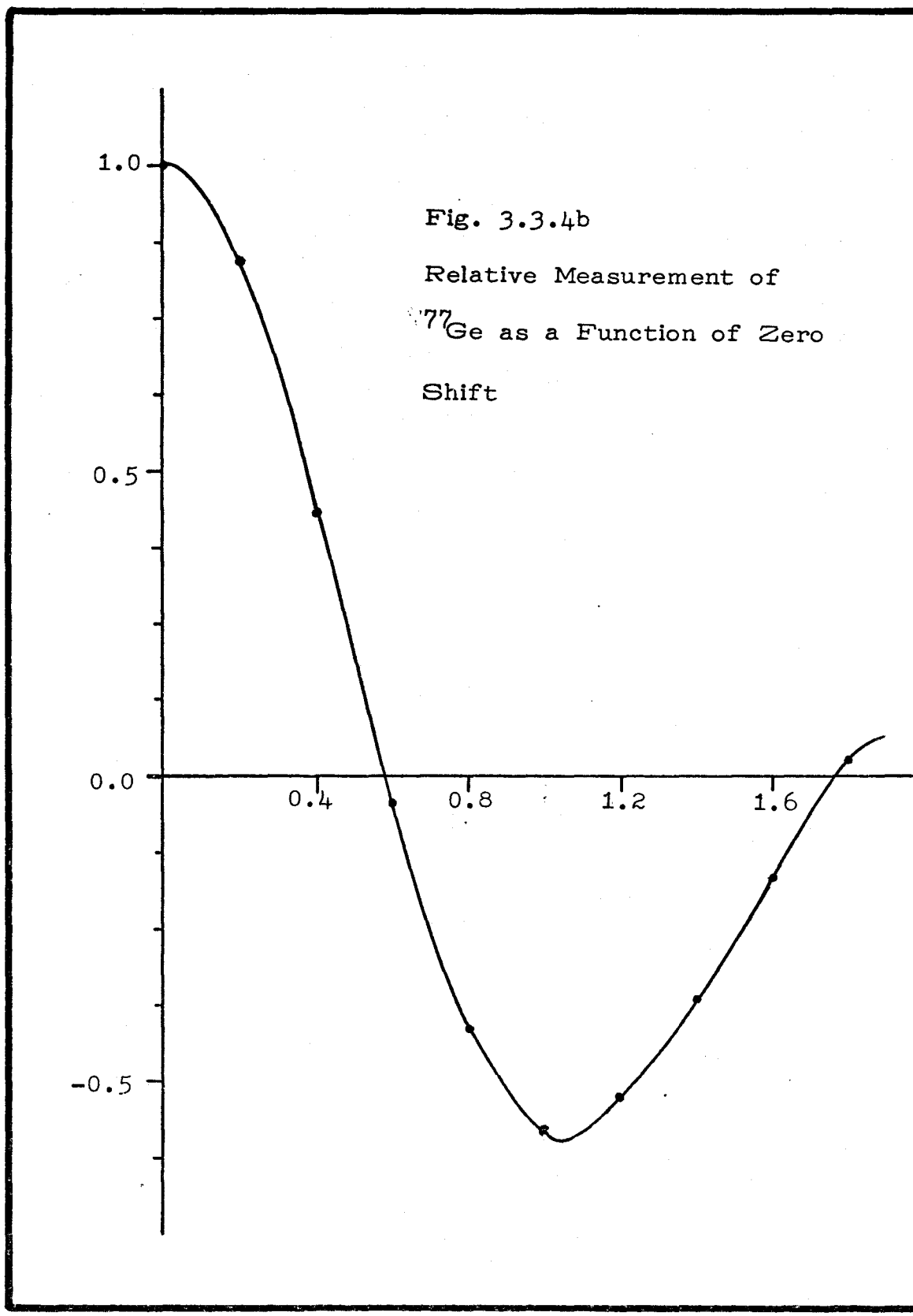

Fig. 3.3.4b

Relative Measurement of ^{77}Ge as a Function of Zero Shift

time and differences of self shielding effects between the samples and the standards. Also included are counter geometry and differences in counting rates. If these effects can not be maintained constant then they must be monitored and corresponding adjustments made to the data.

If the number of samples to be analysed is small it may be possible to irradiate them simultaneously and thus expose them each to the same neutron flux and irradiation time. If this is not possible then it will be necessary to include some form of flux monitoring device. Self shielding effects can be minimized by using very thin standards and samples or by dissolving them in a common solvent. The first method will reduce the self shielding and the second will tend to make it constant for all standards and samples.

When measuring the spectrum the count rate must be maintained at a low enough level to avoid large amounts of random adding (a non-linear effect) and maintain high resolution and at a high enough level to obtain reasonably good statistics. Generally the activities of samples will vary quite widely however and the problem of maintaining a reasonable count rate conflicts with the need to maintain detector geometry. If a flux monitor has been used then the geometry may be changed to accomodate the count rate and a correction ob-

tained by counting the monitor in both the old and new detector configurations.

CHAPTER IV

RESULTS OF SIMULATED SPECTRAL ANALYSIS

To test the accuracy and reliability of the cross correlation procedure and its dependence upon different properties of the spectra five spectra obtained with a Ge(Li) detector were combined in different proportions. Gaussian distributed statistics were then added to the composite spectra by means of a pseudo-random number generator. The five basis spectra ("room background", ^{76}As, ^{82}Br, ^{72}Ga, ^{77}Ge) are shown in Fig. 3.3.3.b in conjunction with the difference spectra.

Of primary interest in the present test was the ability of the correlation technique to identify low intensity components in the presence of high intensity components. Thus the basis spectra were combined in the proportions shown in the "actual quantity" column of Table 4.1a. The composite spectra formed are shown in Fig. 4.1b along with the ^{77}Ge basis spectrum. This spectrum is singled out to draw attention to the degree of overshadadowing of this spectral component by the others. Each of the composite spectra was analysed by the correlation procedure. The results are shown in Table 4.1a. A manual analysis would not even detect the

presence of the ^{77}Ge in Fig. 4.1b$_{iii}$ and yet the cross correlation technique determines the quantity within 30 percent. Although the cross correlation technique does indicate the presence of the ^{77}Ge component in Fig. 4.1b$_{iv}$ to the correct order of magnitude it is clear from the standard deviation that the detection threshold has been reached. Thus it is seen that the cross correlation method offers more sensitivity than a manual analysis.

The relatively large standard deviation associated with the measurement of the room background component is due to the relatively small number of counts in the spectrum as indicated in the total counts column of Table 4.1a.

Table 4.1a

Isotope # 1 - Room Background

Isotope # 2 - ^{76}As

Isotope # 3 - ^{82}Br

Isotope # 4 - ^{72}Ga

Isotope # 5 - ^{77}Ge

	Isotope #	Actual Quantity	Total Counts	Measured Quantity	Standard Deviation	Discrepency
Composite Spectrum #1	1	1.0000	591162	0.99869	0.57000	0.00131
	2	1.0000	6018635	1.00237	0.00830	0.00237
	3	1.0000	5703669	0.99987	0.01800	0.00013
	4	1.0000	4416482	0.99757	0.01300	0.00243
	5	1.0000	6712711	1.00190	0.00650	0.00190

Table 4.1a (con't)

	Isotope #	Actual Quantity	Total Counts	Measured Quantity	Standard Deviation	Discrepency
Composite Spectrum # 2	1	1.0000	591162	0.97454	0.43000	0.02546
	2	1.0000	6018635	1.00812	0.00800	0.00812
	3	1.0000	5703669	1.00724	0.01700	0.00724
	4	1.0000	4416482	0.99422	0.01300	0.00578
	5	0.1000	671271	0.10350	0.00410	0.00350
Composite Spectrum # 3	1	1.0000	591162	0.97313	0.42000	0.02687
	2	1.0000	6018635	1.00811	0.00790	0.00811
	3	1.0000	5703669	1.00717	0.01700	0.00717
	4	1.0000	4416482	0.99427	0.01300	0.00573
	5	0.0100	67127	0.01281	0.00370	0.00281

Table 4.1a (con't)

	Isotope #	Actual Quantity	Total Counts	Measured Quantity	Standard Deviation	Discrepency
Composite Spectrum # 4	1	1.0000	591162	0.97193	0.42000	0.02807
	2	1.0000	6018635	1.00812	0.00790	0.00812
	3	1.0000	5703669	1.00716	0.01700	0.00716
	4	1.0000	4416482	0.99430	0.01300	0.00570
	5	0.0010	6713	0.00373	0.00370	0.00273
Composite Spectrum # 5	1	1.0000	591162	0.98534	0.26000	0.01466
	2	1.0000	6018635	1.00781	0.00740	0.00781
	3	0.0100	57037	0.01204	0.01200	0.00204
	4	0.0100	44165	0.00623	0.00350	0.00377
	5	0.0100	67127	0.01181	0.00250	0.00181

Fig. 4.1b

Composite Spectra Compared with ^{77}Ge Reference

Fig. b_i - Composite contains 1.0000 unit ^{77}Ge

Fig. b_{ii} - Composite contains 0.1000 unit ^{77}Ge

Fig. b_{iii} - Composite contains 0.0100 unit ^{77}Ge

Fig. b_{iv} - Composite contains 0.0010 unit ^{77}Ge

Fig. b_v - Composite contains 0.01000 unit ^{77}Ge

In all figures except b_v there is 1.0 units of each of the other components. In Fig. b_v the background and ^{76}As are present in 1.0 unit quantities while ^{82}Br and ^{72}Ga are present in 0.010 unit quantities.

Fig. $4.1b_i$

Composite Spectrum # 1

Components: Room Background : 1.0000 units

^{76}As : 1.0000 units

^{82}Br : 1.0000 units

^{72}Ga : 1.0000 units

^{77}Ge : 1.0000 units

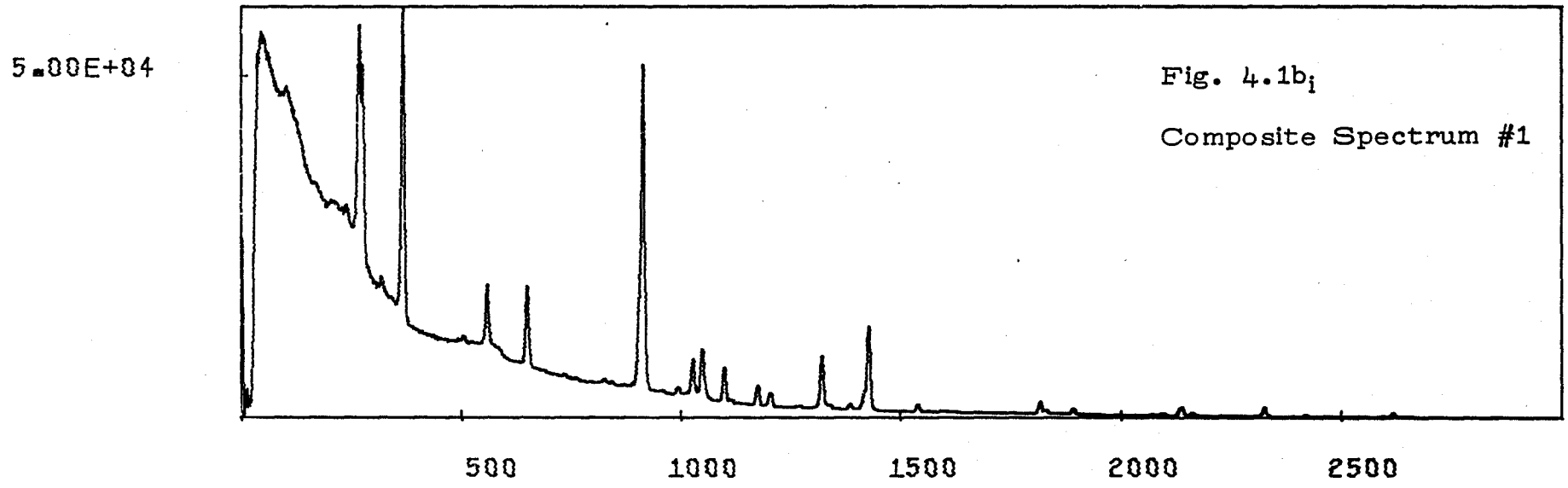

Fig. 4.1b$_i$

Composite Spectrum #1

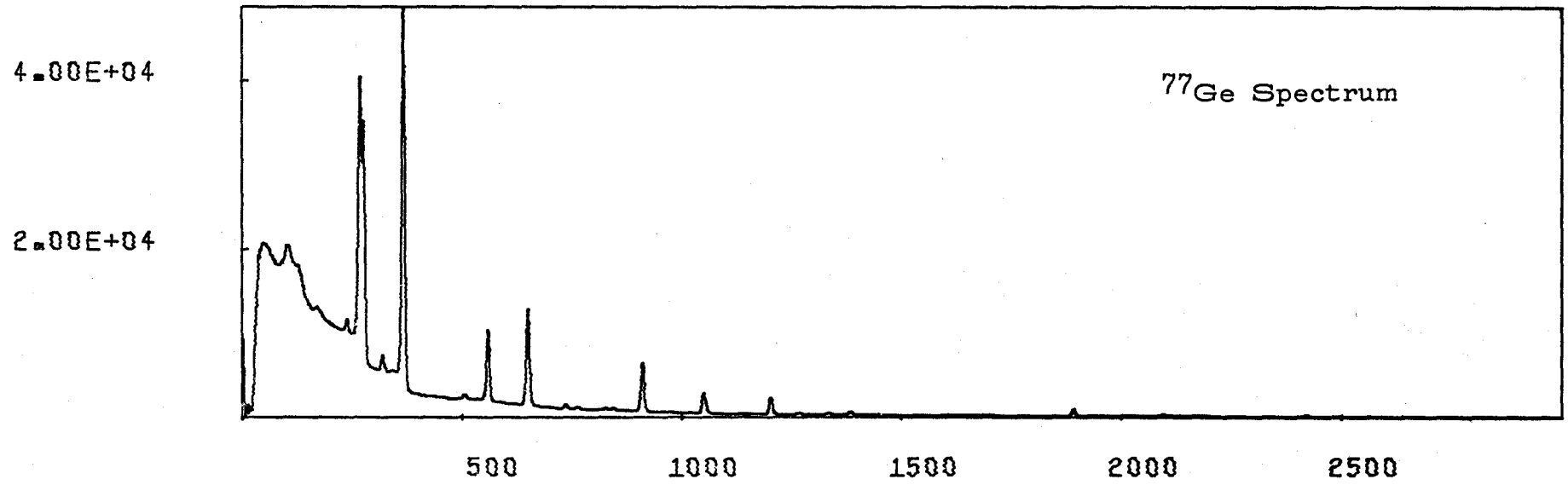

^{77}Ge Spectrum

Fig. $4.1b_{ii}$

Composite Spectrum # 2

Components: Room Background : 1.0000 units

^{76}As : 1.0000 units

^{82}Br : 1.0000 units

^{72}Ga : 1.0000 units

^{77}Ge : 0.1000 units

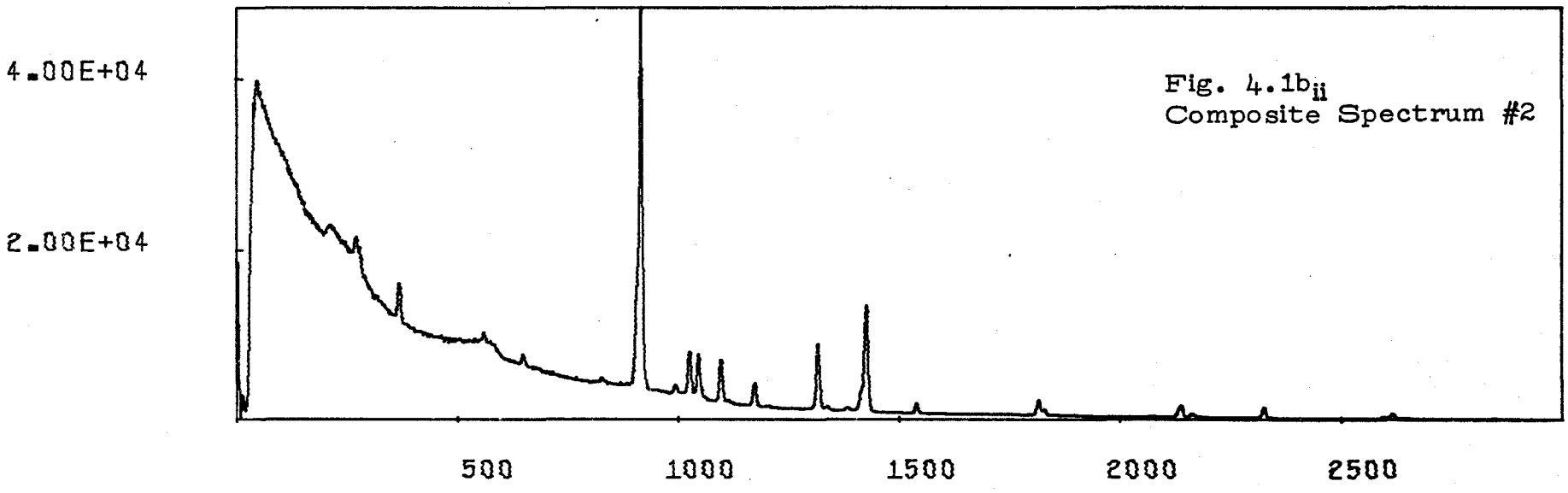

Fig. $4.1b_{ii}$
Composite Spectrum #2

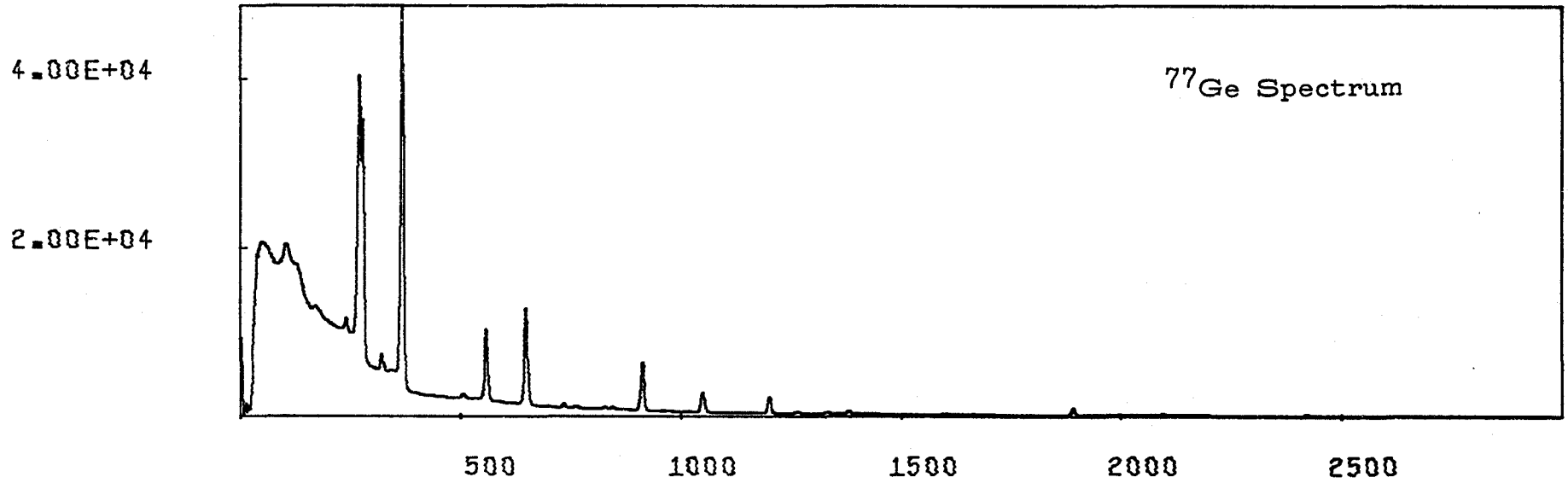

^{77}Ge Spectrum

Fig. 4.1b$_{iii}$ –

Composite Spectrum # 3

Components: Room Background : 1.0000 units

^{76}As : 1.0000 units

^{82}Br : 1.0000 units

^{72}Ga : 1.0000 units

^{77}Ge : 0.0100 units

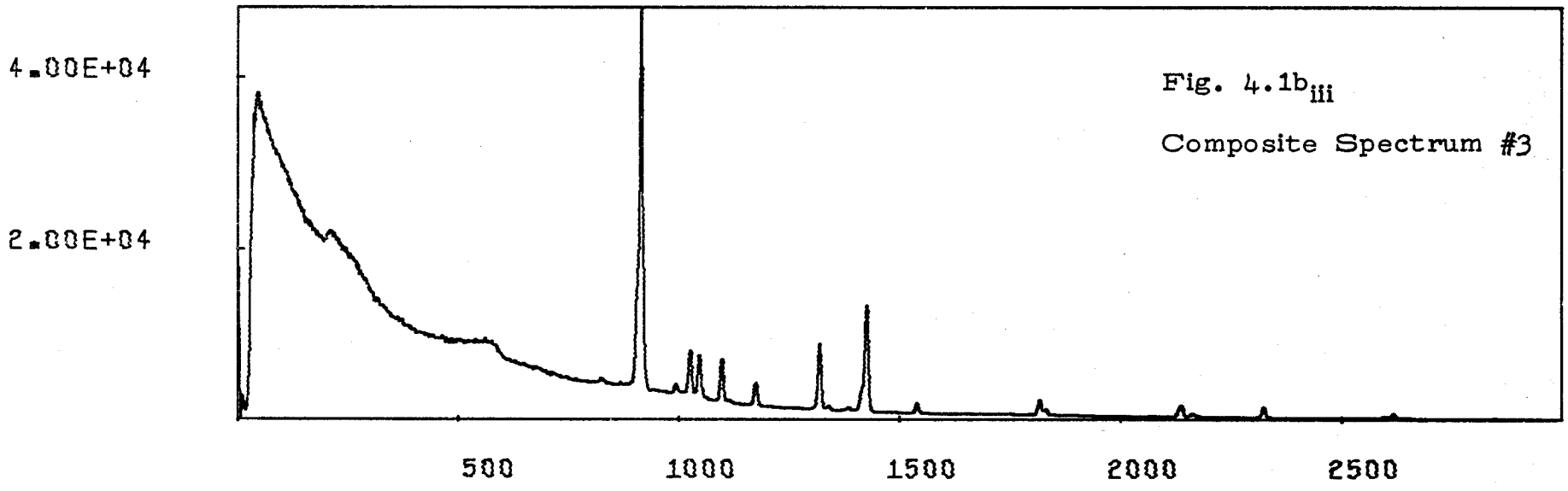

Fig. 4.1b$_{iii}$

Composite Spectrum #3

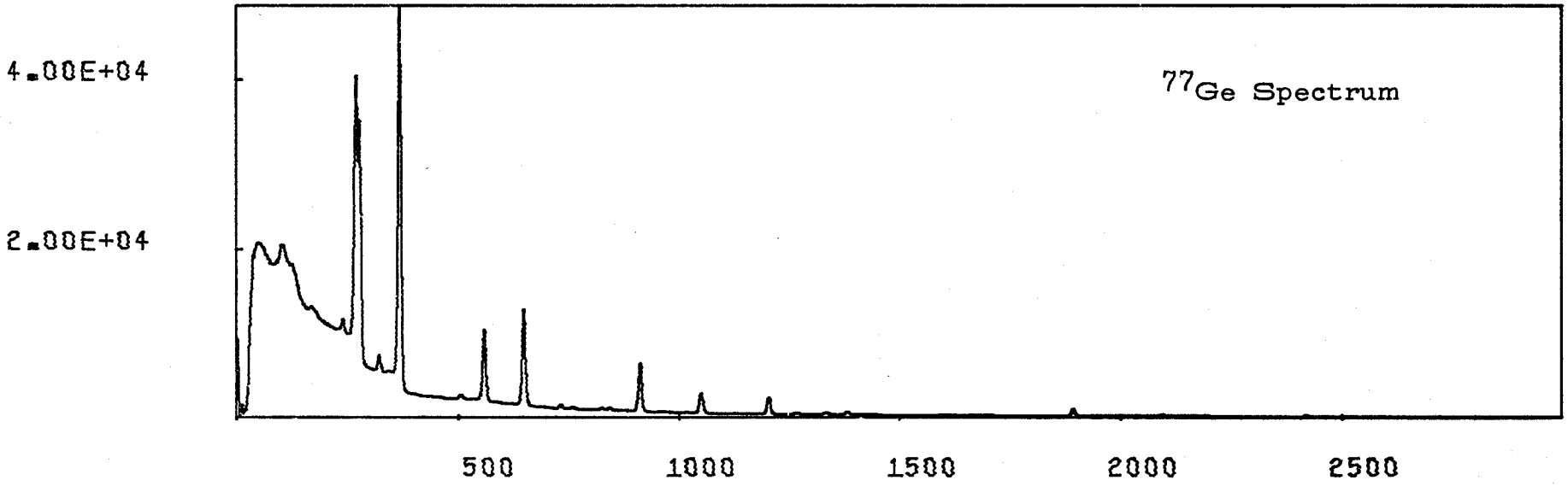

^{77}Ge Spectrum

Fig. 4.1b$_{iv}$

Composite Spectrum # 4

Components: Room Background : 1.0000 units

^{76}As : 1.0000 units

^{82}Br : 1.0000 units

^{72}Ga : 1.0000 units

^{77}Ge : 0.0010 units

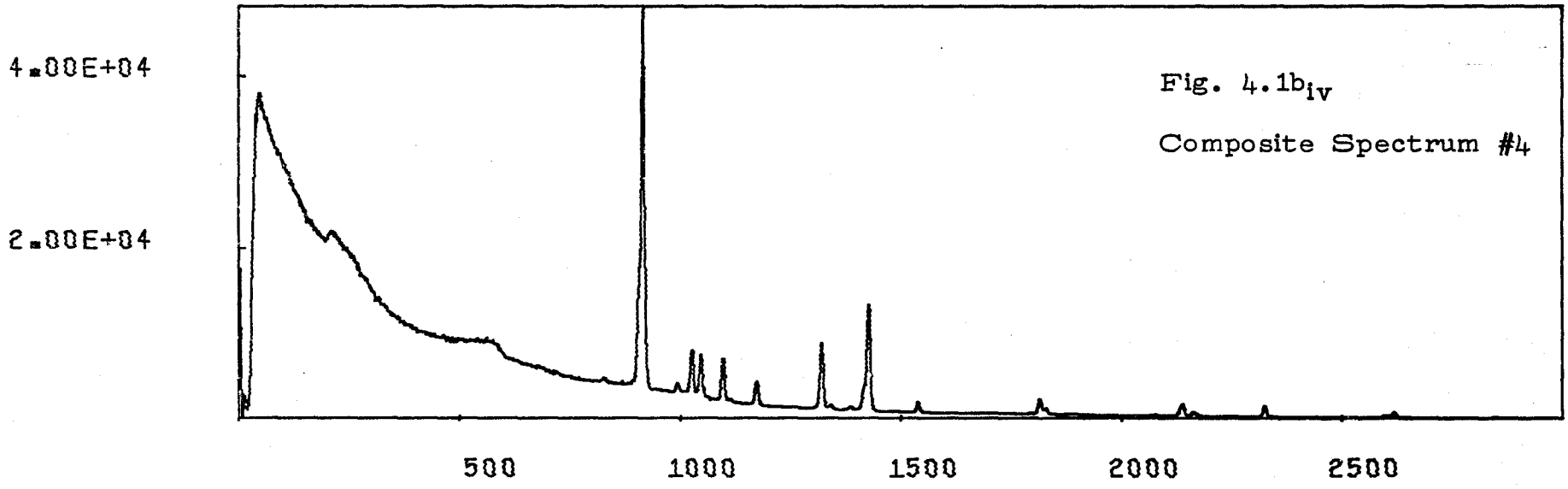

Fig. $4.1b_{iv}$

Composite Spectrum #4

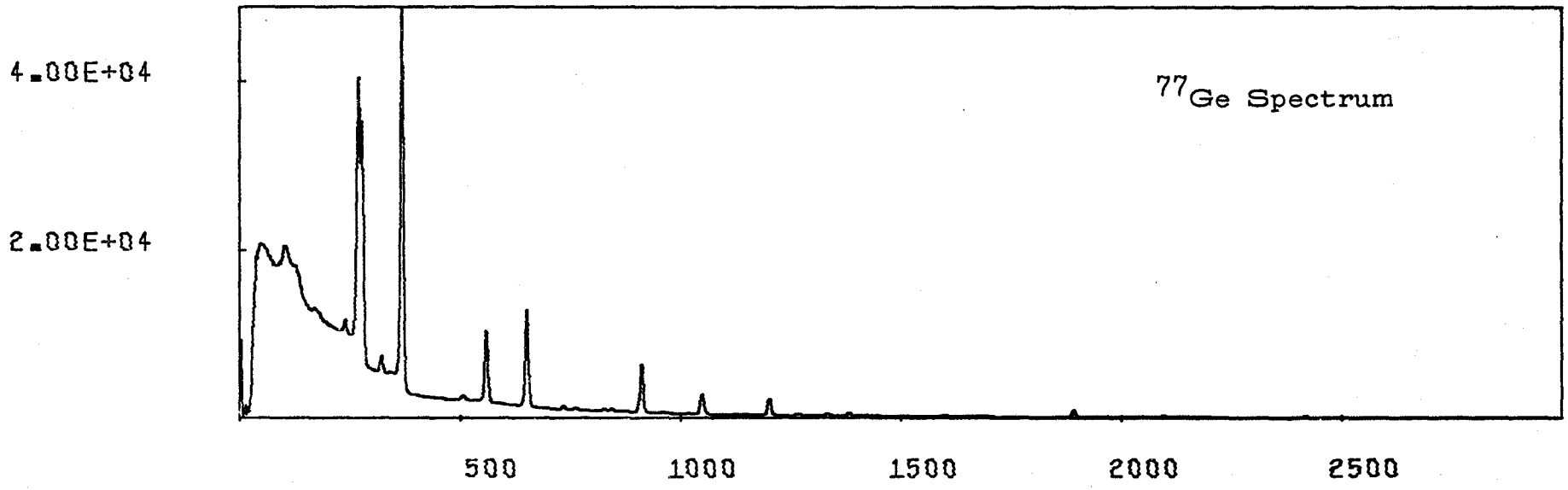

^{77}Ge Spectrum

Fig. $4.1b_v$ –

Composite Spectrum # 5

Components: Room Background : 1.0000 units

^{76}As : 1.0000 units

^{82}Br : 0.0100 units

^{72}Ga : 0.0100 units

^{77}Ge : 0.0100 units

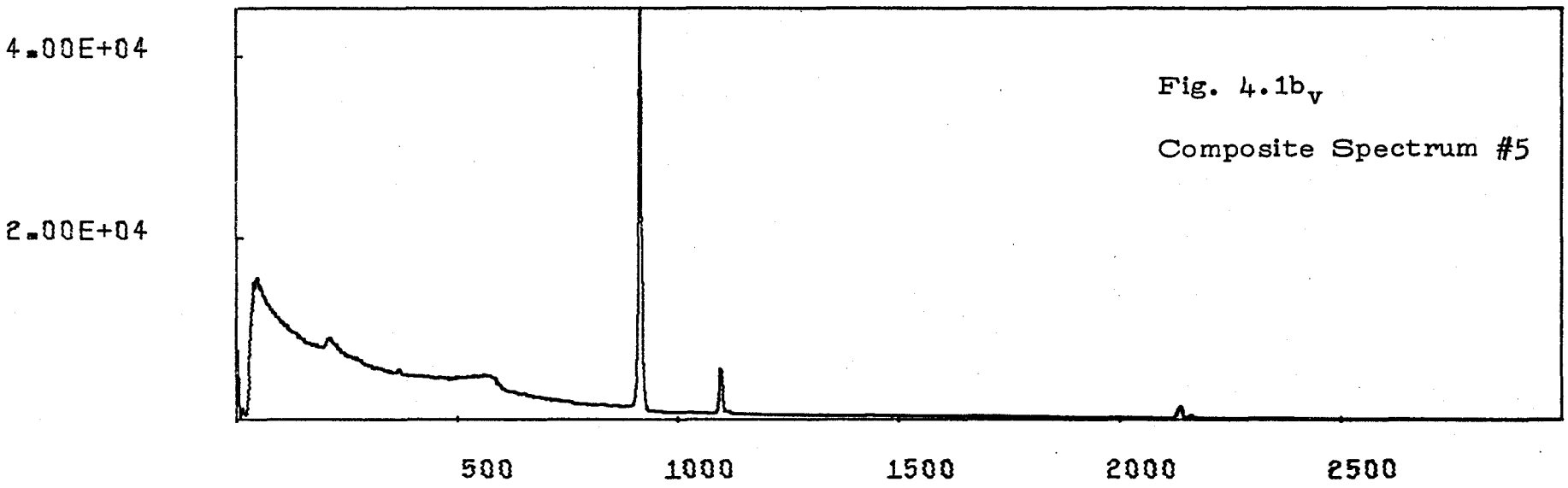

Fig. 4.1b$_v$

Composite Spectrum #5

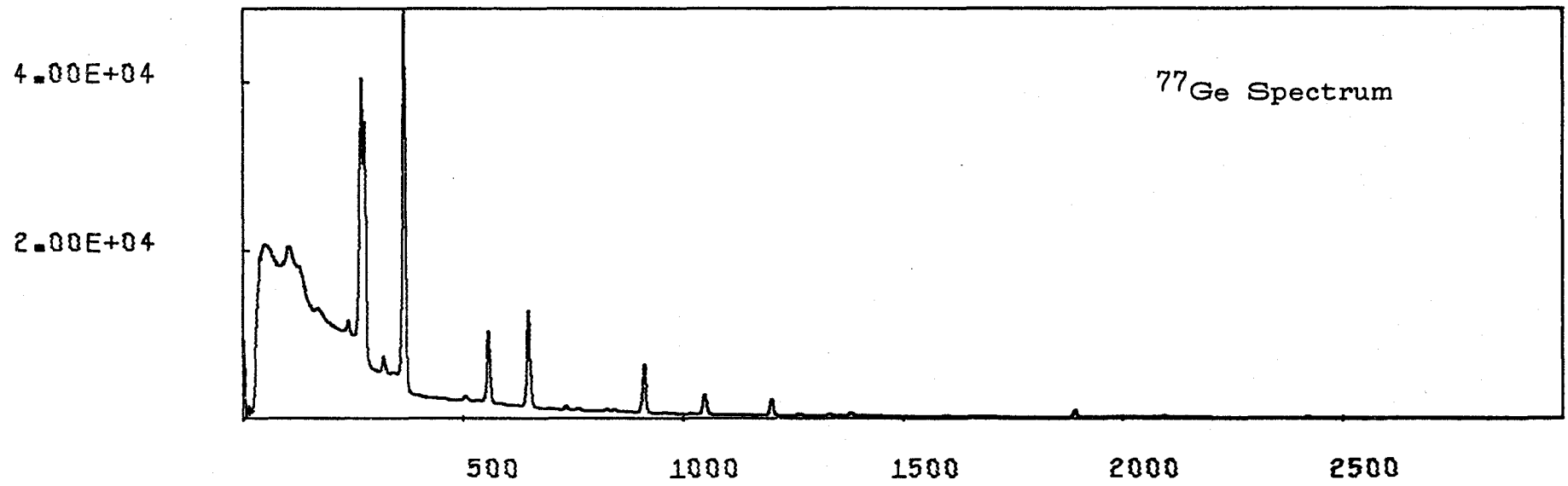

^{77}Ge Spectrum

CHAPTER V

CONCLUSION

In the previous chapters a system for automatic activation analysis has been described. The data reduction algorithm has been developed particularly for small computer systems and this has led to a number of shortcuts for saving memory space and CPU time. The use of the rectangular zero-area filter rather than the exact matched filter saves both memory and CPU time by avoiding the necessity for floating point arithmetic (Section 3.2.2). Time was also saved by avoiding the use of a weighting vector in the cross correlation analysis (Section 3.2.3). The approximate calculation of standard deviations yielded a saving of a factor of 100 to 1000 in CPU time over the standard method of calculation (Section 3.3.1).

It was demonstrated in Chapter IV that the cross correlation technique is more sensitive than manual analysis. Further, it was shown that the effect of any components not included in the analysis may be easily evaluated by examination of a difference spectrum (Section 3.3.3).

Although the method of data reduction was developed

for use with neutron activation spectra it will also be applicable to any similar form of spectral data. In particular it is expected that the method will be applicable to analysis of flame photometry spectra.

It is believed that the analysis system which has been described will form a valuable tool for large volume elemental analysis.

APPENDIX A

ANALYSER - COMPUTER INTERFACE

A.1 Description of Operation

In order to provide rapid data reduction for gamma-ray spectra obtained in activation analysis, an interface was developed to transfer such information from a ND-160 pulse height analyser to a PDP-15 computer. The objective was to design the minimal linkage consistent with the realistic requirements that could be identified for attaining high volume activation analysis. It was decided that accumulated spectra would normally require a block transfer and hence the analyser address register would advance incrementally. Therefore provision for address reset and increment were the only necessary signals to this register. The memory cycle time of the ND-160 and the large number of functions required for reading or writing into memory made the time loss due to a serial transfer between assembly buffers insignificant. The bi-directional transfer provides the computer with an additional 4-K of memory accessable through the accumulator. The option of local or on-line control of the ND-160 was felt necessary in order to make the most efficient use of both the

ND-160 and the PDP-15 while still providing the possibility of completely automatic control.

Local or manual control of the analyser is realized through the use of a 4-position switch which sets the state of a two-bit internal register. The two binaries are identified as analyse "A" and readout "R". The four states are analyse ($A \circ \overline{R}$), readout ($\overline{A} \circ \overline{R}$), stop-1 ($\overline{A} \circ \overline{R}$) and stop-2 (Indeterminate). External control is achieved by selecting the stop-2 mode and providing independent inputs to the A and R registers. The independent inputs are derived from a two bit count up interface register whose state is established by a series of I/O pulses from the computer. This register and the ND-160 address register are reset by a single I/O pulse. A diagram indicating the states of the analyser under local or remote control is shown in Fig. A.1a.

Data transfers between the 18 bit PDP-15 accumulator (AC) and the 18 bit ND-160 memory buffer (MB), AC→MB or MB→AC proceed as shown in Fig. A.1b. Parallel transfers are made from the AC (or the MB) to the accumulator buffer (ACB) (or the analyser buffer (MBB)). The buffer registers are shift registers and the transfers ACB→MBB or MBB→ACB are serial. Through multiplexing,

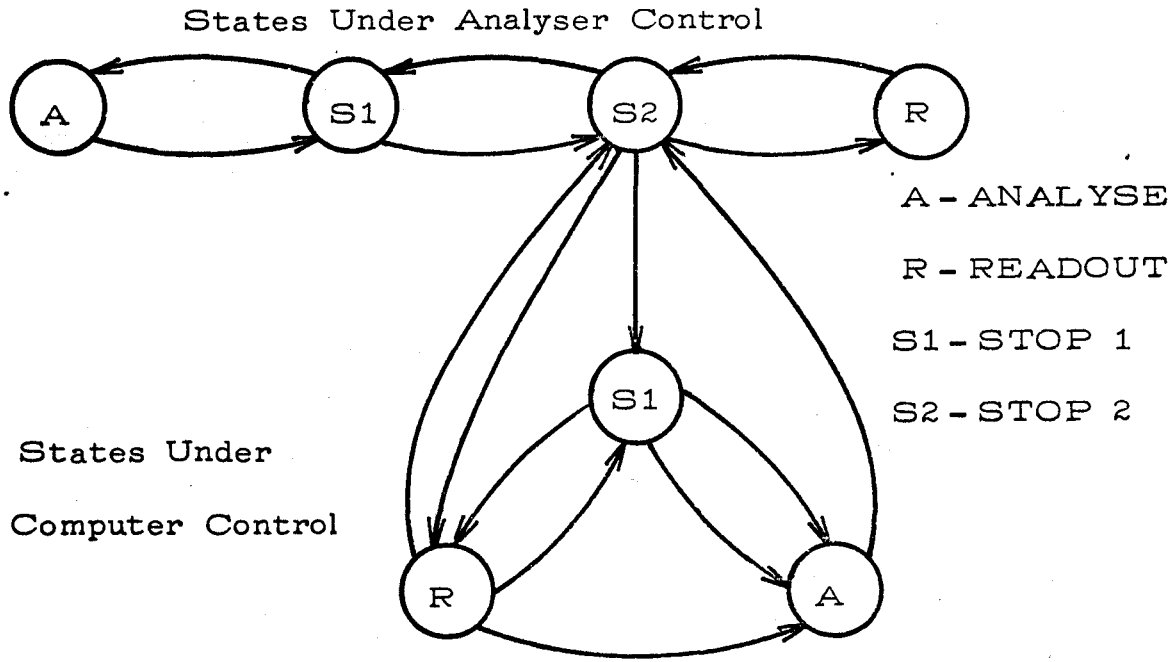
States Under Analyser Control
A
S1
S2
R
A - ANALYSE
R - READOUT
S1 - STOP 1
S2 - STOP 2
S1
States Under
Computer Control
R
A

Fig. A.1a

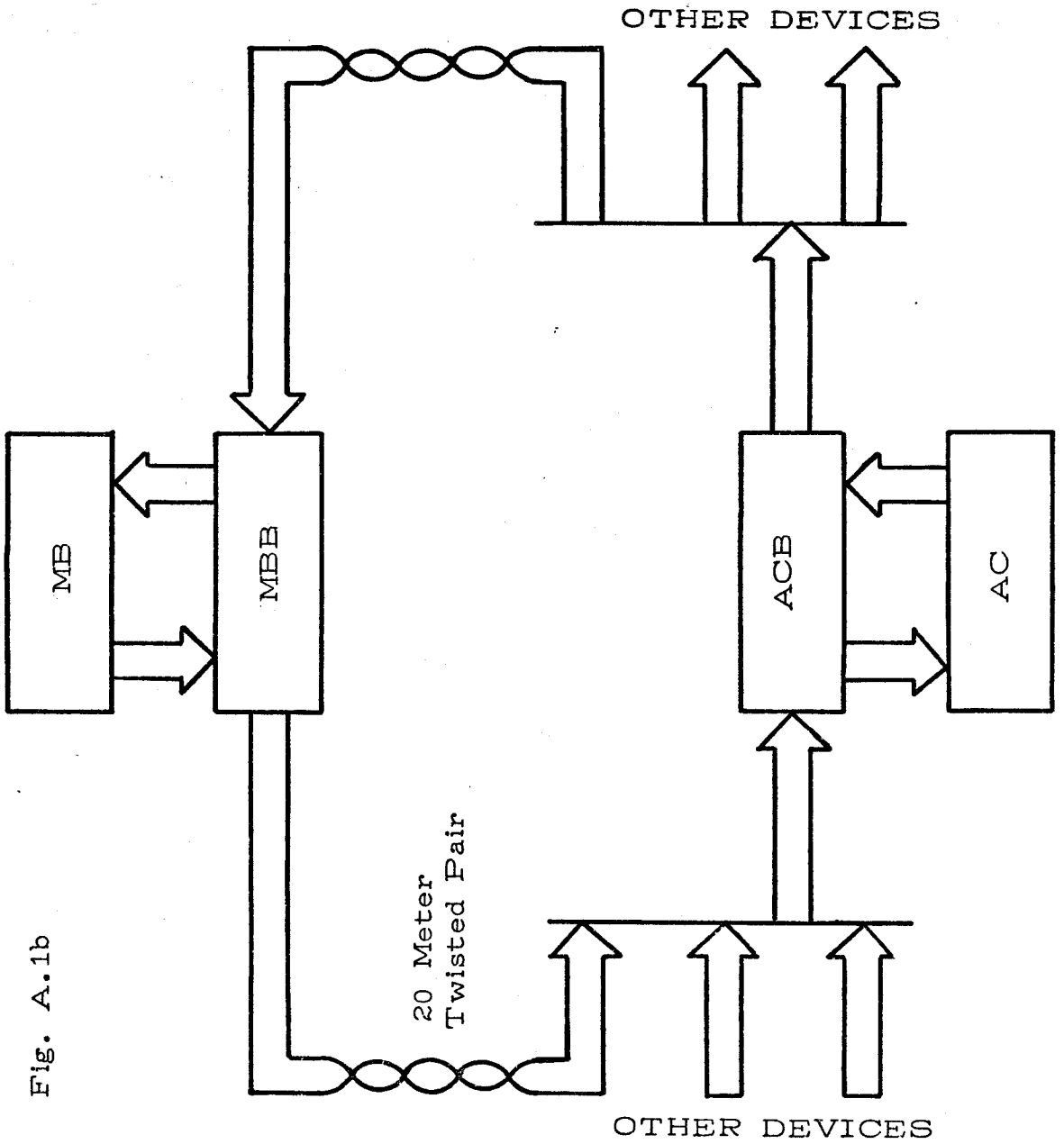
OTHER DEVICES
MB
MBB
ACB
AC
20 Meter
Twisted Pair
OTHER DEVICES

Fig. A.1b

several peripherals can communicate with the AC via the ACB.

Parallel transfers between the accumulator and the accumulator buffer are achieved by one I/O pulse from the computer (4μsec.). Serial transfers between the two buffer registers are initiated by a computer I/O pulse and require 16μsec. to be completed. A developed hardware programmer provides the gated train of shift pulses at a rate of 1.2 MHz to achieve the serial transfer. Transfers between the MB and the MBB require 5 steps. As in the case of the mode control, these steps are generated by an I/O pulse feeding a 3 bit count-up register and decoder. The register is preset by selecting one of the two possible transfer modes: Read MB→MBB or Write MBB→MB. The functions enabled or executed during each state are produced using the circuit shown in Fig. A.2k.

Before writing into the ND-160 memory, it must be set to zero since the R/W cycle results in an inclusive OR with the MB and the accessed location. This is accomplished by performing R/W cycles with the erase toggle enabled, thus holding the MB register in the zero state during the entire cycle. Following complete erasure of the memory, data are transferred into the MB following the read portion of each

cycle.

In order to complement the system with a view to fully automating it, program interrupt and skip facilities have been included. Program interrupt requests are issued either manually or automatically. Manual requests are made by means of a front panel push button. An automatic interrupt arises when the analyser live time has reached a preset value. This mode is enabled through a toggle switch mounted at the analyser station. Flag status may be checked to identify the two preceding conditions by means of a program skip instruction. A skip flag is also set when the analyser is in digital readout mode. This condition must be satisfied before a successful data transfer can take place.

A.2 Schematic Diagrams

The diagrams included on the following pages are divided into two sections:

i. The circuitry at the computer station

ii. The circuitry at the analyser station

i. The Computer Station

Fig. A.2a The Device Selector

Fig. A.2b The Instruction Decoder

Fig. A.2c The Data Flow Controller

Fig. A.2d Interrupt and Skip Logic (Computer)

Fig. A.2e Accumulator Buffer Unit

Fig. A.2f Accumulator Buffer Assembly

Fig. A.2g Output Line Drivers

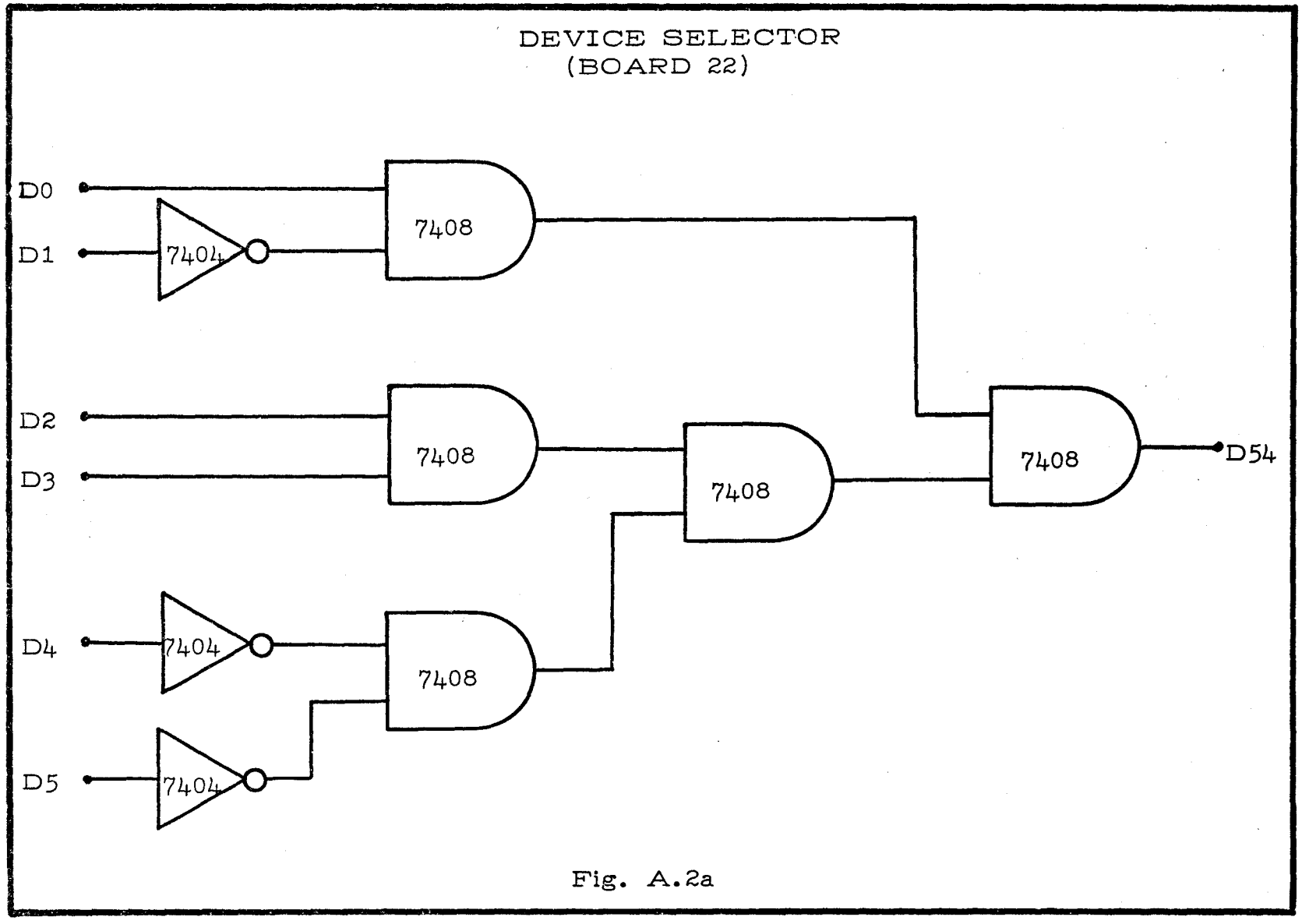
DEVICE SELECTOR
(BOARD 22)
D0
D1
7404
7408
D2
D3
7408
7408
7408
D54
D4
7404
7408
D5
7404

Fig. A.2a

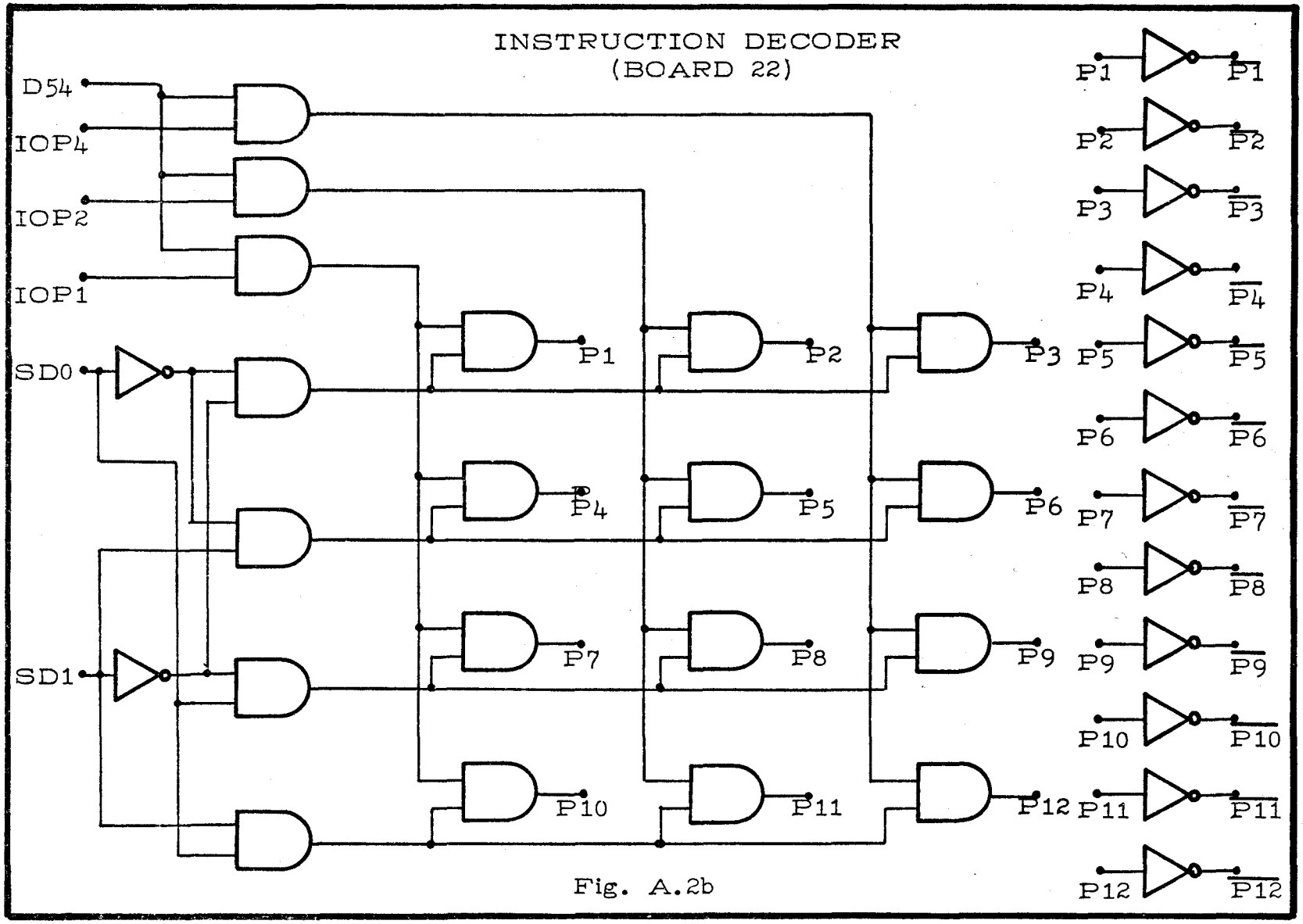
INSTRUCTION DECODER
(BOARD 22)
D54
IOP4
IOP2
IOP1
SD0
SD1
P1
P2
P3
P4
P5
P6
P7
P8
P9
P10
P11
P12
P1
P2
P3
P4
P5
P6
P7
P8
P9
P10
P11
P12

Fig. A.2b

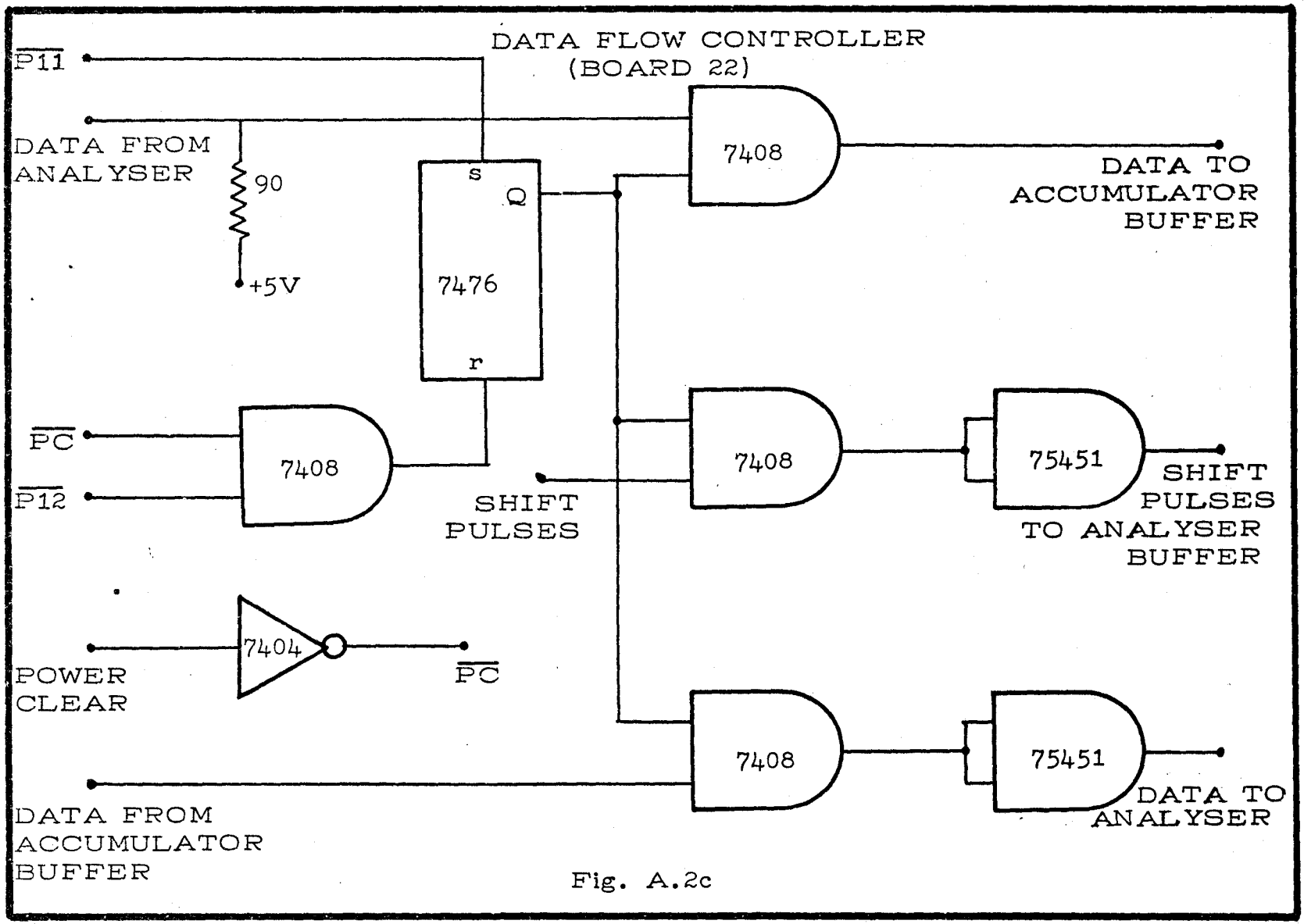
DATA FLOW CONTROLLER
(BOARD 22)
P11
DATA FROM
ANALYSER
90
+5V
S
Q
7476
r
7408
DATA TO
ACCUMULATOR
BUFFER
PC
P12
7408
SHIFT
PULSES
7408
75451
SHIFT
PULSES
TO ANALYSER
BUFFER
7404
POWER
CLEAR
PC
7408
75451
DATA TO
ANALYSER
DATA FROM
ACCUMULATOR
BUFFER

Fig. A.2c

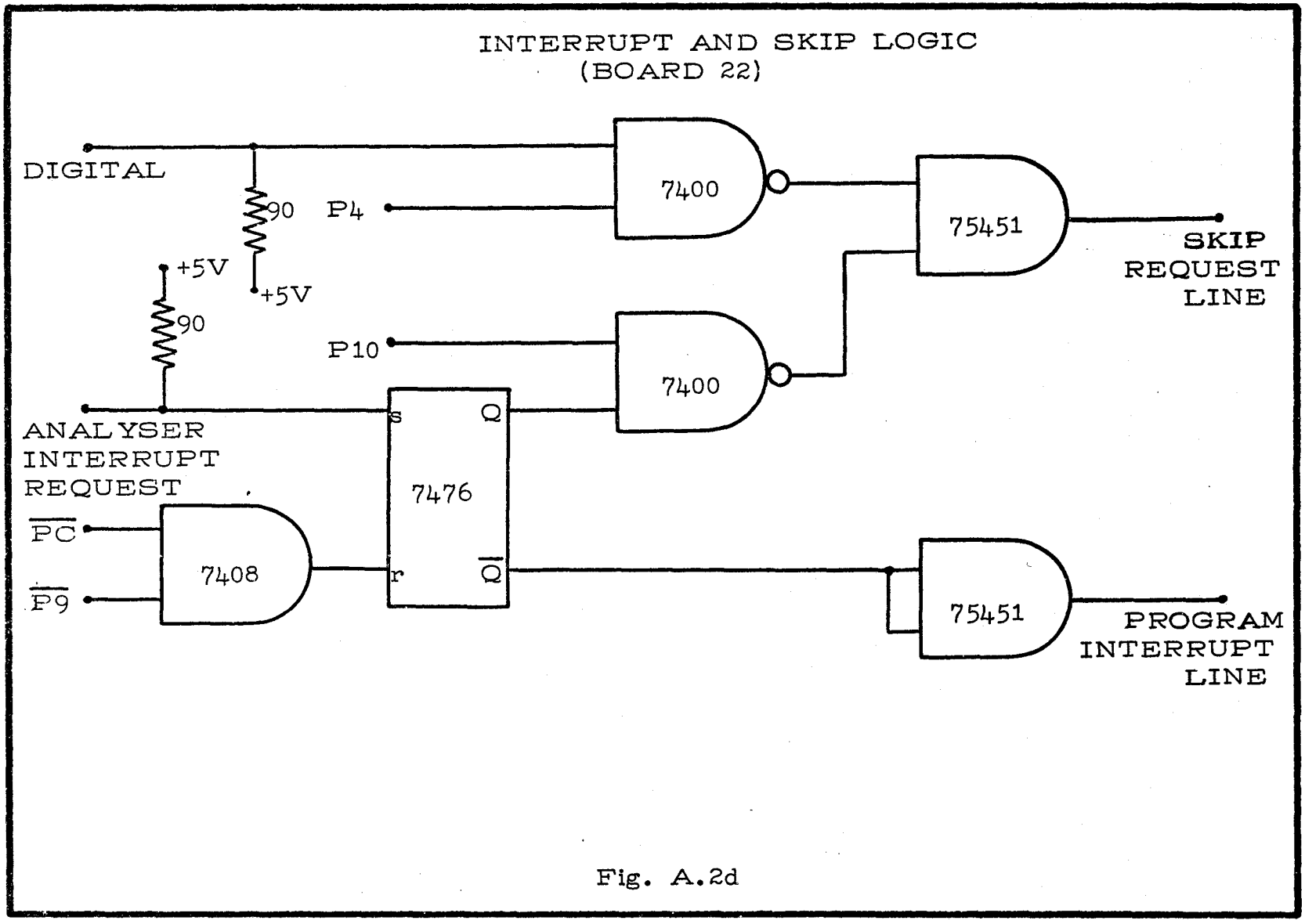
INTERRUPT AND SKIP LOGIC
(BOARD 22)
DIGITAL
90
P4
7400
75451
SKIP
REQUEST
LINE
+5V
+5V
90
P10
7400
ANALYSER
INTERRUPT
REQUEST
S
Q
7476
PC
7408
P9
r
Q
75451
PROGRAM
INTERRUPT
LINE

Fig. A.2d

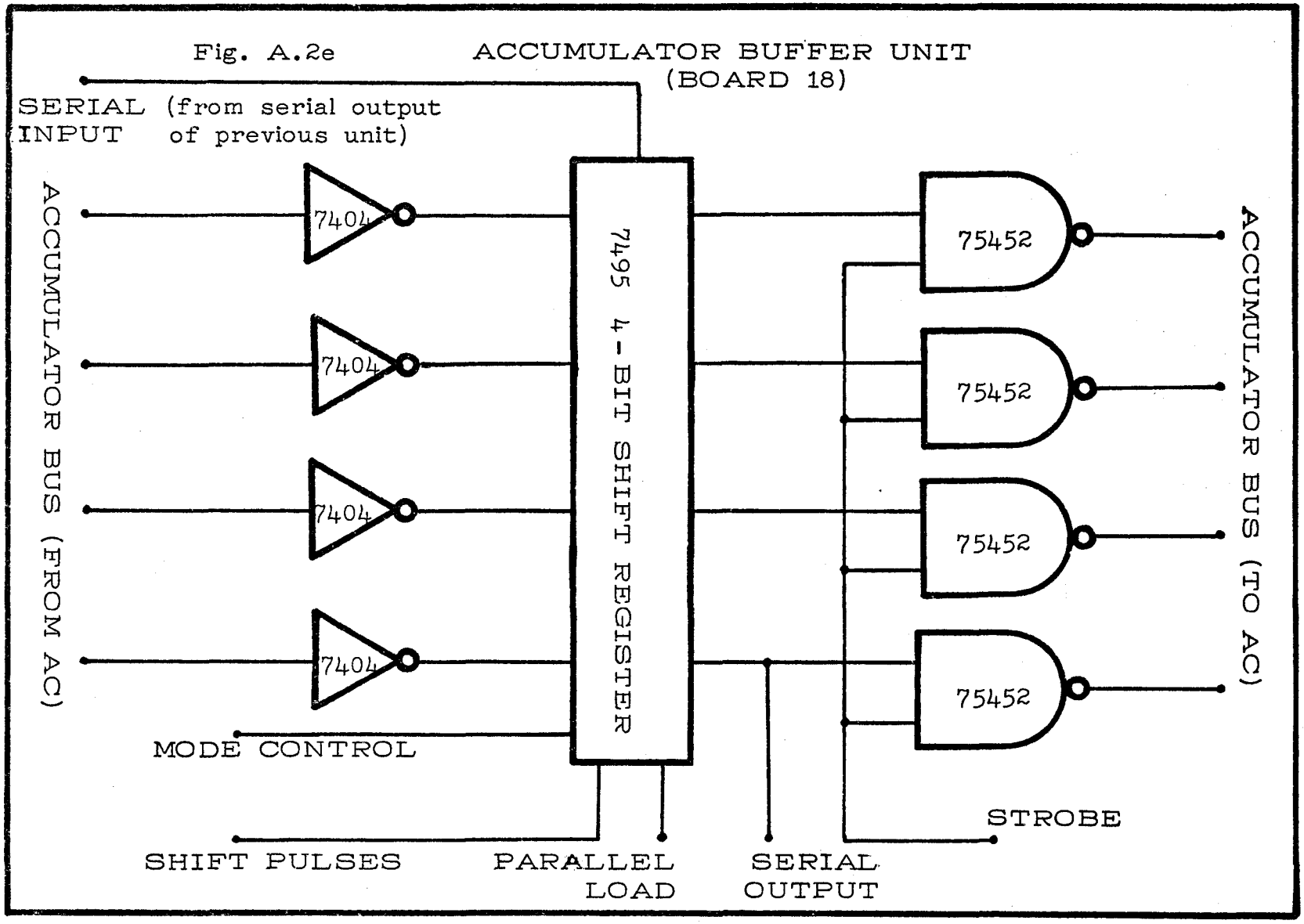
Fig. A.2e
ACCUMULATOR BUFFER UNIT
(BOARD 18)
SERIAL INPUT (from serial output of previous unit)
ACCUMULATOR BUS (FROM AC)
7404
7404
7404
7404
7495 4-BIT SHIFT REGISTER
75452
75452
75452
75452
ACCUMULATOR BUS (TO AC)
MODE CONTROL
STROBE
SHIFT PULSES
PARALLEL LOAD
SERIAL OUTPUT

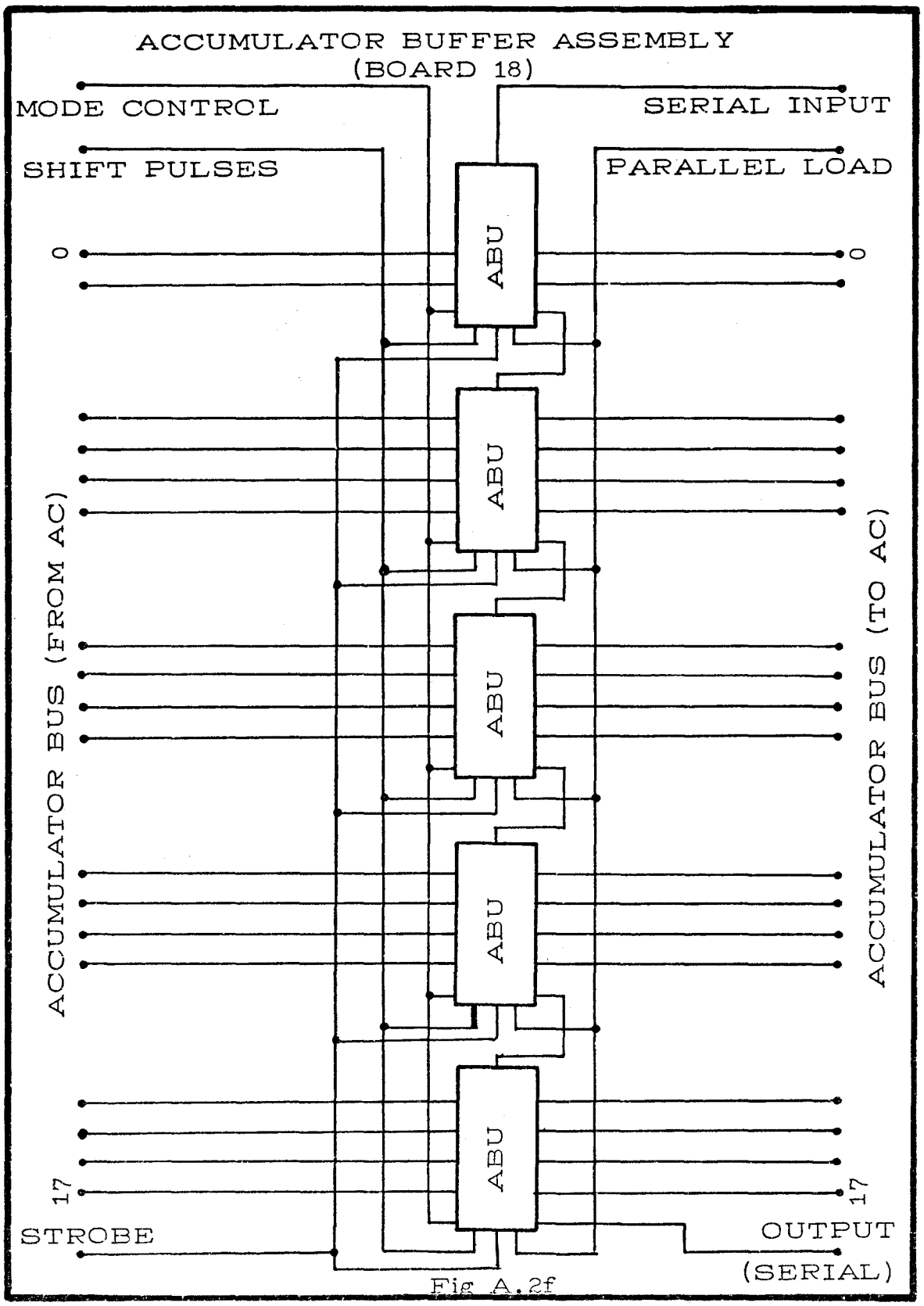
ACCUMULATOR BUFFER ASSEMBLY
(BOARD 18)
MODE CONTROL
SERIAL INPUT
SHIFT PULSES
PARALLEL LOAD
0
0
ABU
ABU
ABU
ABU
ABU
ACCUMULATOR BUS (FROM AC)
ACCUMULATOR BUS (TO AC)
17
17
STROBE
OUTPUT
(SERIAL)

Fig A.2f

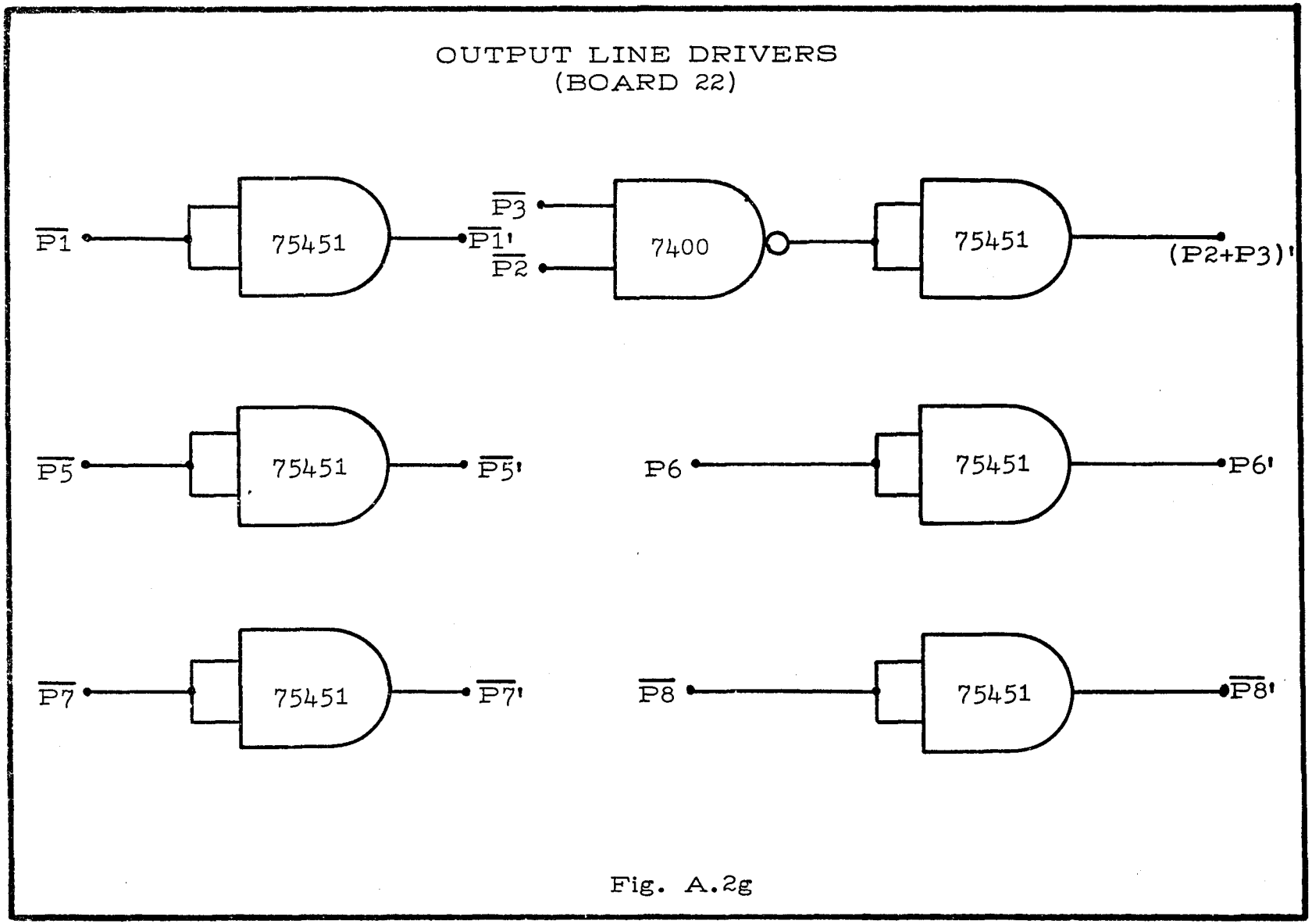
OUTPUT LINE DRIVERS
(BOARD 22)
P1
75451
P1'
P3
P2
7400
75451
(P2+P3)'
P5
75451
P5'
P6
75451
P6'
P7
75451
P7'
P8
75451
P8'

Fig. A.2g

ii. The Analyser Station

Fig. A.2h Analyser Buffer Unit

Fig. A.2i Analyser Buffer Assembly

Fig. A.2j Analyser Mode Controller

Fig. A.2k Read-Write Status Controller

Fig. A.2l Interrupt and Skip Logic (Analyser)

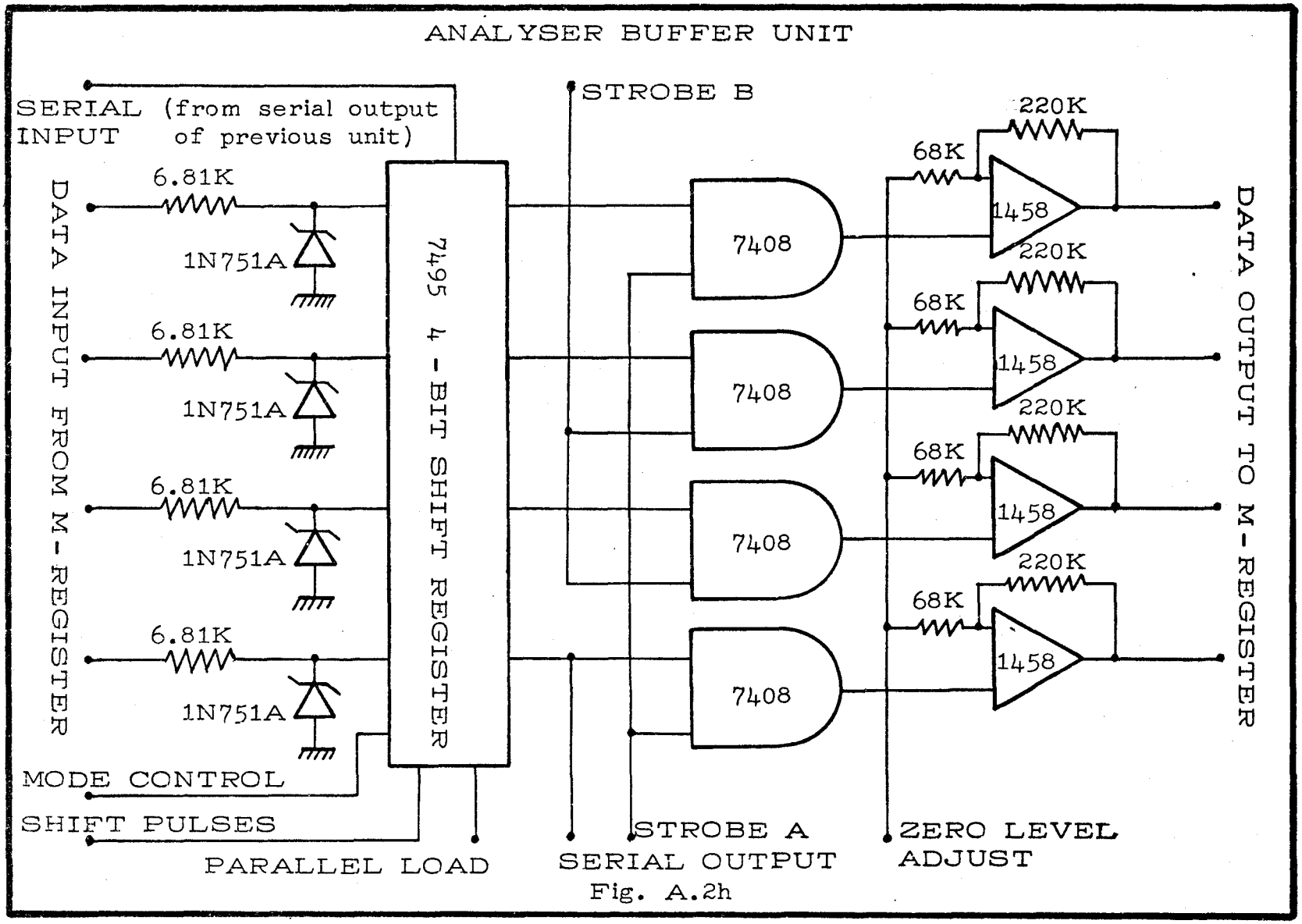
ANALYSER BUFFER UNIT
SERIAL INPUT (from serial output of previous unit)
STROBE B
DATA INPUT FROM M-REGISTER
6.81K
1N751A
7495 4-BIT SHIFT REGISTER
7408
68K
220K
1458
DATA OUTPUT TO M-REGISTER
MODE CONTROL
SHIFT PULSES
PARALLEL LOAD
STROBE A
SERIAL OUTPUT
ZERO LEVEL ADJUST

Fig. A.2h

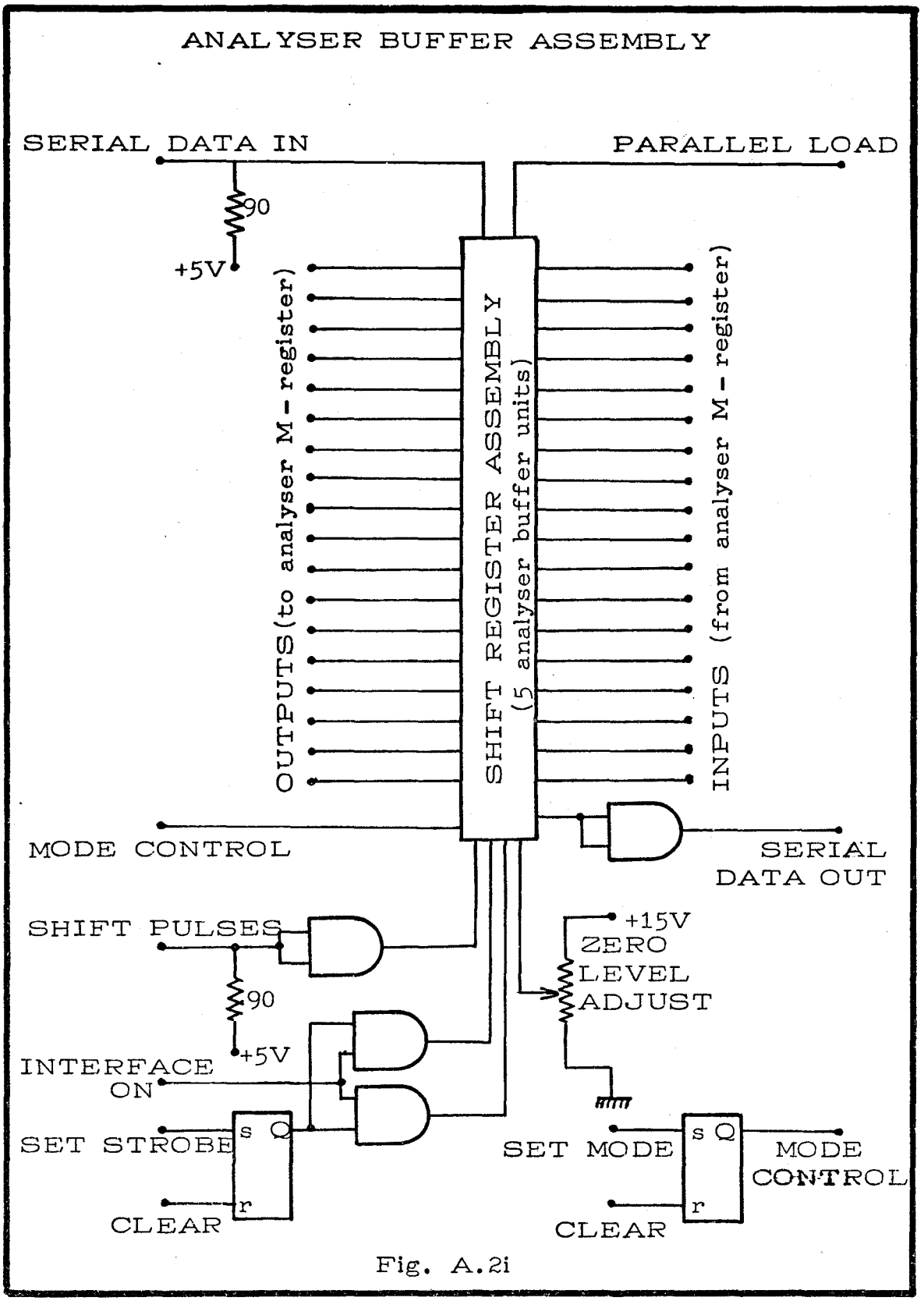
ANALYSER BUFFER ASSEMBLY
SERIAL DATA IN
PARALLEL LOAD
90
+5V
OUTPUTS (to analyser M-register)
SHIFT REGISTER ASSEMBLY
(5 analyser buffer units)
INPUTS (from analyser M-register)
MODE CONTROL
SERIAL
DATA OUT
SHIFT PULSES
90
+5V
+15V
ZERO
LEVEL
ADJUST
INTERFACE
ON
SET STROBE
s Q
r
CLEAR
SET MODE
s Q
r
CLEAR
MODE
CONTROL

Fig. A.2i

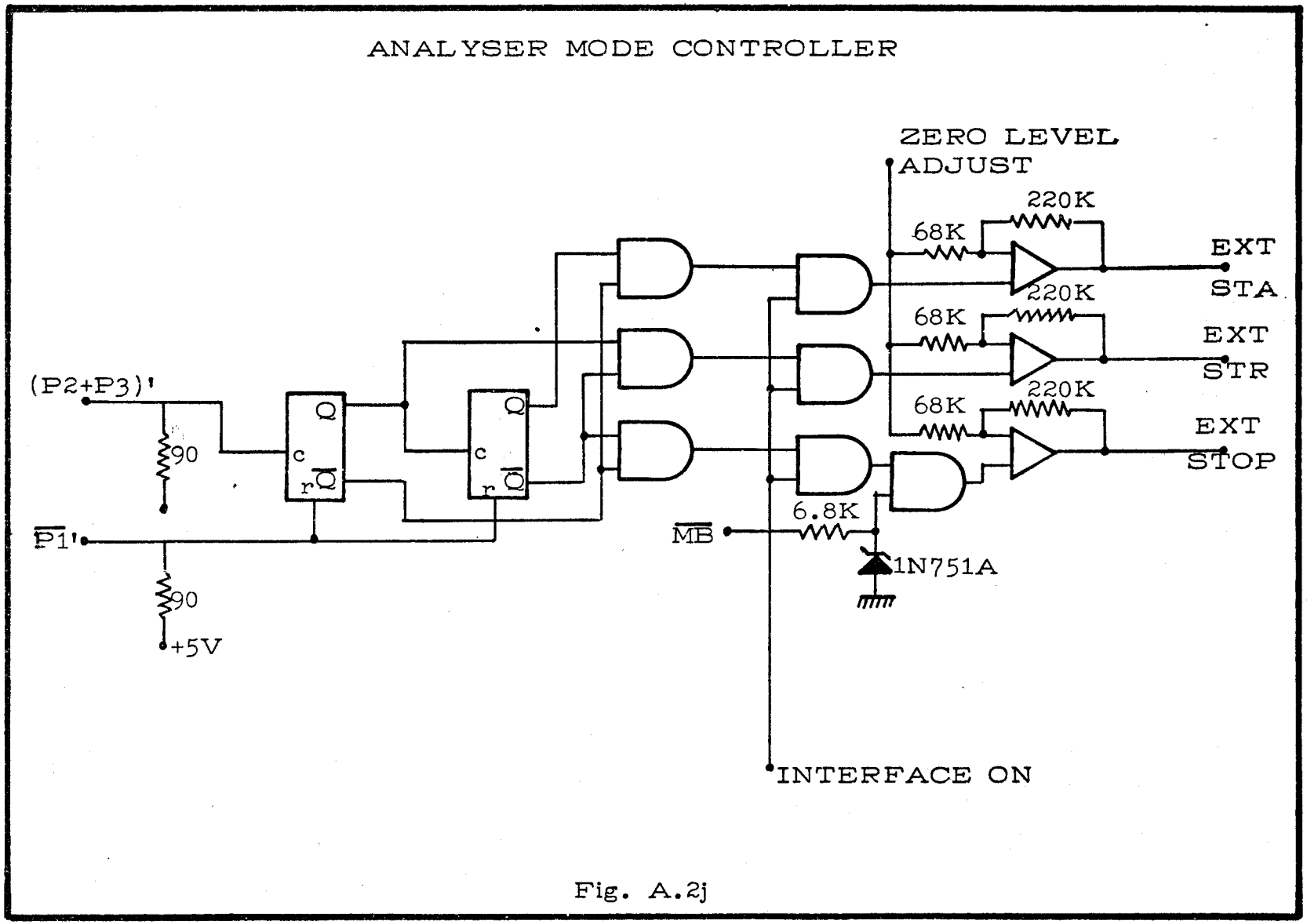
ANALYSER MODE CONTROLLER
ZERO LEVEL
ADJUST
220K
68K
EXT
STA
220K
68K
EXT
STR
220K
68K
EXT
STOP
(P2+P3)'
90
c
Q
r
Q
c
Q
r
Q
P1'
90
+5V
MB
6.8K
1N751A
INTERFACE ON

Fig. A.2j

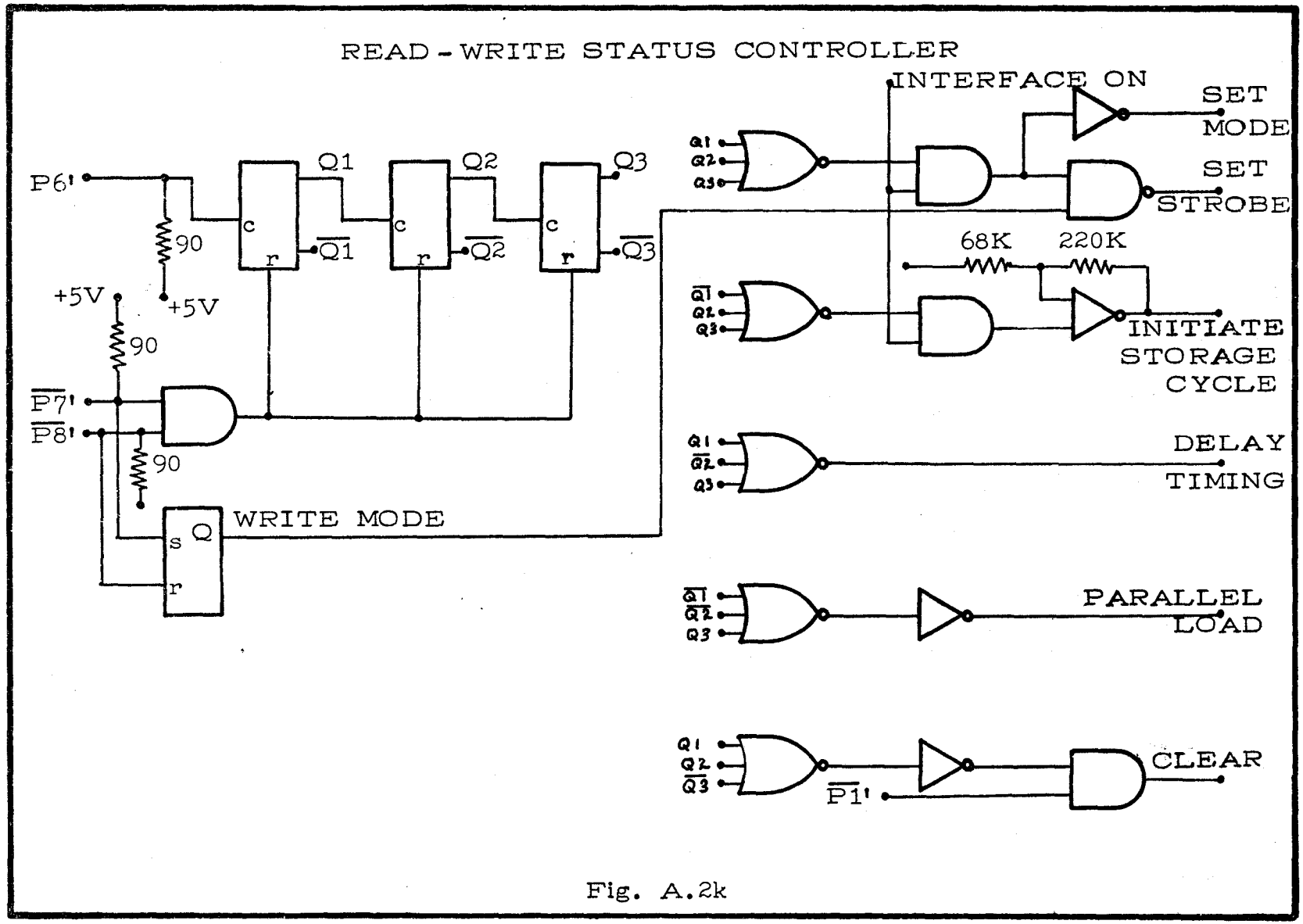
READ - WRITE STATUS CONTROLLER
INTERFACE ON
SET MODE
SET STROBE
P6'
90
Q1
Q2
Q3
+5V
+5V
68K
220K
INITIATE STORAGE CYCLE
P7'
P8'
WRITE MODE
DELAY TIMING
PARALLEL LOAD
CLEAR
P1'

Fig. A.2k

INTERRUPT AND SKIP LOGIC
(ANALYSER STATION)

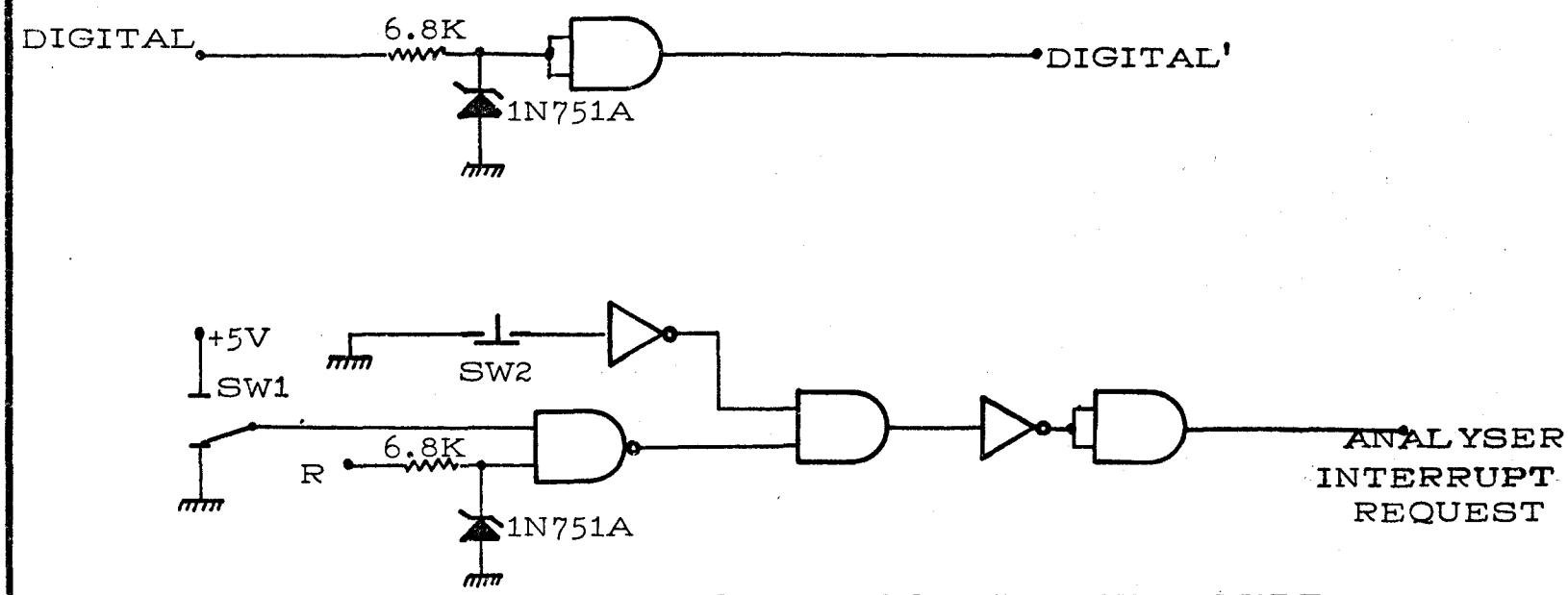

SW1 - AUTOMATIC INTERRUPT
REQUEST SWITCH

SW2 - MANUAL INTERRUPT
REQUEST SWITCH

Fig. A.21

A.3 Instruction List and Software

The interface has been assigned device code 54. The accumulator buffer is considered as a separate unit and has been assigned device code 52. The instructions relevant to the interface are described below followed by some examples of simple data transfer software.

A.3.1 Software Instructions

i Mode Controls

The "Mode"or "State" of the "M" unit may be controlled via the interface by placing the Mode Switch on the "M" unit in the"Stop-2" position.

The mode is then determined by the state of a 2-bit count up register in the interface.

00 - Stop 1

01 - Readout

10 - Analyse

11 - Stop 2 (Indeterminate)

There are 3 instructions relevant to this register and these may be combined or "micro-coded". They are

			Suggested Mnemonic
705401	P1	Reset Mode State	STOP
705402	P2	Advance Mode State	ADV1
705404	P3	Advance Mode State	ADV2

These may be combined as

705403		Set Read Mode	READ
705407		Set Analyse Mode	ANALYSE

For any of these "Instructions" to be properly implemented a delay of at least 12 μseconds is required. Note that the channel scaler is only reset in the Stop1 mode.

ii Skip if Digital is Set

This instruction reads or checks the position of the "CRT-DIGITAL-PEN" switch for DIGITAL. If the switch is in the digital position the next instruction is skipped

705421	P4	Skip if Digital Set	SKPDIG

iii Set Erase Function

This instruction delivers a positive level to reset the "M" register and maintains that level until a "STOP" instruction is encountered. Allow 12 μseconds to take effect.

705422 P5 Set Erase Function ERASE

iv Read Cycle Controls.

The Read M-Write-M cycle is controlled by a 3 bit count up register. Timed pulses are generated by decoding the output of this register. There are 3 relevant instructions. "Set Read Function", "Set Write Function", "Advance Read-Write State". The first two reset the register to all 1's as well as set or reset a READ-WRITE flip-flop.

The third instruction advances the state of the register. The states are:

111	Initial or Reset Value
000	Set Parallel transfer mode Set Strobes if in write mode
001	Initiate ND-160-M unit memory storage cycle (IS). This state must ordinarily be terminated within 32 μsec. to prevent the initiation of another storage cycle. Recommended delay - 4 μsec.
010	Pause - allows stabilization of M-register before parallel load of shift register buffer.
011	Strobe data into shift register buffer
100	Reset Mode, Reset Strobe

101	Unused	
110	Unused	

705424	P6	Advance Read-Write State	EXEC
705441	P7	Set Write Function	SETW
705442	P8	Set Read Function	SETR

v Interrupt Instructions

The interface is equipped with an automatic and a manual "Interrupt" request. The manual request is accomplished via the pushbutton on the Interface Panel. The automatic mode is set by the switch directly below this push button. When in "Automatic Interrupt Mode" an interrupt request will be issued whenever the analyser is in readout mode. There are two instructions associated with this. "Clear Analyser Interrupt Flag" and "Skip if Analyser Interrupt Flag is off".

705444	P9	Clear Analyser Interrupt Flag	CLAI
705461	P10	Skip Analyser Interrupt off	SKAI

vi Transfer Instructions

In order to accomplish the transfer between the shift registers it is necessary to state which device is requesting the transfer. This is accomplished in conjunction with the

starting of the clock producing the shift pulses. When the transfer is complete the connection to analyse buffer may be broken with an "Analyser Off" instruction. Delay 20 μsec. on transfers.

705462	P11	Interchange Shift Register Buffers	TRAN
705464	P12	Disconnect Analyser Buffer	ANOFF

vii Accumulator Buffer Control

There are two instructions to be used for data transfer to the AC from the accumulator buffer and vice versa. The first is "Place the Buffer in the AC". Note that the buffer is "ORED" to the AC so the AC must be cleared (CLA) before executing the instruction. The second is "Place Accumulator in AC Buffer".

705202	Place ACB in AC	PBA
705222	Place AC in ACB	PAB

viii Summary of Instructions

705401	P1	STOP
705402	P2	ADV1
705404	P3	ADV2
705403	P1+P2	READ
705407	P1+P2+P3	ANALYSE

705421	P4	SKPDIG
705422	P5	ERASE
705424	P6	EXEC
705441	P7	SETW
705442	P8	SETR
705444	P9	CLAI
705461	P10	SKAI
705462	P11	TRAN
705464	P12	ANOFF
705202		PBA
705212		LAB (Clears AC before transfer)
705222		PAB

A.3.2 Software Examples

i Analyser read routine

The following subroutine reads the analyser into the second page of the PDP-15 memory. The instruction DEL is an unused IOT instruction and therefore provides a 4 μsec. delay. It is important to note that the timing of the first 3 instructions following the label ANRD1 is critical and thus the program interrupt must be disabled at this point.

Read Analyser into Upper 4-K

```
100          ANRD      0                          000000
101                    STOP                       705401
102                    DEL                        705444
103                    DEL                        705444
104                    DEL                        705444
105                    READ                       705403
106                    SETR                       705442
107                    LAC       (7777            200142
110                    DAC       10               040010
111          ANRD1     EXEC                       705424
112                    EXEC                       705424
113                    DEL                        705444
114                    EXEC                       705424
115                    EXEC                       705424
116                    EXEC                       705424
117                    SETR                       705442
120                    TRAN                       705462
121                    DEL                        705444
122                    DEL                        705444
123                    DEL                        705444
124                    DEL                        705444
125                    DEL                        705444
126                    LAC       10               200010
127                    SAD       (17776           540142
130                    JMP       ANRD2            600135
131                    CLA                        750000
132                    PBA                        705202
133                    DAC    *  10               060010
134                    JMP       ANRD1            600111
135          ANRD2     CLA                        750000
136                    PBA                        705202
137                    DAC    *  10               060010
140                    JMP    *  ANRD             620100
141                  007777                       007777
142                  177776                       017776
```

ii Erase the Analyser Memory

The following example is a subroutine to erase the entire 4-K analyser memory. The inclusion of the long delay sequence is to allow completion of the ND-160- M memory cycle

before starting a second cycle.

```
300     ERASE     00                      000000
301               STOP                    705401
302               SEM                     705422
303               SETR                    705442
304               ADV1                    705402
305               LAC       (770000       200344
306               DAC       CNT           040345
307               CLA                     750000
310     ERASE1    IAC                     740030
311               EXEC                    705424
312               EXEC                    705424
313               DEL                     705444
314               EXEC                    705424
315               EXEC                    705424
316               EXEC                    705424
317               SETR                    705442
320               DEL                     705444
321               DEL                     705444
322               DEL                     705444
323               DEL                     705444
324               DEL                     705444
325               DEL                     705444
326               DEL                     705444
327               DEL                     705444
330               DEL                     705444
331               DEL                     705444
332               DEL                     705444
333               DEL                     705444
334               DEL                     705444
335               ISZ       CNT           440345
336               JMP       ERASE1        600310
337               STOP                    705401
340               DEL                     705444
341               DEL                     705444
342               DEL                     705444
343               JMP*      ERASE         620300
344     CNTO      770000                  770000
345     CNT       00                      000000
```

iii Write into the Analyser Memory

This subroutine transfers the second page of PDP-15 memory to the ND-160-M unit. Note that before transfer can take place the memory of the ND-160-M unit must be erased. This is accomplished by means of the previous subroutine.

```
500     WRITE   - 00                    000000
501               JMS       ERASE       100300
502               STOP                  705401
503               DEL                   705444
504               DEL                   705444
505               DEL                   705444
506               READ                  705403
507               SETW                  705441
510               LAC       (7777       200540
511               DAC       10          040010
512     WRITE1    LAC *     10          220010
513               PAB                   705222
514               TRAN                  705462
515               DEL                   705444
516               DEL                   705444
517               DEL                   705444
520               DEL                   705444
521               DEL                   705444
522               EXEC                  705424
523               DEL                   705444
524               DEL                   705444
525               DEL                   705444
526               DEL                   705444
527               EXEC                  705424
530               DEL                   705444
531               EXEC                  705424
532               EXEC                  705424
533               EXEC                  705424
534               SETW                  705441
535               LAC       10          200010
536               SAD       (17777      540547
537               SKP                   741000
540               JMP       WRITE1      600512
541               STOP                  705401
542               DEL                   705444
543               DEL                   705444
544               DEL                   705444
545               JMP *     WRITE       620500
546                7777                 007777
547               17777                 017777
```

APPENDIX B

THE FILTER

B.1 The Optimum Filter

For the high resolution detectors being used for the activation analysis measurements the spectra obtained consist of a number of sharp Gaussian peaks (signal portion) superimposed on a relatively smooth background. If we denote the background by B(E) we may denote the spectrum as a sum of the desired signal portion and the background.

$$x(E) = S(E) + B(E)$$

Application of a filter to this spectrum results in a correlation spectrum

$$y(E') + b(E') = \int F(E-E')(S(E) + B(E))dE$$

If the background spectrum is considered to form the primary contributant to the noise, the noise in the correlation spectrum may be identified with $\sigma^2_{b(E')}$.

As shown in Section 3.3 equation (8)

$$\sigma^2_{b(E')} = \int_E F^2(E-E')B(E')dE$$

Since B(E) is slowly varying it may be considered to be constant over the width of the filter.

$$\sigma^2_{b(E')} = \overline{B}\int_E F^2(E-E')dE$$

Then the signal to noise ratio of the correlation spectrum is

$$R_{y(E')} = \frac{\left(\int F(E-E')S(E)dE\right)^2}{\overline{B}\int_E F^2(E-E')dE}$$

Adopting a vectorial viewpoint the integral of the numerator is seen to be the inner product of the vector

$$F(E) = F(E-E')$$

and the vector S(E). The Schwartz inequality states

$$\Big(F(E)\circ S(E)\Big)^2 \leq (F(E)\circ F(E))(S(E)\circ S(E))$$

the equality holding for $F(E) = S(E)$. Hence the correlation signal to noise ratio $R_{y(E')}$ is maximized for $F(E) = S(E)$ and optimization is achieved if the correlator is identical with the spectral line shape.

B.2 Fourier Transforms of Filters

The correlation spectrum

$$y(E') = \int_{\varepsilon} F(E'-E)X(E)dE$$

is seen to be a convolution of the filter function, $F(E)$, with the original data, $x(E)$. Invoking the convolution theorem

$$Y(w) = H(w)X(w)$$

where $Y(w)$, $X(w)$ and $H(w)$ are the Fourier transforms of $y(E)$, $x(E)$ and $F(E)$ respectively. The Fourier transforms of three different forms of zero area filters are shown in Fig. $3.2.2_c$. The calculations of the transforms is performed

below.

By definition, the Fourier transform of a function F(E) is defined as

$$H(w) = \mathcal{F} F(E) = \frac{1}{\sqrt{2\pi}} \int_{E=-\infty}^{\infty} e^{-iwE} F(E)\,dE$$

The three filter functions considered may be formed as the difference of:

i. two rectangular functions

ii. a Gaussian and a rectangular function

iii. two Gaussian functions

Thus the Fourier transforms of the filters will be the difference of the Fourier transforms of the simpler rectangular and Gaussian functions. For the Gaussian

$$G_{\sigma}(E) = \mathrm{EXP}\left(-\frac{E^2}{2\sigma^2} \right)$$

we have the transform

$$H_G(w) = \frac{1}{\sqrt{2\pi}} \mathrm{EXP}(-iwE)\, \mathrm{EXP}\left(-\frac{E^2}{2\sigma^2} \right) dE$$

$$H_G(w) = \frac{1}{\sqrt{2\pi}} \int_{-\infty}^{\infty} EXP\left\{-\left(\frac{E}{\sqrt{2}\sigma} + \frac{i\sigma w}{\sqrt{2}}\right)^2\right\} EXP\left\{-\frac{\sigma^2 w^2}{2}\right\} dE$$

$$= EXP\left\{-\frac{\sigma^2 w^2}{2}\right\} \frac{1}{\sqrt{2\pi}} \int_{-\infty}^{\infty} EXP(-x^2)\sqrt{2}\sigma\, dx$$

$$H_G(w) = EXP\left\{-\frac{\sigma^2 w^2}{2}\right\}$$

It is seen that the transform of a Gaussian is again a Gaussian whose width is inversely proportional to the width of the original. For the rectangular function

$$R_N(E) = \begin{cases} 1 & |E| \leq N \\ 0 & |E| > N \end{cases}$$

the Fourier transform is

$$H_{R_N}(w) = \frac{1}{\sqrt{2\pi}} \int_{-\infty}^{\infty} e^{-iwE} R_N(E)\, dE$$

$$H_{R_N}(w) = \frac{1}{\sqrt{2\pi}} \int_{-N}^{N} e^{-iwE}\, dE$$

$$= \frac{1}{\sqrt{2\pi}} \left(\frac{e^{-iwE}}{-iw} \right) \Bigg|_{-N}^{N}$$

$$= \frac{1}{\sqrt{2\pi}}\, 2\, \frac{\mathrm{Sin}(wN)}{w}$$

and we note that the width of the sinc function is also inversely proportional to the width of the filter function.

The zero area rectangular filter with upper width N and lower width L may be written

$$F_{R-R}(E) = \frac{L}{L-N} R_N(E) - \frac{N}{L-N} R_L(E)$$

The Fourier transform of this filter is

$$H_{R-R}(w) = \frac{2}{\sqrt{2\pi}(L-N)w} (L \operatorname{Sin} wN - N \operatorname{Sin} wL)$$

and is plotted in Fig. 3.2c$_i$ for a filter with N = 2.5 and L = 5.5.

The filter consisting of a Gaussian minus a rectangular section to achieve a net area of zero may be written

$$F_{G-R}(E) = \operatorname{EXP}\left\{-\frac{E^2}{2\sigma_1^2}\right\} - \sqrt{\frac{\pi}{2}}\frac{\sigma_1}{L} R_L(E)$$

and will have the Fourier transform

$$H_{G-R}(w) = \sigma_1 \operatorname{EXP}\left\{-\frac{\sigma_1^2 w^2}{2}\right\} - \sqrt{\frac{\pi}{2}}\frac{1}{L}\sqrt{\frac{2}{\pi}}\frac{\operatorname{Sin} wL}{w}$$

$$= \sigma_1 \operatorname{EXP}\left\{-\frac{\sigma_1^2 w^2}{2}\right\} - \frac{1}{Lw}\operatorname{Sin} wL$$

This function is plotted in Fig. $3.2c_{ii}$ for a Gaussian with HWHM = 2.5 and a lower rectangle with L = 5.5.

For the double Gaussian filter we may write

$$F_{G-G}(E) = \sigma_2 \text{EXP}\left\{-\frac{E}{2\sigma_1^2}\right\} - \sigma_1 \text{EXP}\left\{-\frac{E}{2\sigma_2^2}\right\}$$

and the corresponding Fourier transform will be

$$H_{G-G}(w) = \sigma_1\sigma_2 \text{EXP}\left\{-\frac{\sigma_1^2 w^2}{2}\right\} - \sigma_1\sigma_2 \text{EXP}\left\{-\frac{\sigma_2^2 w^2}{2}\right\}$$

which is plotted in Fig. $3.2c_{iii}$ for Gaussians with HWHM = 2.5 and 5.5 respectively.

REFERENCES

(1) M.A. Mariscotti (Nucl. Instr. and Meth., 50 (1967) page 309).

(2) W.W. Bowman (Nucl. Instr. and Meth., 96 (1971) page 135).

(3) A. Robertson, W.V. Prestwich, T.J. Kennett (Nucl. Instr. and Meth., 100 (1972) page 317).

(4) J.T. Routti (Nucl. Instr. and Meth., 72 (1969) page 125).

(5) L. Varnell, J. Trischuk (Nucl. Instr. and Meth., 76 (1969) page 109).

(6) Z. Kosina (Nucl. Instr. and Meth., 88 (1970) page 163).

(7) D. Goss (Nucl. Instr. and Meth., 89 (1970) page 221).

(8) I.A. Slavic, S.P. Bingulac (Nucl. Instr. and Meth., 84 (1970) page 261).

(9) A. Connelly, W.W. Black (Nucl. Instr. and Meth., 82 (1970) page 141).

(10) T. Inouye, T. Harper, N.C. Rasmussen (Nucl. Instr. and Meth., 67 (1969) page 125).

(11) H. Tominaga, M. M. Dojyo, M. Tanaka (Nucl. Instr. and Meth., 98 (1972) page 69).

(12) J.H. Head (Nucl. Instr. and Meth., 98 (1972) page 419).

(13) P. Quittner (Nucl. Instr. and Meth., 76 (1969) page 115).

(14) N.V. De Castra Faria, J.P. Martin, R.J.A. Levesque (Nucl. Instr. and Meth., 85 (1970) page 49).

(15) A.B. Tanner, R.C. Bhargava, F.E. Senftle, J.M. Brinkerhoff (Nucl. Instr. and Meth., 102 (1972) page 61).

REFERENCES (cont.)

(16) N.D. Eckhoff (Nucl. Instr. and Meth., 74 (1969) page 77).

(17) J.A. Blackburn (Analytical Chemistry, 65 (1965) page 1000).

(18) J.S. Bendat, A.G. Piersol (Random Data, Analysis and Measurement Procedures).

(19) D.L. Summers, D.D. Babb (Unfolding Pulse Height Distributions by Vector Analysis) Applications of Computers to Nuclear and Radiochemistry, U.S. Atomic Energy Commission, (1962).

(20) A.J. Tavendale, Ewan (Nucl. Instr. and Meth., 25 (1963) page 185).

(21) B.J. Wall, Thesis, McMaster University, Hamilton, Ont. (1966)